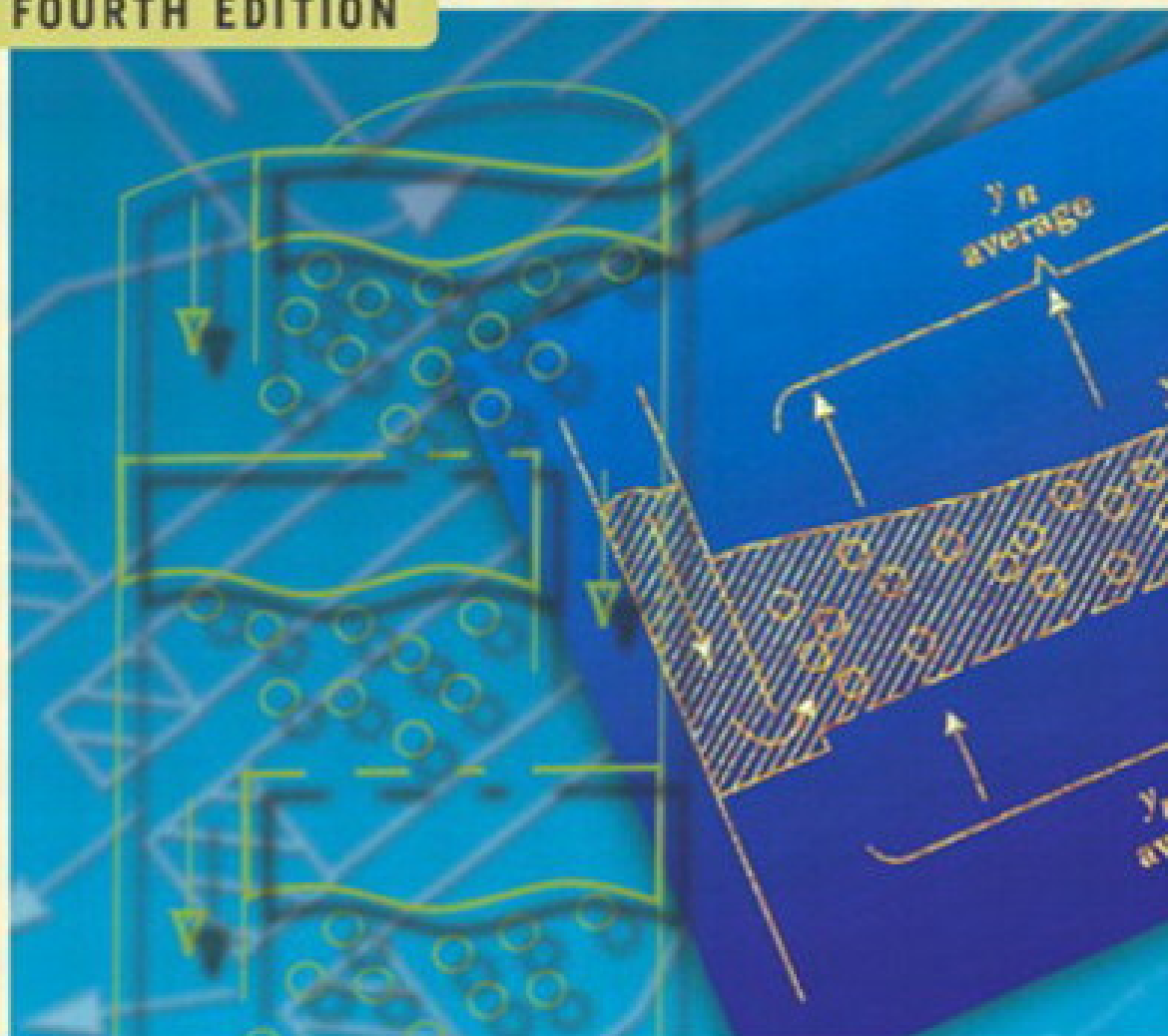


Transport Processes AND Separation Process Principles

(INCLUDES UNIT OPERATIONS)

FOURTH EDITION



CHRISTIE JOHN GEANKOPLIS

| | |
|---|----------|
| Chapter 12. Liquid–Liquid and Fluid–Solid Separation Processes..... | 1 |
| Section 12.1. INTRODUCTION TO ADSORPTION PROCESSES..... | 1 |
| Section 12.2. BATCH ADSORPTION..... | 4 |
| Section 12.3. DESIGN OF FIXED-BED ADSORPTION COLUMNS..... | 5 |
| Section 12.4. ION-EXCHANGE PROCESSES..... | 12 |
| Section 12.5. SINGLE-STAGE LIQUID–LIQUID EXTRACTION PROCESSES..... | 18 |
| Section 12.6. TYPES OF EQUIPMENT AND DESIGN FOR LIQUID–LIQUID EXTRACTION..... | 25 |
| Section 12.7. CONTINUOUS MULTISTAGE COUNTERCURRENT EXTRACTION..... | 33 |
| Section 12.8. INTRODUCTION AND EQUIPMENT FOR LIQUID–SOLID LEACHING..... | 46 |
| Section 12.9. EQUILIBRIUM RELATIONS AND SINGLE-STAGE LEACHING..... | 52 |
| Section 12.10. COUNTERCURRENT MULTISTAGE LEACHING..... | 56 |
| Section 12.11. INTRODUCTION AND EQUIPMENT FOR CRYSTALLIZATION..... | 61 |
| Section 12.12. CRYSTALLIZATION THEORY..... | 67 |
| PROBLEMS..... | 75 |
| REFERENCES..... | 82 |

Chapter 12. Liquid–Liquid and Fluid–Solid Separation Processes

INTRODUCTION TO ADSORPTION PROCESSES

Introduction

In adsorption processes one or more components of a gas or liquid stream are adsorbed on the surface of a solid adsorbent and a separation is accomplished. In commercial processes, the adsorbent is usually in the form of small particles in a fixed bed. The fluid is passed through the bed and the solid particles adsorb components from the fluid. When the bed is almost saturated, the flow in this bed is stopped and the bed is regenerated thermally or by other methods so that desorption occurs. The adsorbed material (adsorbate) is thereby recovered and the solid adsorbent is ready for another cycle of adsorption.

Applications of liquid-phase adsorption include removal of organic compounds from water or organic solutions, colored impurities from organics, and various fermentation products from fermentor effluents. Separations include paraffins from aromatics and fructose from glucose using zeolites.

Applications of gas-phase adsorption include removal of water from hydrocarbon gases, sulfur compounds from natural gas, solvents from air and other gases, and odors from air.

Physical Properties of Adsorbents

Many adsorbents have been developed for a wide range of separations. Typically, the adsorbents are in the form of small pellets, beads, or granules ranging from about 0.1 mm to 12 mm in size, with the larger particles being used in packed beds. A particle of adsorbent has a very porous structure, with many fine pores and pore volumes up to 50% of total particle volume. The adsorption often occurs as a monolayer on the surface of the fine pores, although several layers sometimes occur. Physical adsorption, or van der Waals adsorption, usually occurs between the adsorbed molecules and the solid internal pore surface and is readily reversible.

The overall adsorption process consists of a series of steps in series. When the fluid is flowing past the particle in a fixed bed, the solute first diffuses from the bulk fluid to the gross exterior surface of the particle. Then the solute diffuses inside the pore to the surface of the pore. Finally, the solute is adsorbed on the surface. Hence, the overall adsorption process is a series of steps.

There are a number of commercial adsorbents and some of the main ones are described below. All are characterized by very large pore surface areas of 100 to over 2000 m²/g.

1. **Activated carbon.** This is a microcrystalline material made by thermal decomposition of wood, vegetable shells, coal, and so on, and has surface areas of 300 to 1200 m²/g with average pore diameters of 10 to 60 Å. Organics are generally adsorbed by activated carbon.

2. **Silica gel.** This adsorbent is made by acid treatment of sodium silicate solution and then drying. It has a surface area of 600 to 800 m²/g and average pore diameters of 20 to 50 Å. It is primarily used to dehydrate gases and liquids and to fractionate hydrocarbons.
3. **Activated alumina.** To prepare this material, hydrated aluminum oxide is activated by heating to drive off the water. It is used mainly to dry gases and liquids. Surface areas range from 200 to 500 m²/g, with average pore diameters of 20 to 140 Å.
4. **Molecular sieve zeolites.** These zeolites are porous crystalline aluminosilicates that form an open crystal lattice containing precisely uniform pores, which makes it different from other types of adsorbents, which have a range of pore sizes. Different zeolites have pore sizes from about 3 to 10 Å. Zeolites are used for drying, separation of hydrocarbons, mixtures, and many other applications.
5. **Synthetic polymers or resins.** These are made by polymerizing two major types of monomers. Those made from aromatics such as styrene and divinylbenzene are used to adsorb nonpolar organics from aqueous solutions. Those made from acrylic esters are usable with more-polar solutes in aqueous solutions.

Equilibrium Relations for Adsorbents

The equilibrium between the concentration of a solute in the fluid phase and its concentration on the solid resembles somewhat the equilibrium solubility of a gas in a liquid. Data are plotted as adsorption isotherms as shown in Fig. 12.1-1. The concentration in the solid phase is expressed as q , kg adsorbate (solute)/kg adsorbent (solid), and in the fluid phase (gas or liquid) as c , kg adsorbate/m³ fluid.

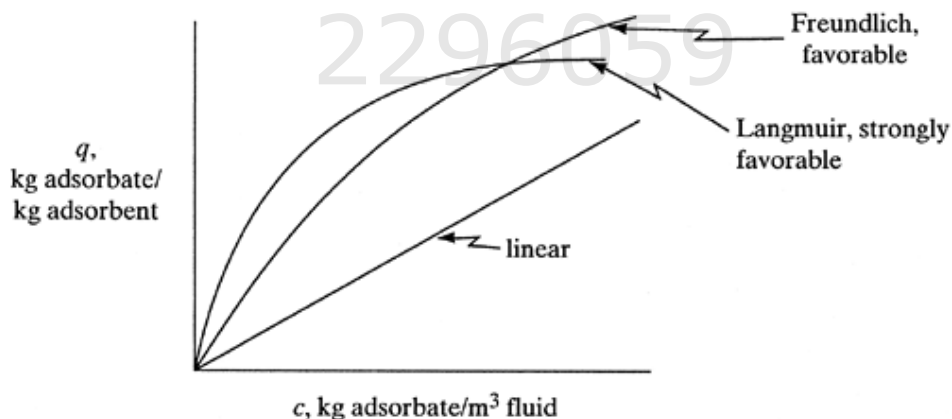


Figure 12.1-1. Some common types of adsorption isotherms.

Data that follow a linear law can be expressed by an equation similar to Henry's law:

Equation 12.1-1.

$$q = Kc$$

where K is a constant determined experimentally, m³/kg adsorbent. This linear isotherm is not common, but in the dilute region it can be used to approximate data for many systems.

The Freundlich isotherm equation, which is empirical, often approximates data for many physical adsorption systems and is particularly useful for liquids:

Equation 12.1-2.

$$q = Kc^n$$

where K and n are constants and must be determined experimentally. If a log–log plot is made for q versus c , the slope is the dimensionless exponent n . The dimensions of K depend on the value of n . This equation is sometimes used to correlate data for hydrocarbon gases on activated carbon.

The Langmuir isotherm has a theoretical basis and is given by the following, where q_o and K are empirical constants:

Equation 12.1-3.

$$q = \frac{q_o c}{K + c}$$

where q_o is kg adsorbate/kg solid and K is kg/m³. The equation was derived assuming that there are only a fixed number of active sites available for adsorption, that only a monolayer is formed, and that the adsorption is reversible and reaches an equilibrium condition. By plotting $1/q$ versus $1/c$, the slope is K/q_o and the intercept is $1/q_o$.

Almost all adsorption systems show that as temperature is increased, the amount adsorbed by the adsorbent decreases strongly. This is useful since adsorption is normally at room temperatures and desorption can be attained by raising the temperature.

EXAMPLE 12.1-1. Adsorption Isotherm for Phenol in Wastewater

Batch tests were performed in the laboratory using solutions of phenol in water and particles of granular activated carbon (R5). The equilibrium data at room temperature are shown in Table 12.1-1. Determine the isotherm that fits the data.

Table 12.1-1. Equilibrium Data for Example 12.1-1 (R5)

| $c,$ $\left(\frac{\text{kg phenol}}{\text{m}^3 \text{ solution}} \right)$ | $q,$ $\left(\frac{\text{kg phenol}}{\text{kg carbon}} \right)$ |
|---|--|
| 0.322 | 0.150 |
| 0.117 | 0.122 |
| 0.039 | 0.094 |
| 0.0061 | 0.059 |
| 0.0011 | 0.045 |

Solution: Plotting the data as $1/q$ versus $1/c$, the results are not a straight line and do not follow the Langmuir equation (12.1-3). A plot of $\log q$ versus $\log c$ in Fig. 12.1-2 gives a straight line and, hence, follows the Freundlich isotherm, Eq. (12.1-2). The slope n is 0.229 and the constant K is 0.199, to give

$$q = 0.199c^{0.229}$$

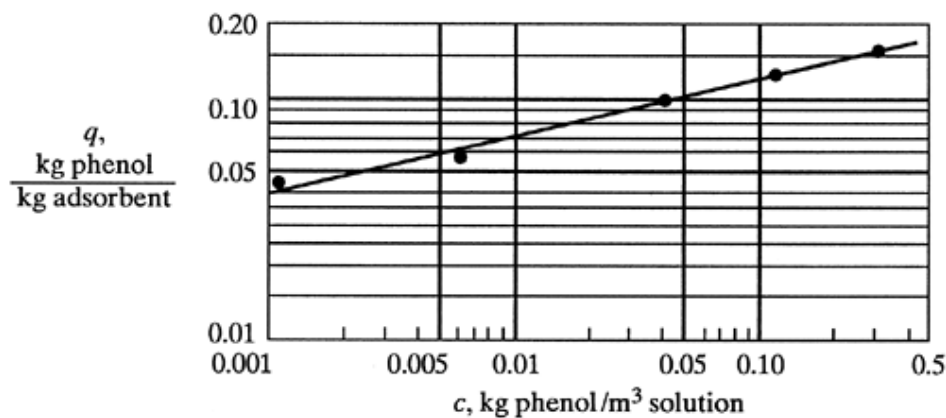


Figure 12.1-2. Plot of data for Example 12.1-1.

BATCH ADSORPTION

Batch adsorption is often used to adsorb solutes from liquid solutions when the quantities treated are small in amount, as in the pharmaceutical or other industries. As with many other processes, an equilibrium relation such as the Freundlich or Langmuir isotherm and a material balance are needed. The initial feed concentration is c_F and the final equilibrium concentration is c . Also, the initial concentration of the solute adsorbed on the solid is q_F and the final equilibrium value is q . The material balance on the adsorbate is

Equation 12.2-1.

$$q_F M + c_F S = q M + c S$$

where M is the amount of adsorbent, kg; and S is the volume of feed solution, m^3 .

When the variable q in Eq. (12.2-1) is plotted versus c , the result is a straight line. If the equilibrium isotherm is also plotted on the same graph, the intersection of both lines gives the final equilibrium values of q and c .

EXAMPLE 12.2-1. Batch Adsorption on Activated Carbon

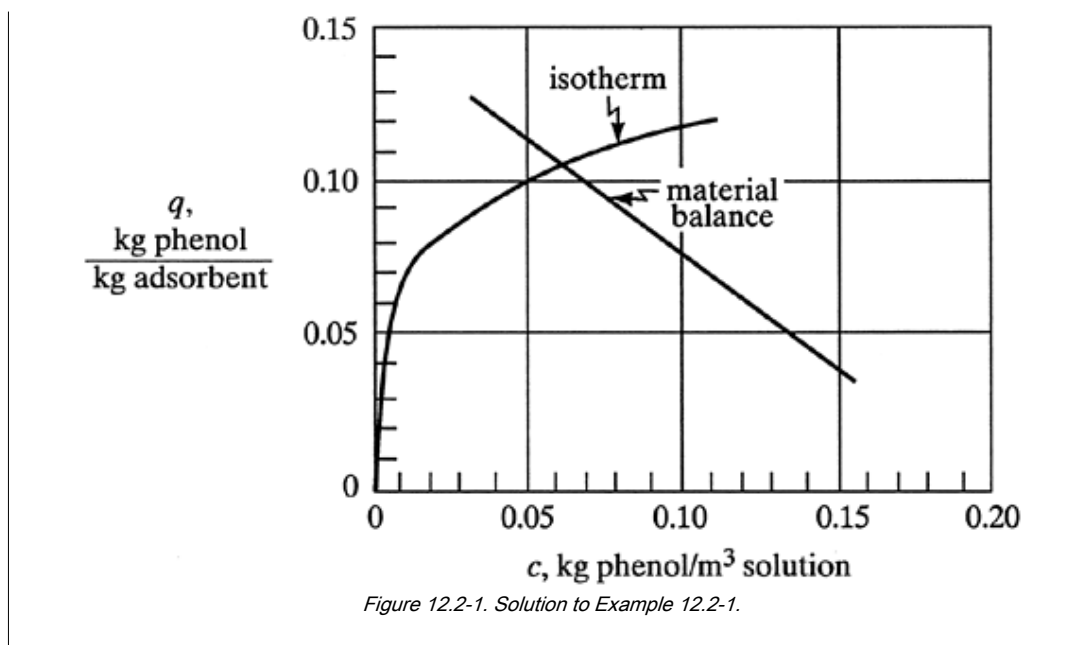
A wastewater solution having a volume of 1.0 m^3 contains $0.21 \text{ kg phenol/m}^3$ of solution (0.21 g/L). A total of 1.40 kg of fresh granular activated carbon is added to the solution, which is then mixed thoroughly to reach equilibrium. Using the isotherm from Example 12.1-1, what are the final equilibrium values, and what percent of phenol is extracted?

Solution: The given values are $c_F = 0.21 \text{ kg phenol/m}^3$, $S = 1.0 \text{ m}^3$, $M = 1.40 \text{ kg carbon}$, and q_F is assumed as zero. Substituting into Eq. (12.2-1),

$$0(1.40) + 0.21(1.0) = q(1.40) + c(1.0)$$

This straight-line equation is plotted in Fig. 12.2-1. The isotherm from Example 12.1-1 is also plotted in Fig. 12.2-1. At the intersection, $q = 0.106 \text{ kg phenol/kg carbon}$ and $c = 0.062 \text{ kg phenol/m}^3$. The percent of phenol extracted is

$$\% \text{ extracted} = \frac{c_F - c}{c_F}(100) = \frac{0.210 - 0.062}{0.210}(100) = 70.5$$



DESIGN OF FIXED-BED ADSORPTION COLUMNS

Introduction and Concentration Profiles

A widely used method for adsorption of solutes from liquid or gases employs a fixed bed of granular particles. The fluid to be treated is usually passed down through the packed bed at a constant flow rate. The situation is more complex than that for a simple stirred-tank batch process which reaches equilibrium. Mass-transfer resistances are important in the fixed-bed process, and the process is unsteady state. The overall dynamics of the system determine the efficiency of the process, rather than just the equilibrium considerations.

The concentrations of the solute in the fluid phase and of the solid adsorbent phase change with time and with position in the fixed bed as adsorption proceeds. At the inlet to the bed, the solid is assumed to contain no solute at the start of the process. As the fluid first comes in contact with the inlet of the bed, most of the mass transfer and adsorption takes place here. As the fluid passes through the bed, the concentration in this fluid drops very rapidly with distance in the bed and reaches zero well before the end of the bed is reached. The concentration profile at the start at time t_1 is shown in Fig. 12.3-1a, where the concentration ratio c/c_o is plotted versus bed length. The fluid concentration c_o is the feed concentration and c is the fluid concentration at a point in the bed.

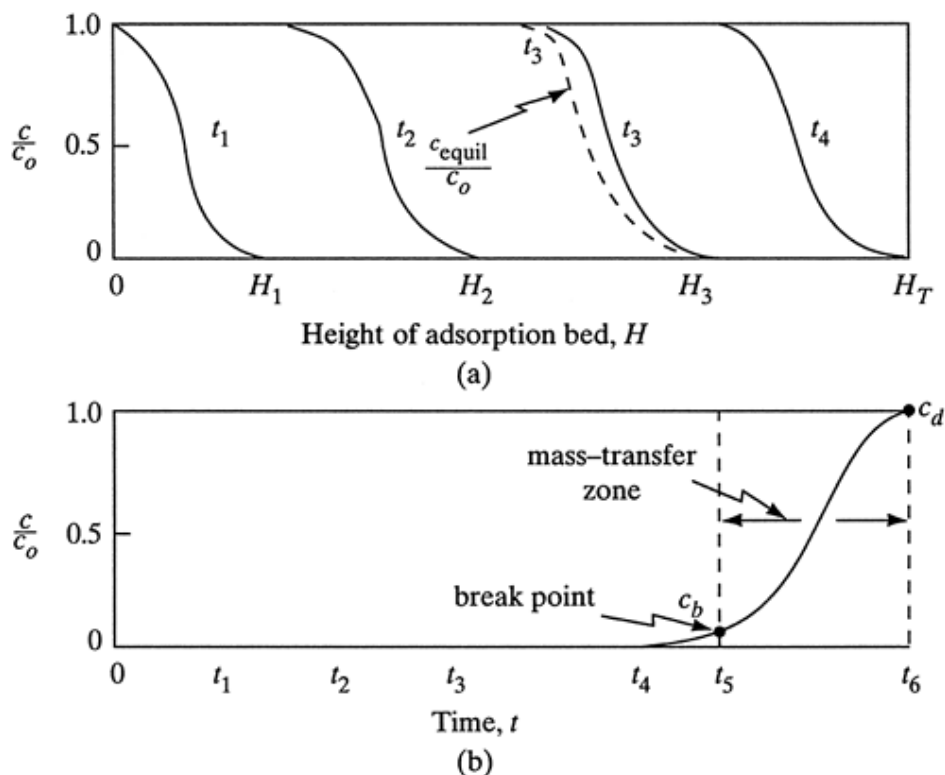


Figure 12.3-1. Concentration profiles for adsorption in a fixed bed: (a) profiles at various positions and times in the bed, (b) breakthrough concentration profile in the fluid at outlet of bed.

After a short time, the solid near the entrance to the tower is almost saturated, and most of the mass transfer and adsorption now takes place at a point slightly farther from the inlet. At a later time t_2 , the profile or mass-transfer zone where most of the concentration change takes place has moved farther down the bed. The concentration profiles shown are for the fluid phase. Concentration profiles for the concentration of adsorbates on the solid would be similar. The solid at the entrance would be nearly saturated, and this concentration would remain almost constant down to the mass-transfer zone, where it would drop off rapidly to almost zero. The dashed line for time t_3 shows the concentration in the fluid phase in equilibrium with the solid. The difference in concentrations is the driving force for mass transfer.

Breakthrough Concentration Curve

As seen in Fig. 12.3-1a, the major part of the adsorption at any time takes place in a relatively narrow adsorption or *mass-transfer zone*. As the solution continues to flow, this mass-transfer zone, which is S-shaped, moves down the column. At a given time t_3 in Fig. 12.3-1a, when almost half of the bed is saturated with solute, the outlet concentration is still approximately zero, as shown in Fig. 12.3-1b. This outlet concentration remains near zero until the mass-transfer zone starts to reach the tower outlet at time t_4 . Then the outlet concentration starts to rise, and at t_5 the outlet concentration has risen to c_b , which is called the *break point*.

After the break-point time is reached, the concentration c rises very rapidly up to point c_d , which is the end of the breakthrough curve, where the bed is judged ineffective. The break-point concentration represents the maximum that can be discarded and is often taken as 0.01 to 0.05 for c_b/c_o . The value c_d/c_o is taken as the point where c_d is approximately equal to c_o .

For a narrow mass-transfer zone, the breakthrough curve is very steep and most of the bed capacity is used at the break point. This makes efficient use of the adsorbent and lowers energy costs for regeneration.

If the mass-transfer rate were infinitely fast and if no axial dispersion were present, the mass-transfer-zone width would be zero and the breakthrough curve would be a vertical line from $d/c_o = 0$ to $d/c_o = 1.0$.

Mass-Transfer Zone

As shown in Fig. 12.3-1a, on entering the bed the concentration profile in the fluid starts to develop. For systems with a favorable isotherm, similar to the Freundlich and Langmuir isotherms (Fig. 12.1-1), which are concave downward (L1), the concentration profile in the mass-transfer zone soon acquires the typical S shape of the mass-transfer zone. Then the mass-transfer zone is constant in height as it moves through the column.

This constant height of the mass-transfer zone can then be used in scale-up when the height of the overall bed is large relative to the mass-transfer zone (L1, T1). Many industrial applications fall within these restrictions, which are applicable to adsorption from gases and liquids. Note that if the isotherm is linear or an unfavorable isotherm, the mass-transfer-zone width increases with bed length. A favorable isotherm for adsorption is unfavorable for effective regeneration (P4).

Capacity of Column and Scale-Up Design Method

The mass-transfer-zone width and shape depend on the adsorption isotherm, flow rate, mass-transfer rate to the particles, and diffusion in the pores. A number of theoretical methods have been published which predict the mass-transfer zone and concentration profiles in the bed. The predicted results may be inaccurate because of many uncertainties due to flow patterns and correlations for predicting diffusion and mass transfer. Hence, experiments in laboratory scale are needed in order to scale up the results.

The total or stoichiometric capacity of the packed-bed tower, if the entire bed comes to equilibrium with the feed, can be shown to be proportional to the area between the curve and a line at $d/c_o = 1.0$, as shown in Fig. 12.3-2. The total shaded area represents the total or stoichiometric capacity of the bed as follows (R6):

Equation 12.3-1.

$$t_i = \int_0^\infty \left(1 - \frac{c}{c_o}\right) dt$$

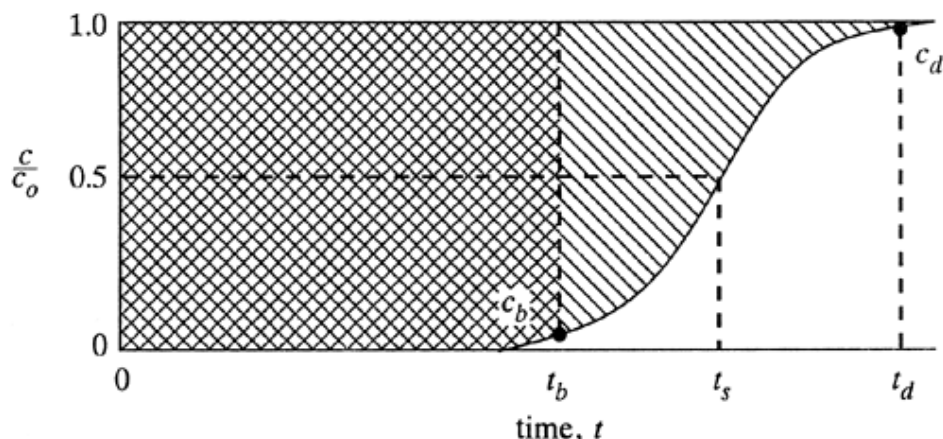


Figure 12.3-2. Determination of capacity of column from breakthrough curve.

where t_t is the time equivalent to the total or stoichiometric capacity. The usable capacity of the bed up to the break-point time t_b is the crosshatched area:

Equation 12.3-2.

$$t_u = \int_0^{t_b} \left(1 - \frac{c}{c_o}\right) dt$$

where t_u is the time equivalent to the usable capacity or the time at which the effluent concentration reaches its maximum permissible level. The value of t_u is usually very close to that of t_b . Numerical integration of Eqs. (12.3-1) and (12.3-2) can be done using a spreadsheet.

The ratio t_u/t_t is the fraction of the total bed capacity or length utilized up to the break point (C3, L1, M1). Hence, for a total bed length of H_T m, H_B is the length of bed used up to the break point,

Equation 12.3-3.

$$H_B = \frac{t_u}{t_t} H_T$$

The length of unused bed H_{UNB} in m is then the unused fraction times the total length:

Equation 12.3-4.

$$H_{UNB} = \left(1 - \frac{t_u}{t_t}\right) H_T$$

The H_{UNB} represents the mass-transfer section or zone. It depends on the fluid velocity and is essentially independent of total length of the column. The value of H_{UNB} may, therefore, be measured at the design velocity in a small-diameter laboratory column packed with the desired adsorbent. Then the full-scale adsorber bed can be designed simply by first calculating the length of bed needed to achieve the required usable capacity, H_B , at the break point. The value of H_B is directly proportional to t_b . Then the length H_{UNB} of the mass-transfer section is simply added to the length H_B needed to obtain the total length, H_T :

Equation 12.3-5.

$$H_T = H_{UNB} + H_B$$

This design procedure is widely used; its validity depends on the conditions in the laboratory column being similar to those for the full-scale unit. The small-diameter unit must be well insulated to be similar to the large-diameter tower, which operates adiabatically. The mass velocity in both units must be the same and the bed must be of sufficient length to contain a steady-state mass-transfer zone (L1). Axial dispersion or axial mixing may not be exactly the same in both towers, but if caution is exercised, this is a useful design method.

An approximate alternative procedure to use instead of integrating and obtaining areas is to assume that the breakthrough curve in Fig. 12.3-2 is symmetrical at $d/c_o = 0.5$ and t_s . Then the value of t_t in Eq. (12.3-1) is simply t_s . This assumes that the area below the curve between t_b and t_s is equal to the area above the curve between t_s and t_d .

EXAMPLE 12.3-1. Scale-Up of Laboratory Adsorption Column

A waste stream of alcohol vapor in air from a process was adsorbed by activated carbon particles in a packed bed having a diameter of 4 cm and length of 14 cm containing 79.2 g of carbon. The inlet gas stream having a concentration c_o of 600 ppm and a density of 0.00115 g/cm^3 entered the bed at a flow rate of $754 \text{ cm}^3/\text{s}$. Data in Table 12.3-1 give the concentrations of the breakthrough curve. The break-point concentration is set at $c/c_o = 0.01$. Do as follows:

- Determine the break-point time, the fraction of total capacity used up to the break point, and the length of the unused bed. Also determine the saturation loading capacity of the carbon.
- If the break-point time required for a new column is 6.0 h, what is the new total length of the column required?

Table 12.3-1. Breakthrough Concentration for Example 12.3-1

| Time, h | c/c_o | Time, h | c/c_o |
|---------|---------|---------|---------|
| 0 | 0 | 5.5 | 0.658 |
| 3 | 0 | 6.0 | 0.903 |
| 3.5 | 0.002 | 6.2 | 0.933 |
| 4 | 0.030 | 6.5 | 0.975 |
| 4.5 | 0.155 | 6.8 | 0.993 |
| 5 | 0.396 | | |

Solution: The data from Table 12.3-1 are plotted in Fig. 12.3-3. For part (a), for $c/c_o = 0.01$, the break-point time is $t_b = 3.65 \text{ h}$ from the graph. The value of t_d is approximately 6.95 h. Numerically or graphically integrating, the areas are $A_1 = 3.65 \text{ h}$ and $A_2 = 1.51 \text{ h}$. Then from Eq. (12.3-1), the time equivalent to the total or stoichiometric capacity of the bed is

$$t_t = \int_0^\infty \left(1 - \frac{c}{c_o}\right) dt = A_1 + A_2 = 3.65 + 1.51 = 5.16 \text{ h}$$

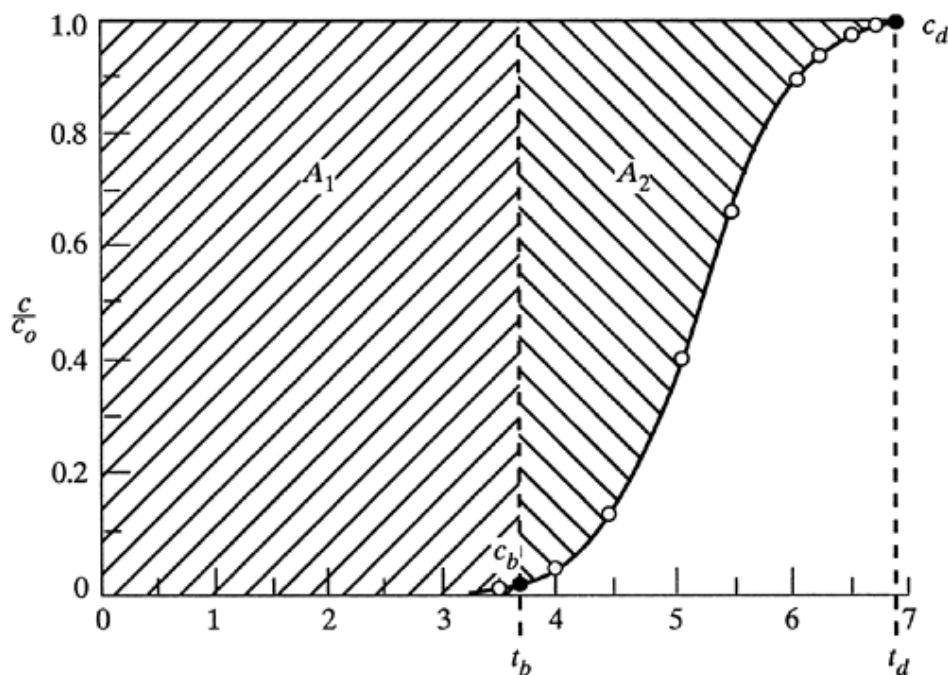


Figure 12.3-3. Breakthrough curve for Example 12.3-1.

The time equivalent to the usable capacity of the bed up to the break-point time is, using Eq. (12.3-2),

$$t_u = \int_0^{t_b=3.65} \left(1 - \frac{c}{c_o}\right) dt = A_1 = 3.65 \text{ h}$$

Hence, the fraction of total capacity used up to the break point is $t_b/t_t = 3.65/5.16 = 0.707$. From Eq. (12.3-3) the length of the used bed is $H_B = 0.707(14) = 9.9 \text{ cm}$. To calculate the length of the unused bed from Eq. (12.3-4),

$$H_{UNB} = \left(1 - \frac{t_u}{t_t}\right) H_T = (1 - 0.707)14 = 4.1 \text{ cm}$$

For part (b), for a new t_b of 6.0 h, the new H_B is obtained simply from the ratio of the break-point times multiplied by the old H_B :

$$H_B = \frac{6.0}{3.65} (9.9) = 16.3 \text{ cm}$$

$$H_T = H_B + H_{UNB} = 16.3 + 4.1 = 20.4 \text{ cm}$$

We determine the saturation capacity of the carbon:

$$\text{Air flow rate} = (754 \text{ cm}^3/\text{s})(3600 \text{ s})(0.00115 \text{ g/cm}^3) = 3122 \text{ g air/h}$$

$$\begin{aligned} \text{Total alcohol adsorbed} &= \left(\frac{600 \text{ g alcohol}}{10^6 \text{ g air}}\right)(3122 \text{ g air/h})(5.16 \text{ h}) \\ &= 9.67 \text{ g alcohol} \end{aligned}$$

$$\begin{aligned} \text{Saturation capacity} &= 9.67 \text{ g alcohol}/79.2 \text{ g carbon} \\ &= 0.1220 \text{ g alcohol/g carbon} \end{aligned}$$

The fraction of the new bed used up to the break point is now $16.3/20.4$, or 0.799 .

In the scale-up, not only may it be necessary to change the column height, but also the actual throughput of fluid might be different from that used in the experimental laboratory unit. Since the mass velocity in the bed must remain constant for scale-up, the diameter of the bed should be adjusted to keep it constant.

Typical gas adsorption systems use heights of fixed beds of about 0.3 to 1.5 m with downflow of the gas. Low superficial gas velocities of 15–50 cm/s (0.5–1.7 ft/s) are used. Adsorbent particle sizes range from about 4 to 50 mesh (0.3 to 5 mm). Pressure drops are low, only a few inches of water per foot of bed. The adsorption time is about 0.5 h up to 8 h. For liquids the superficial velocity of the liquid in the bed is about 0.3 to 0.7 cm/s (4 to 10 gpm/ft²).

Practical bed depths usually need to be 5–10 times the length of bed of the mass-transfer zone to be economical (W1). The adsorption step usually uses downward flow in the bed. For desorption the flow is usually upward for greater efficiency (S3).

Basic Models for Predicting Adsorption

Adsorption in fixed beds is the most important method used for this process. A fixed or packed bed consists of a vertical cylindrical pipe filled or packed with the adsorbent particles. Adsorbers are mainly designed using laboratory data and the methods described in Section 12.3D. In this section, the basic equations for isothermal adsorption are described so that the fundamentals involved in this process can be better understood.

An unsteady-state solute material balance in the fluid is as follows for a section dz length of bed:

Equation 12.3-6.

$$\varepsilon \frac{\partial c}{\partial t} + (1 - \varepsilon)\rho_p \frac{\partial q}{\partial t} = -v \frac{\partial c}{\partial z} + E \frac{\partial^2 c}{\partial z^2}$$

where ε is the external void fraction of the bed; v is superficial velocity in the empty bed, m/s; ρ_p is density of particle, kg/m³; and E is an axial dispersion coefficient, m²/s. The first term represents accumulation of solute in the liquid. The second term is accumulation of solute in the solid. The third term represents the amount of solute flowing in by convection to the section dz of the bed minus that flowing out. The last term represents axial dispersion of solute in the bed, which leads to mixing of the solute and solvent.

The second differential equation needed to describe this process relates the second term of Eq. (12.3-6) for accumulation of solute in the solid to the rate of external mass transfer of the solute from the bulk solution to the particle and the diffusion and adsorption on the internal surface area. The actual physical adsorption is very rapid. The third equation is the equilibrium isotherm.

There are many solutions for these three equations which are nonlinear and coupled. These solutions frequently do not fit experimental results very well and will not be discussed here.

Processing Variables and Adsorption Cycles

Large-scale adsorption processes can be divided into two broad classes. The first and most important is the cyclic batch system, in which the adsorption fixed bed is alternately saturated and then regenerated in a cyclic manner. The second is a continuous flow system, which involves a continuous flow of adsorbent countercurrent to a flow of feed.

There are four basic methods in common use for the cyclic batch adsorption system using fixed beds. These methods differ from each other mainly in the means used to regenerate the adsorbent after the adsorption cycle. In general, these four basic methods operate with two or sometimes three fixed beds in parallel, one in the adsorption cycle and the other one or two in a desorbing cycle, to provide continuity of flow. After a bed has completed the adsorption cycle, the flow is switched to the second newly regenerated bed for adsorption. The first bed is then regenerated by any of the following methods.

1. **Temperature-swing cycle.** This is also called the thermal-swing cycle. The spent adsorption bed is regenerated by heating it with embedded stream coils or with a hot purge gas stream to remove the adsorbate. The elevation in temperature is used to shift the adsorption equilibrium curve and affect regeneration of the adsorbent. Finally, the bed must be cooled so that it can be used for adsorption in the next cycle. The time for regeneration is generally a few hours or more.
2. **Pressure-swing cycle.** In this case the bed is desorbed by reducing the pressure at essentially constant temperature and then purging the bed at this low pressure with a small fraction of the product stream. Reduction in pressure shifts the adsorption equilibrium and affects the regeneration of the adsorbent. This process for gases uses a very short cycle time for regeneration compared to that for the temperature-swing cycle.

3. **Inert-purge gas stripping cycle.** In this cycle the adsorbate is removed by passing a nonadsorbing or inert gas through the bed. This lowers the partial pressure or concentration around the particles and desorption occurs. Regeneration cycle times are usually only a few minutes.
4. **Displacement-purge cycle.** The pressure and temperature are kept essentially constant as in purge-gas stripping, but a gas or liquid is used that is adsorbed more strongly than the adsorbate and displaces the adsorbate. Again, cycle times are usually only a few minutes.

Steam stripping is often used in regeneration of solvent-recovery systems using activated-carbon adsorbent. This can be considered a combination of the temperature-swing cycle and the displacement-purge cycle.

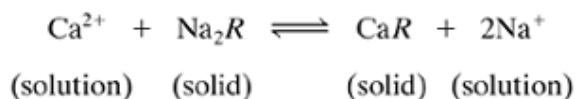
ION-EXCHANGE PROCESSES

Introduction and Ion-Exchange Materials

Ion-exchange processes are basically chemical reactions between ions in solution and ions in an insoluble solid phase. The techniques used in ion exchange so closely resemble those used in adsorption that for the majority of engineering purposes ion exchange can be considered as a special case of adsorption.

In ion exchange, certain ions are removed by the ion-exchange solid. Since electroneutrality must be maintained, the solid releases replacement ions to the solution. The first ion-exchange materials were natural-occurring porous sands called zeolites, which are cation exchangers. Positively charged ions in solution such as Ca^{2+} diffuse into the pores of the solid and exchange with the Na^+ ions in the mineral:

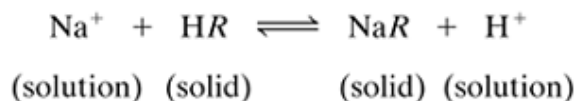
Equation 12.4-1.



where R represents the solid. This is the basis for “softening” water. To regenerate, a solution of NaCl is added, which drives the reversible reaction above to the left. Almost all of these inorganic ion-exchange solids exchange only cations.

Most present-day ion-exchange solids are synthetic resins or polymers. Certain synthetic polymeric resins contain sulfonic, carboxylic, or phenolic groups. These anionic groups can exchange cations:

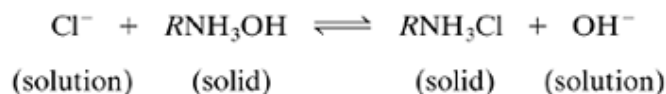
Equation 12.4-2.



Here R represents the solid resin. The Na^+ in the solid resin can be exchanged with H^+ or other cations.

Similar synthetic resins containing amine groups can be used to exchange anions and OH^- in solution:

Equation 12.4-3.



Equilibrium Relations in Ion Exchange

The ion-exchange isotherms have been developed using the law of mass action. For example, for the case of a simple ion-exchange reaction such as Eq. (12.4-2), HR and NaR represent the ion-exchange sites on the resin filled with a proton H^+ and a sodium ion Na^+ . It is assumed that all of the fixed number of sites are filled with H^+ or Na^+ . At equilibrium,

Equation 12.4-4.

$$K = \frac{[NaR][H^+]}{[Na^+][HR]}$$

Since the total concentration of the ionic groups $[\bar{R}]$ on the resin is fixed (B7),

Equation 12.4-5.

$$[\bar{R}] = \text{constant} = [NaR] + [HR]$$

Combining Eqs. (12.4-4) and (12.4-5),

Equation 12.4-6.

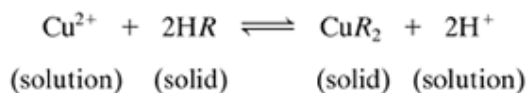
$$[NaR] = \frac{K[\bar{R}][Na^+]}{[H^+] + K[Na^+]}$$

If the solution is buffered, so that $[H^+]$ is constant, the above equation for sodium exchange or adsorption is similar to the Langmuir isotherm.

The ion-exchange process functions for strong acid or strong base exchangers by replacing the ions of a solution with ions such as H^+ or OH^- . These replaced ions from the solution are taken up by the resin. Then, to regenerate the resin, a small amount of solution with a high concentration of H^+ is used for cation exchangers or a high concentration of OH^- ions for anion exchangers. These high concentrations of H^+ or OH^- for regeneration shift the equilibrium to the left, making the regeneration process more favorable.

A typical ion-exchange process for removal of metals from solution is shown for copper cation being removed from a stream containing dilute $CuSO_4$ and H_2SO_4 :

Equation 12.4-7.



For regeneration, the bed of resin is contacted with a high concentration of H_2SO_4 to shift the equilibrium to the left.

Use of Equilibrium Relations and Relative-Molar-Selectivity Coefficients

Convenient tables for relative-molar-selectivity coefficients K have been prepared for various types of ion-exchange resins. Data are given in Table 12.4-1 for a polystyrene resin with 8% divinylbenzene (DVB) cross-linking (B8, P4) for strong-acid and strong-base resins. For cation exchangers, values are given for cation A entering the resin and displacing the cation Li^+ , and for anion exchangers, values for anion A replacing Cl^- .

Table 12.4-1. Relative-Molar-Selectivity Coefficients K for Polystyrene Cation and Anion Exchangers with 8% DVB Cross-Linking (B8, P4)

| Strong-Base Anion Exchanger (Relative to Cl^- as 1.0) | | Strong-Acid Cation Exchanger (Relative to Li^+ as 1.0) | |
|--|-----------|---|------|
| Cl^- | 1.0 | Li^+ | 1.0 |
| Iodide | 8.7 | H^+ | 1.27 |
| Nitrate | 3.8 | Na^+ | 1.98 |
| Acetate | 0.2 | NH_4^+ | 2.55 |
| Sulfate | 0.15 | K^+ | 2.90 |
| Hydroxide | 0.05–0.07 | Mg^{2+} | 3.29 |
| | | Cu^{2+} | 3.85 |
| | | Ca^{2+} | 5.16 |

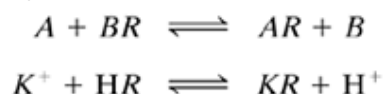
The equilibrium constant or selectivity coefficient for exchange of any two ions A and B can be approximated from Table 12.4-1 using values of K_A and K_B :

Equation 12.4-8.

$$K_{A,B} = K_A/K_B$$

For example, for the reaction of cation K^+ (A) displacing cation H^+ (B),

Equation 12.4-9.



Substituting into Eq. (12.4-8), $K_{A,B} = K_A/K_B = 2.90/1.27 = 2.28$.

For dilute solutions, activity coefficients are relatively constant and simple concentration units are used. For Eq. (12.4-9), the equilibrium constant is as follows:

Equation 12.4-10.

$$K_{A,B} = \frac{c_B q_{AR}}{c_A q_{BR}} = \frac{(c_{\text{H}^+})(q_{\text{KR}})}{(c_{\text{K}^+})(q_{\text{HR}})}$$

where, for the resin phase, concentrations q_{KR} and q_{HR} are in equivalents/L of bulk bed volume of water-swelled resin, and for the liquid phase, concentrations c_{H^+} and c_{K^+} are in equivalents/L of volume of solution.

The total concentration C in the liquid solution and the total concentration Q in the resin remain constant during the exchange process because of electroneutrality in Eq. (12.4-9). Then,

Equation 12.4-11.

$$C = c_A + c_B, \quad Q = q_{AR} + q_{BR}$$

In the case of Eq. (12.4-7), where the ion Cu^{2+} (A) replaces H^+ (B) and the charges are unequal,

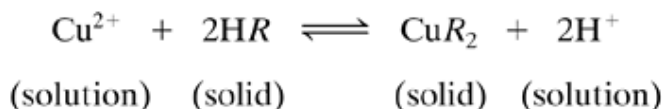
Equation 12.4-12.

$$K_{A,B} = \frac{(c_B)^2 (q_{AR_2})}{(c_A) (q_{BR})^2} = \frac{(c_{\text{H}^+})^2 (q_{\text{CuR}_2})}{(c_{\text{Cu}^{2+}}) (q_{\text{HR}})^2}$$

EXAMPLE 12.4-1. Removal of Cu^{2+} Ion from Acid Solution by an Ion-Exchange Resin

A waste acidic stream contains copper in solution which is being removed by a strong acid–cation resin. The cation Cu^{2+} (*A*) is displacing the cation H^+ (*B*) in the resin. A polystyrene resin similar to that in Table 12.4-1 is being used. The total resin capacity Q is approximately 1.9 equivalents/L of wet bed volume. For a total concentration C of 0.10 N (0.10 equivalents/L) in the solution, calculate at equilibrium the total equivalents of Cu^{2+} in the resin when the concentration of Cu^{2+} in solution is 0.02 M (0.04 N).

Solution: The known values are $C = 0.10$ N or equivalents/L of Cu^{2+} (*A*) and H^+ (*B*) in solution and $Q = 1.9$ equivalents/L of *A* and *B* in the resin. The equilibrium relation is Eq. (12.4-7):



or,



From Table 12.4-1, $K_A = K_{\text{Cu}^{2+}} = 3.85$ and $K_B = K_{\text{H}^+} = 1.27$. Then, from Eq. (12.4-8),

$$K_{A,B} = K_A/K_B = 3.85/1.27 = 3.03$$

Using Eq. (12.4-12),

$$K_{A,B} = \frac{(c_B)^2(q_{AR_2})}{(c_A)(q_{BR})^2} = \frac{(c_{\text{H}^+})^2(q_{\text{CuR}_2})}{(c_{\text{Cu}^{2+}})(q_{\text{HR}})^2}$$

From Eq. (12.4-11), $C = 0.10$ equivalents/L = $2c_{\text{Cu}^{2+}} + c_{\text{H}^+}$. Also, $Q = 1.9 = q_{\text{HR}} + 2q_{\text{CuR}_2}$. The values to substitute into Eq. (12.4-12) are $K_{A,B} = 3.03$, $q_{\text{CuR}_2} = 1.9/2 - q_{\text{HR}}/2$, $c_{\text{Cu}^{2+}} = 0.02$, and $c_{\text{H}^+} = 0.10 - 2c_{\text{Cu}^{2+}} = 0.10 - 0.04 = 0.06$.

$$3.03 = \frac{(0.06)^2(1.9/2 - q_{\text{HR}}/2)}{(0.02)(q_{\text{HR}})^2}$$

Rearranging,

$$(q_{\text{HR}})^2 + 0.02970q_{\text{HR}} - 0.05644 = 0$$

Solving this quadratic equation, $q_{\text{HR}} = 0.2232$. Then $q_{\text{CuR}_2} = 1.9/2 - 0.2232/2 = 0.8384$. Hence, the equivalents of Cu^{2+} in the resin is $2(0.8384) = 1.677$ compared to a value of 1.9 when fully loaded with copper. The result shows that the removal of Cu^{2+} from the solution by the resin is highly favored.

Concentration Profiles and Breakthrough Curves

Basic models in ion exchange

The rate of ion exchange depends on mass transfer of ions from the bulk solution to the particle surface, diffusion of the ions in the pores of the solid to the surface, exchange of the ions at the surface, and diffusion of the exchange ions back to the bulk solution. This is similar to adsorption. The differential equations derived are also very similar to those for adsorption. The design methods used for ion exchange and adsorption are similar.

Concentration profiles in packed beds

Concentration profiles in packed beds for ion exchangers are very similar to those given in Fig. 12.3-1a for adsorption. The typical S-shaped curves occur and pass through the bed. The major part of the ion exchange at any time takes place in a relatively narrow mass-transfer zone. This mass-transfer zone moves down the column. In Fig. 12.3-1b the breakthrough curve is shown, which is similar for adsorption and ion exchange.

Mass-transfer zone

As the mass-transfer zone travels down the column, the height of this zone becomes constant. This behavior is generally characteristic in cases where the ion to be removed from the feed stream has a greater affinity for the solid resin than the ion originally present in the solid. The majority of industrial ion-exchange processes fall in this category (M1). This constant height of the mass-transfer zone can then be used for scale-up, similar to adsorption scale-up.

Capacity of Columns and Scale-Up Design Method

Capacity of column

The design method for fixed-bed ion exchangers is quite similar to that used for adsorption processes. Theoretical predictions of concentration profiles, the mass-transfer zone, and mass transfer may be inaccurate because of uncertainties due to flow patterns, and so forth. Hence, experiments using small packed-bed laboratory-scale columns are needed for scale-up.

The total stoichiometric capacity of the packed bed is the total shaded area in the breakthrough curve in Fig. 12.3-2. The time t_t is the time equivalent to the total capacity:

Equation 12.3-1.

$$t_t = \int_0^{\infty} (1 - c/c_o) dt$$

The usable capacity up to the break-point time t_b is the cross-hatched area from $t = 0$ to t_b . Then t_u , the time equivalent to the usable capacity, is

Equation 12.3-2.

$$t_u = \int_0^{t_b} (1 - c/c_o) dt$$

Numerical integration of Eqs. (12.3-1) and (12.3-2) can also be done using spreadsheets. Then the fraction of the total bed length or capacity utilized up to the break point is t_u/t_t . For a total bed length of H_T m, H_B is the length of the bed used up to the break point:

Equation 12.3-3.

$$H_B = (t_u/t_i)H_T$$

The length of the mass-transfer section or unused bed H_{UNB} in m is then

Equation 12.3-4.

$$H_{UNB} = (1 - t_u/t_i)H_T$$

This H_{UNB} is essentially independent of the total column length. The experimental value of H_{UNB} is measured at the desired velocity in a small-diameter laboratory column. To design the full-scale column, the length of the bed H_B is calculated to achieve the desired capacity at the break point. Then the total column length is

Equation 12.3-5.

$$H_T = H_{UNB} + H_B$$

The mass velocity of both the laboratory- and full-scale columns must be the same. The diameter of the large-scale column is calculated using the same given mass velocity.

Typical process variables

Some typical operating process variables are as follows. The laboratory column should be at least 2.5 cm in diameter and 0.3 m in length. Liquid flow rates commercially (W1) can be from 1 to 12 gpm/ft² (0.041–0.489 m/min) but are usually 6–8 gpm/ft² (0.244–0.326 m/min). Commercial columns are usually 1–3 m in height. Usually a freeboard of 50% or more open space is needed to accommodate bed expansion when regenerant flow is upward.

The resin gel can swell due to exchange by about 10 to 20%. Particle sizes used range from 0.2 mm to 1.0 mm. Typical moisture contents of the resins vary from 50 to 70%. The equilibrium exchange capacities of strong-acid or -base exchange resins are typically 3–5 meq/g of dry resin and 1–2 meq/ml of wet resin bed.

Regeneration flow rates are typically quite low, in the range of 0.5 to 5.0 bed volumes/h, in order to attain equilibrium while using minimum amounts of solution (W1). A bed volume is the total volume of the packed bed of resin as calculated from the column diameter and height of the packed bed.

Pressure drop can be predicted by using the equations for flow in packed beds. Typical pressure drops for beds are about 0.6 to 0.9 psi/ft height (13.6–20.4 kPa/m height) for flow rates of 6 to 8 gpm/ft². Excessive pressure drops should be avoided, since the gel-resin particles can be deformed.

A useful method for correlating experimental breakthrough curves at different flow velocities and the mass-transfer zone is as follows: Instead of plotting dC_o versus time t , as in Fig. 12.3-1b, a plot of dC_o versus the number of bed volumes (BV) is made. Data for different flow velocities will then tend to fall on the same curve.

Operating cycles

The operating cycles for ion-exchange processes in a packed bed are more complicated than those for gas adsorption. These usually consist of the following four steps, with experimental data usually needed to define each operating time (S3, W1). (1) Downflow loading of the process feed for a proper time. At the end of loading, the bed voids are filled with feed solution. (2) Displacement of the feed solution with upward flow of the regeneration solution. Thus, displacement of the occluded feed solution first occurs as a wave front. (3) Regeneration of the bed with continued upward flow of the regeneration solution. This occurs as a second wavefront. (4) Rinse upward to remove occluded regenerant from the bed. A rinse can be used instead of step (2) for recovering possibly valuable occluded process solution (W1).

For the actual design and for continuous feed flow, at least two columns are needed, so that one column is used to process the feed while the other is used for regeneration. When breakthrough occurs, the towers are switched. The total number of beds depends on the loading and regeneration times. Alternatively, a three-column system can be used for better utilization of the columns. The feed enters column 2 and then column 3 in series while column 1 is being regenerated. When breakthrough occurs in column 3, column 2 is removed for regeneration. The feed is then rerouted and goes to column 3 and then to column 1.

SINGLE-STAGE LIQUID–LIQUID EXTRACTION PROCESSES

Introduction to Extraction Processes

In order to separate one or more of the components in a mixture, the mixture is brought into contact with another phase. The two-phase pair can be gas–liquid, which was discussed in Chapter 10; vapor–liquid, which was covered in Chapter 11; liquid–liquid; or fluid–solid. In this section *liquid–liquid extraction separation processes* are considered first. Alternative terms for the same process are *liquid extraction* or *solvent extraction*.

In distillation, the liquid is partially vaporized to create another phase, which is a vapor. The separation of the components depends on the relative vapor pressures of the substances. The vapor and liquid phases are similar chemically. In liquid–liquid extraction, the two phases are chemically quite different, which leads to a separation of the components according to physical and chemical properties.

Solvent extraction can sometimes be used as an alternative to separation by distillation or evaporation. For example, acetic acid can be removed from water by distillation or by solvent extraction using an organic solvent. The resulting organic solvent–acetic acid solution is then distilled. Choice of distillation or solvent extraction would depend on relative costs (C7). In another example, high-molecular-weight fatty acids can be separated from vegetable oils by extraction with liquid propane or by high-vacuum distillation, which is more expensive.

In the pharmaceutical industry, products such as penicillin occur in fermentation mixtures that are quite complex, and liquid extraction can be used to separate the penicillin. Many metal separations are being done commercially by extraction of aqueous solutions, such as copper–iron, uranium–vanadium, and tantalum–columbium.

Equilibrium Relations in Extraction

Phase rule

Generally in a liquid–liquid system we have three components, A , B , and C , and two phases in equilibrium. Substituting into the phase rule, Eq. (10.2-1), the number of degrees of freedom is 3. The variables are temperature, pressure, and four concentrations. Four concentrations occur because only two of the three mass-fraction concentrations in a phase can be specified. The third must make the total mass fractions equal to 1.0: $x_A + x_B + x_C = 1.0$. If pressure and temperature are set, which is the usual case, then, at equilibrium, setting one concentration in either phase fixes the system.

Triangular coordinates and equilibrium data

Equilateral triangular coordinates are often used to represent the equilibrium data for a three-component system, since there are three axes. This is shown in Fig. 12.5-1. Each of the three corners represents a pure component, A , B , or C . The point M represents a mixture of A , B , and C . The perpendicular distance from the point M to the base AB represents the mass fraction x_C of C in the mixture at M , the distance to base CB the mass fraction x_A of A , and the distance to base AC the mass fraction x_B of B . Thus,

Equation 12.5-1.

$$x_A + x_B + x_C = 0.40 + 0.20 + 0.40 = 1.0$$

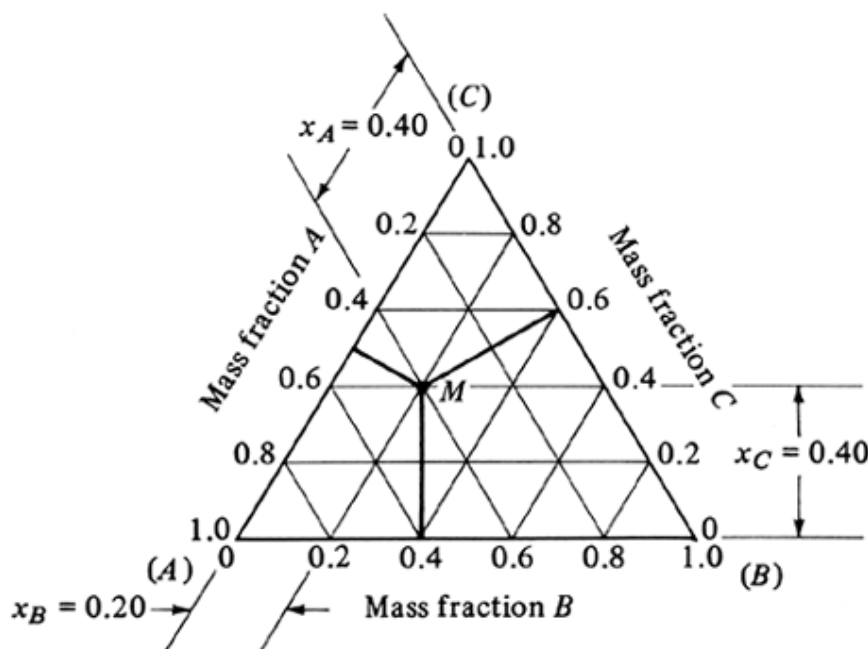


Figure 12.5-1. Coordinates for a triangular diagram.

A common phase diagram where a pair of components A and B are partially miscible is shown in Fig. 12.5-2. Typical examples are methyl isobutyl ketone (A)–water (B)–acetone (C), water (A)–chloroform (B)–acetone (C), and benzene (A)–water (B)–acetic acid (C). Referring to Fig. 12.5-2, liquid C dissolves completely in A or in B . Liquid A is only slightly soluble in B and B slightly soluble in A . The two-phase region is included inside below the curved envelope. An original mixture of composition M will separate into two phases a and b which are on the equilibrium tie line through point M . Other tie lines are also shown. The two phases are identical at point P , the *Plait point*.

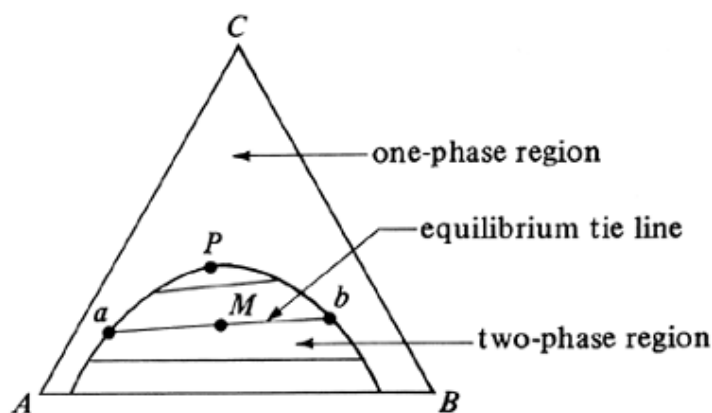


Figure 12.5-2. Liquid–liquid phase diagram where components A and B are partially miscible.

Equilibrium data on rectangular coordinates

Since triangular diagrams have some disadvantages due to the special coordinates, a more useful method of plotting the three-component data is to use rectangular coordinates. This is shown in Fig. 12.5-3 for the system acetic acid (A)–water (B)–isopropyl ether solvent (C). Data for this system are from Appendix A.3. The solvent pair B and C are partially miscible. The concentration of component C is plotted on the vertical axis and that of A on the horizontal axis. The concentration of component B is obtained by difference from Eq. (12.5-2) or (12.5-3):

Equation 12.5-2.

$$x_B = 1.0 - x_A - x_C$$

Equation 12.5-3.

$$y_B = 1.0 - y_A - y_C$$

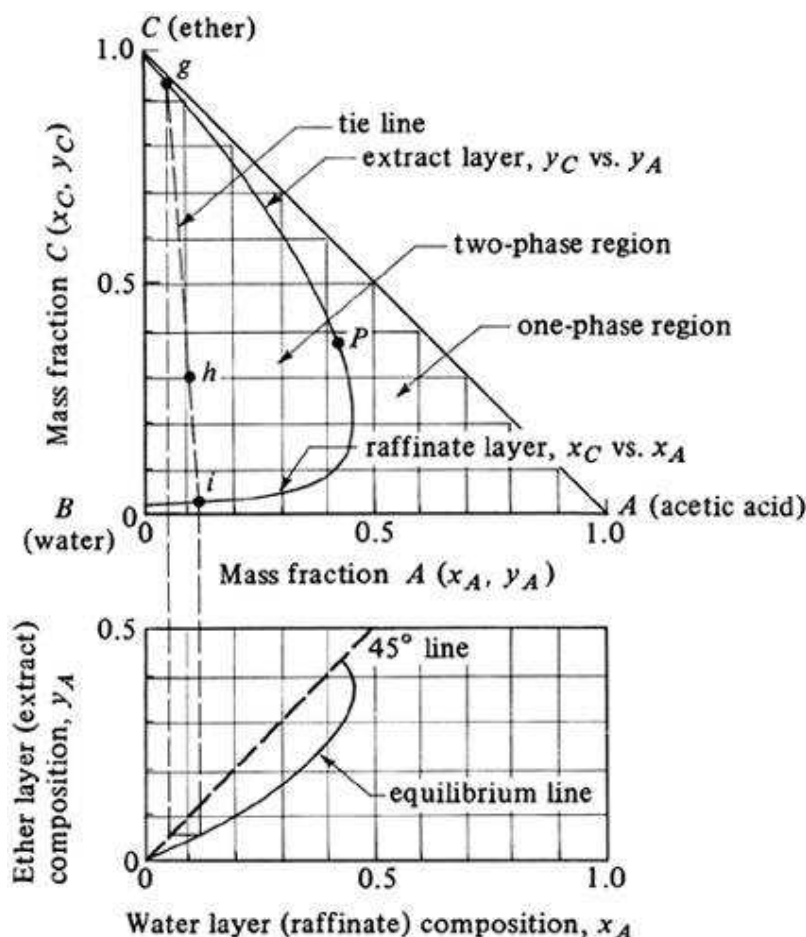


Figure 12.5-3. Acetic acid (A)–water (B)–isopropyl ether (C) liquid–liquid phase diagram at 293 K (20°C).

The two-phase region in Fig. 12.5-3 is inside the envelope and the one-phase region outside. A tie line gi is shown connecting the water-rich layer i , called the *raffinate layer*, and the ether-rich solvent layer g , called the *extract layer*. The raffinate composition is designated by x and the extract by y . Hence, the mass fraction of C is designated as y_C in the extract layer and as x_C in the raffinate layer. To construct the tie line gi using the equilibrium $y_A - x_A$ plot below the phase diagram, vertical lines to g and i are drawn.

EXAMPLE 12.5-1. Material Balance for Equilibrium Layers

An original mixture weighing 100 kg and containing 30 kg of isopropyl ether (C), 10 kg of acetic acid (A), and 60 kg water (B) is equilibrated and the equilibrium phases separated. What are the compositions of the two equilibrium phases?

Solution: The composition of the original mixture is $x_C = 0.30$, $x_A = 0.10$, and $x_B = 0.60$. This composition of $x_C = 0.30$ and $x_A = 0.10$ is plotted as point h on Fig. 12.5-3. The tie line gi is drawn through point h by trial and error. The composition of the extract (ether) layer at g is $y_A = 0.04$, $y_C = 0.94$, and $y_B = 1.00 - 0.04 - 0.94 = 0.02$ mass fraction. The raffinate (water)-layer composition at i is $x_A = 0.12$, $x_C = 0.02$, and $x_B = 1.00 - 0.12 - 0.02 = 0.86$.

Another common type of phase diagram is shown in Fig. 12.5-4, where the solvent pairs B and C and A and C are partially miscible. Examples are the system styrene (A)–ethylbenzene (B)–diethylene glycol (C) and the system chlorobenzene (A)–methyl ethyl ketone (B)–water (C).

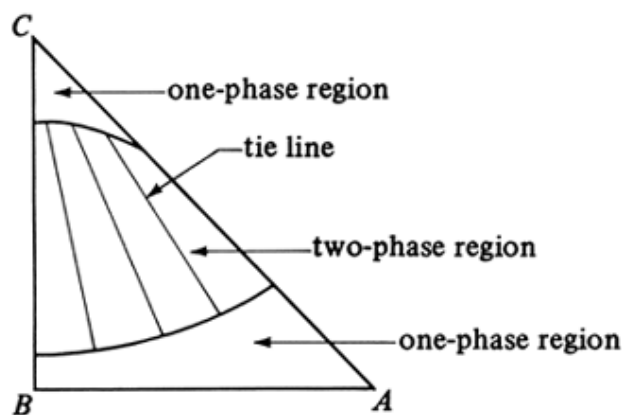


Figure 12.5-4. Phase diagram where the solvent pairs B–C and A–C are partially miscible.

Single-Stage Equilibrium Extraction

Derivation of lever-arm rule for graphical addition

This will be derived for use with the rectangular extraction-phase-diagram charts. In Fig. 12.5-5a two streams, L kg and V kg, containing components A , B , and C , are mixed (added) to give a resulting mixture stream M kg total mass. Writing an overall mass balance and a balance on A ,

Equation 12.5-4.

$$V + L = M$$

Equation 12.5-5.

$$Vy_A + Lx_A = Mx_{AM}$$

where x_{AM} is the mass fraction of A in the M stream. Writing a balance for component C ,

Equation 12.5-6.

$$Vy_C + Lx_C = Mx_{CM}$$

Combining Eqs. (12.5-4) and (12.5-5),

Equation 12.5-7.

$$\frac{L}{V} = \frac{y_A - x_{AM}}{x_{AM} - x_A}$$

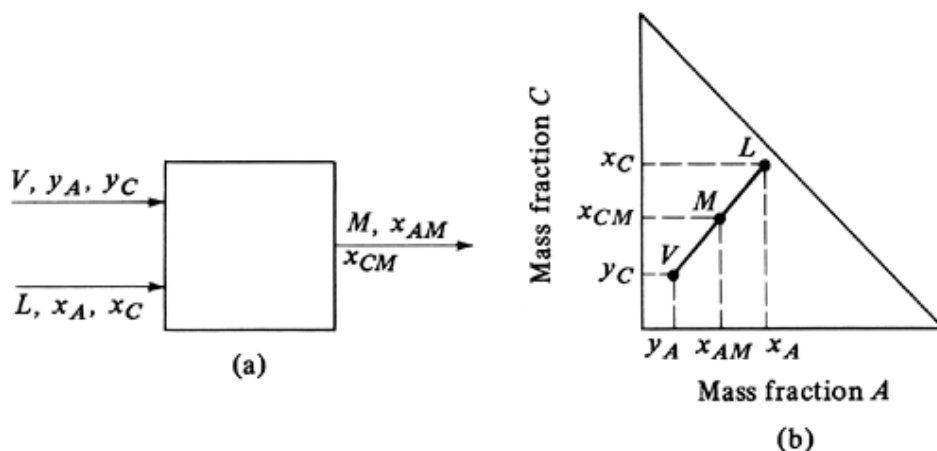


Figure 12.5-5. Graphical addition and lever-arm rule: (a) process flow, (b) graphical addition.

Combining Eqs. (12.5-4) and (12.5-6),

Equation 12.5-8.

$$\frac{L}{V} = \frac{y_C - x_{CM}}{x_{CM} - y_C}$$

Equating Eqs. (12.5-7) and (12.5-8) and rearranging,

Equation 12.5-9.

$$\frac{x_C - x_{CM}}{x_A - x_{AM}} = \frac{x_{CM} - y_C}{x_{AM} - y_A}$$

This shows that points L , M , and V must lie on a straight line. By using the properties of similar right triangles,

Equation 12.5-10.

$$\frac{L \text{ (kg)}}{V \text{ (kg)}} = \frac{\overline{VM}}{\overline{LM}}$$

This is the lever-arm rule, which states that $\text{kg } L/\text{kg } V$ is equal to the length of line \overline{VM} /length of line \overline{LM} . Also,

Equation 12.5-11.

$$\frac{L \text{ (kg)}}{M \text{ (kg)}} = \frac{\overline{VM}}{\overline{LV}}$$

These same equations also hold for kg mol and mol frac , lb_m , and so on.

EXAMPLE 12.5-2. Amounts of Phases in Solvent Extraction

The compositions of the two equilibrium layers in Example 12.5-1 are for the extract layer (V), $y_A = 0.04$, $y_B = 0.02$, and $y_C = 0.94$, and for the raffinate layer (L), $x_A = 0.12$, $x_B = 0.86$, and $x_C = 0.02$. The original mixture contained 100 kg and $x_{AM} = 0.10$. Determine the amounts of V and L .

Solution: Substituting into Eq. (12.5-4),

$$V + L = M = 100$$

Substituting into Eq. (12.5-5), where $M = 100$ kg and $x_{AM} = 0.10$,

$$V(0.04) + L(0.12) = 100(0.10)$$

Solving the two equations simultaneously, $L = 75.0$ and $V = 25.0$. Alternatively, using the lever-arm rule, the distance hg in Fig. 12.5-3 is measured as 4.2 units and gi as 5.8 units. Then, by Eq. (12.5-11),

$$\frac{L}{M} = \frac{L}{100} = \frac{\overline{hg}}{\overline{gi}} = \frac{4.2}{5.8}$$

Solving, $L = 72.5$ kg and $V = 27.5$ kg, which is in reasonably close agreement with the material-balance method.

Single-stage equilibrium extraction

We now study the separation of A from a mixture of A and B by a solvent C in a single equilibrium stage. The process is shown in Fig. 12.5-6a, where the solvent, as stream V_2 , enters together with the stream L_0 . The streams are mixed and equilibrated and the exit streams L_1 and V_1 leave in equilibrium with each other.

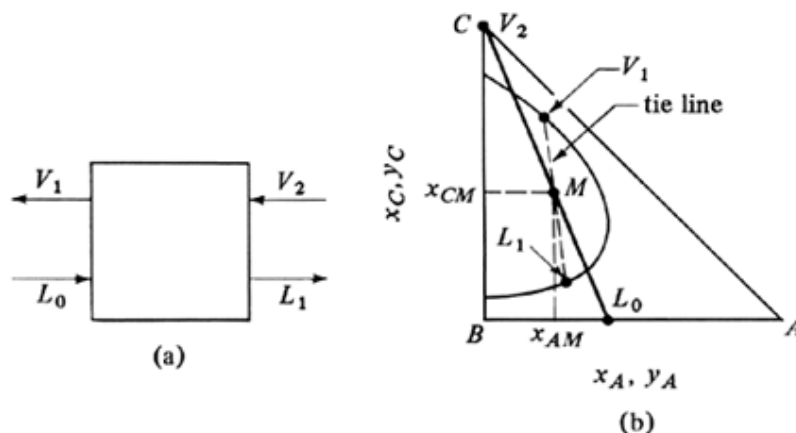


Figure 12.5-6. Single-stage equilibrium liquid–liquid extraction: (a) process flow diagram, (b) plot on phase diagram.

The equations for this process are the same as those given in Section 10.3 for a single equilibrium stage, where y represents the composition of the V streams and x the L streams:

Equation 12.5-12.

$$L_0 + V_2 = L_1 + V_1 = M$$

Equation 12.5-13.

$$L_0 x_{A0} + V_2 y_{A2} = L_1 x_{A1} + V_1 y_{A1} = M x_{AM}$$

Equation 12.5-14.

$$L_0 x_{C0} + V_2 y_{C2} = L_1 x_{C1} + V_1 y_{C1} = M x_{CM}$$

Since $x_A + x_B + x_C = 1.0$, an equation for B is not needed. To solve the three equations, the equilibrium-phase diagram in Fig. 12.5-6b is used. Since the amounts and compositions of L_0 and V_2 are known, we can calculate values of M , x_{AM} , and x_{CM} from Eqs. (12.5-12)–(12.5-14). The points L_0 , V_2 , and M can be plotted as shown in Fig. 12.5-6b. Then, using trial and error, a tie line is drawn through point M , which locates the compositions of L_1 and V_1 . The amounts of L_1 and V_1 can be determined by substitution into Eqs. (12.5-12)–(12.5-14) or by using the lever-arm rule.

TYPES OF EQUIPMENT AND DESIGN FOR LIQUID–LIQUID EXTRACTION

Introduction and Equipment Types

As in the separation processes of absorption and distillation, the two phases in liquid–liquid extraction must be brought into intimate contact with a high degree of turbulence in order to obtain high mass-transfer rates. After this contact of the two phases, they must be separated. In both absorption and distillation, this separation is rapid and easy because of the large difference in density between the gas or vapor phase and the liquid phase. In solvent extraction, the density difference between the two phases is not large and separation is more difficult.

There are two main classes of solvent-extraction equipment, vessels in which mechanical agitation is provided for mixing, and vessels in which the mixing is done by the flow of the fluids themselves. The extraction equipment can be operated batchwise or continuously as in absorption and in distillation.

Mixer–Settlers for Extraction

To provide efficient mass transfer, a mechanical mixer is often used to provide intimate contact between the two liquid phases. One phase is usually dispersed into the other in the form of small droplets. Sufficient time of contact should be provided for the extraction to take place. Small droplets produce large interfacial areas and faster extraction. However, the droplets must not be so small that the subsequent settling time in the settler is too large.

The design and power requirements for baffled agitators or mixers have been discussed in detail in Section 3.4. In Fig. 12.6-1a a typical mixer–settler is shown, where the mixer or agitator is entirely separate from the settler. The feed of aqueous phase and organic phase are mixed in the mixer, and then the mixed phases are separated in the settler. In Fig. 12.6-1b a combined mixer–settler is shown, which is sometimes used in the extraction of uranium salts or copper salts from aqueous solutions. Both types of mixer–settlers can be used in series for countercurrent or multiple-stage extraction. Typical stage efficiencies for a mixer–settler are 75–100%.

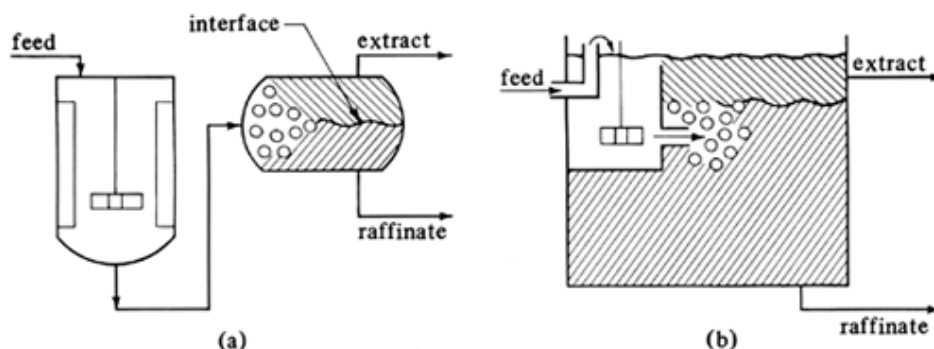


Figure 12.6-1. Typical mixer–settlers for extraction: (a) separate mixer–settler, (b) combined mixer–settler.

Spray Extraction Towers

Packed and spray-tower extractors give differential contact, where mixing and settling proceed continuously and simultaneously (C8). In the plate-type towers or mixer–settler contactors, the extraction and settling proceeds in discrete stages. In Fig. 12.6-2 the heavy liquid enters at the top of the spray tower, fills the tower as the continuous phase, and flows out through the bottom. The light liquid enters through a nozzle distributor at the bottom, which disperses or sprays the droplets upward. The light liquid coalesces at the top and flows out. In some cases the heavy liquid is sprayed downward into a rising, light continuous phase.

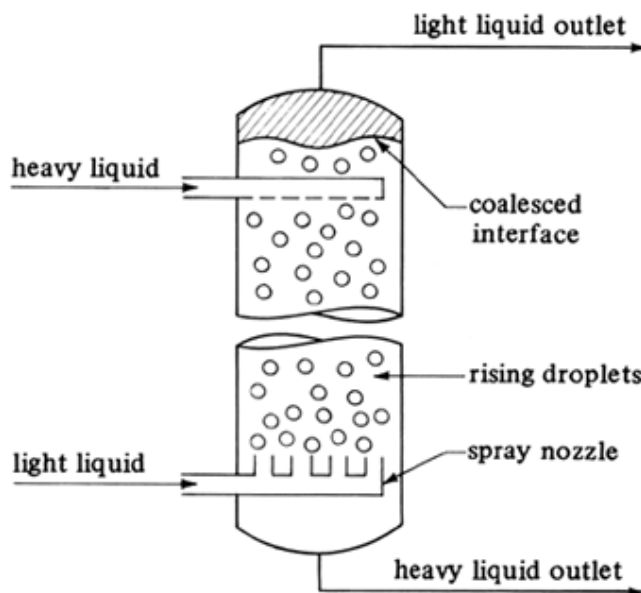


Figure 12.6-2. Spray-type extraction tower.

The spray tower has a very large axial dispersion (back-mixing) in the continuous phase. Hence, only one or two stages are usually present in such a tower. Typical performance parameters for a spray tower are given in Table 12.6-1. Despite its very low cost, this type of tower is rarely used. It can be used when a rapid, irreversible chemical reaction occurs, as in neutralization of waste acids (W1).

Table 12.6-1. Typical Performance for Several Types of Commercial Extraction Towers

| Type | Capacity of Combined Streams, $(V_D + V_C), \text{m}^3/\text{m}^2 \cdot \text{h}$ | Approximate Flooding, $(V_D + V_C), \text{m}^3/\text{m}^2 \cdot \text{h}$ | Spacing between Stages, T, cm | Overall Height of Transfer Unit, H_{OL}, m | Plate Efficiency, $E_O, \%$ | Height of Equilibrium Stage, HETS, m | Ref. |
|--------------------------|---|---|--|---|-----------------------------|---|------------|
| Spray Tower | 15–75 | | | 3–6 | | 3–6 | M4, S5 |
| Packed Tower | 12–30 | | | 0.9–1.7 | | 0.4–1.5 | S4, S5, W1 |
| Structured Packing Tower | 65–90 | | | | | 0.5–1.6 | H4 |
| Sieve-Tray Tower | 27–60 | | 10–25 | | 8–30 | 0.8–1.2 | M4, P4, S4 |

| Type | Capacity of Combined Streams, $(V_D + V_C)$, $m^3/m^2 \circ h$ | Approximate Flooding, $(V_D + V_C)$, $m^3/m^2 \circ h$ | Spacing between Stages, T , cm | Overall Height of Transfer Unit, H_{OL} , m | Plate Efficiency, E_O , % | Height of Equilibrium Stage, HETS, m | Ref. |
|-------------------------|---|---|----------------------------------|---|-----------------------------|--------------------------------------|----------------|
| Pulsed Packed Tower | 17–23 | 40 | | | | 0.15–0.3 | P4, S4, W1 |
| Pulsed Sieve Tray Tower | 25–35 | 60 | 5.1 | | | 0.15–0.3 | S4, W1 |
| Scheibel Tower | 10–14* | 40 | 2.5–20 | | | 0.1–0.3 | P4, S2, S3, W1 |
| Karr Tower | 30–40 | 80–100 | 5–15 | | | 0.2–0.6 | S2, S4 |

*Throughput for diameter $D_1 = 7.6$ cm. For larger towers of D_2 diameter see Eq. (12.6-3).

Packed Extraction Towers

A more effective type of tower is made by packing the column with random packing such as Raschig rings, Berl saddles, Pall rings, and so on, which cause the droplets to coalesce and redisperse at frequent intervals throughout the tower. The axial mixing is reduced considerably. A packed tower is more efficient than a spray tower, but back-mixing still occurs and the HETS (height equivalent to a theoretical stage) is generally greater than for the pulsed and mechanically agitated towers discussed later in Sections 12.6F and G.

Packed towers are used where only a few stages are needed (S3) and generally with low-interfacial-tension systems of about 10 dyn/cm or so (W1). When using random packings, it is preferable to choose a material that is preferentially wetted by the continuous phase. For example, stoneware Raschig rings or Berl saddles are used for water as the continuous phase and carbon rings or saddles for toluene as the continuous phase (T2). Packed towers more often use random packing and less often structured packing. Some typical performance values for packed towers are given in Table 12.6-1.

The few data available for structured packing have similar HETS values as packed or sieve-tray towers but give higher capacities (H4). The structured packings used for extraction are similar to those used for distillation.

In packed absorption towers, flooding occurs when the gas velocity is increased until the liquid cannot flow downward and is carried up by the gas out of the tower. In packed liquid-extraction towers, flooding occurs when increasing the dispersed or continuous flow rates causes both phases to leave at the outlet of the continuous phase.

A *flooding correlation* by Crawford and Wilke (C9) is given in Fig. 12.6-3, where V_C and V_D are superficial velocities of continuous and dispersed phases in ft/h, ρ_C and ρ_D are densities of continuous and dispersed phases in lb_m/ft^3 , $\Delta\rho$ is $|\rho_C - \rho_D|$, μ_c is viscosity of continuous phase in $lb_m/ft \cdot h$, a is specific surface area of packing in ft^2/ft^3 (Table 10.6-1), ε is void fraction of packed section (Table 10.6-1), and σ is interfacial tension between phases in lb_m/h^2 . Note: 1.0 dyn/cm = 28 572 lb_m/h^2 . It is recommended that the design flow rates be set at 50% of flooding due to uncertainties in the correlation.

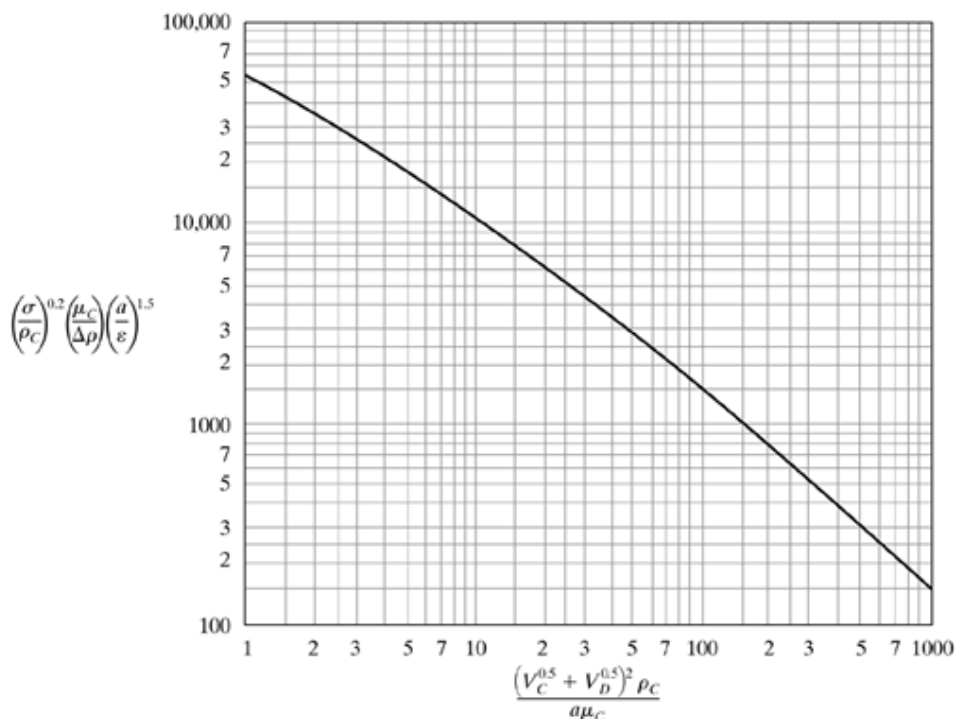


Figure 12.6-3. Flooding correlation for packed extraction towers. [From J. W. Crawford and C. R. Wilke, *Chem. Eng. Prog.*, 47, 423 (1951). With permission.]

EXAMPLE 12.6.1. Prediction of Flooding and Packed-Tower Diameter

Toluene as the dispersed phase is being used to extract diethylamine from a dilute water solution in a packed tower of 1-in. Pall rings at 26.7°C. The flow rate of toluene $V = 84 \text{ ft}^3/\text{h}$ and of water solution $L = 56 \text{ ft}^3/\text{h}$. The physical properties of the dilute solutions are: for the aqueous continuous phase (C), $\rho_C = 62.2 \text{ lb}_m/\text{ft}^3$, $\mu_C = 0.860 \text{ cp} = 0.860(2.4191) = 2.080 \text{ lb}_m/\text{ft} \cdot \text{h}$; for the dispersed phase, $\rho_D = 54.0 \text{ lb}_m/\text{ft}^3$. The interfacial tension $\sigma = 25 \text{ dyn/cm}$ (T2). Do as follows:

- Predict the flooding velocity.
- Using 50% of flooding, determine the tower diameter.
- If the separation requires 5.0 theoretical stages, calculate the tower height.

Solution: For part (a), from Table 10.6-1 for 1-in. Pall rings, the surface area $a = 63 \text{ ft}^2/\text{ft}^3$ and $\epsilon = 0.94$ void fraction. Also, $\sigma = (25 \text{ dyn/cm})(28\,572 \text{ lb}_m/\text{h}^2)/(\text{dyn/cm}) = 714\,300 \text{ lb}_m/\text{h}^2$. Then, for the ordinate in Fig. 12.6-3,

$$\left(\frac{\sigma}{\rho_C}\right)^{0.2} \left(\frac{\mu_C}{\Delta\rho}\right) \left(\frac{a}{\epsilon}\right)^{1.5} = \left(\frac{714\,300}{62.2}\right)^{0.2} \left(\frac{2.080}{62.2 - 54.0}\right) \left(\frac{63}{0.94}\right)^{1.5} = 902.8$$

From Fig. 12.6-3, the abscissa value is 170. Hence,

$$170 = \frac{(V_C^{0.5} + V_D^{0.5})^2 \rho_C}{a \mu_C} = \frac{(V_C^{0.5} + V_D^{0.5})^2 (62.2)}{(63)(2.080)}$$

Solving, $(V_C^{0.5} + V_D^{0.5}) = 18.92$. Also, since $V_D/V_C = V/L = 84/56 = 1.5$, the final result gives $V_D = 108.45 \text{ ft}^3/\text{h}$ and $V_C = 72.30 \text{ ft}^3/\text{h}$ for the flooding velocity.

For part (b), using 50% of flooding, $V_D = 54.2$, $V_C = 36.15$ ft/h, and $V_C + V_D = 90.35$ ft/h = $90.35/3.2808 = 27.54$ m/h. This is still in the typical range given for packed towers in Table 12.6-1 of 12–30 m/h.

The tower cross-sectional area = $L/V_C = (56 \text{ ft}^3/\text{h})/(36.15 \text{ ft/h}) = 1.549 \text{ ft}^2$. Then, $\pi D^2/4 = 1.549$ and $D = 1.404$ ft (0.428 m).

For part (c), use the average HETS for packed towers from Table 12.6-1 of $(0.4 + 1.5)/2$, or 0.95 m (3.117 ft). Then the tower height is (HETS ft/stage) (number of stages) or $3.117(5.0) = 15.58$ ft (4.75 m). Adding about 2 ft to the top and bottom for inlet nozzles and settling zones, the total height = $15.58 + 2 + 2 = 19.58$ ft (5.97 m).

To use Fig. 12.6-3, the value of the interfacial tension σ is needed. This is a very important variable for extraction and can vary from about 5 to 50 dyn/cm. The interfacial tension between immiscible phases that must be settled must be sufficiently high for rapid coalescence. Also, high values of σ mean that often extra energy or agitation must be used in the tower for dispersion of one phase in the other. However, too low a value may result in too-slow coalescence or stable emulsions.

To estimate the *interfacial tension* of a two-phase system when experimental data are not available, Eq. (12.6-1) can be used for type one ternary systems, with an average deviation of about $\pm 15\%$ (T2):

Equation 12.6-1.

$$\sigma = -7.34 \ln[x_{AB} + x_{BA} + (x_{CA} + x_{CB})/2] - 4.90$$

where σ is the interfacial tension in dyn/cm, x_{AB} is the mole fraction of solvent *A* in the saturated solvent-rich *B* layer, x_{BA} is the mole fraction of *B* in the saturated solvent-rich *A* layer, x_{CA} is the mole fraction of the distributed solute *C* in *A*, and x_{CB} is the mole fraction of solute *C* in *B*. This equation holds only for a range of values for $[x_{AB} + x_{BA} + (x_{CA} + x_{CB})/2]$ between 0.0004 and 0.30. A value of 1.0 indicates complete solution of the phases at the plait point. The range of σ values is 4–52.5 dyn/cm.

EXAMPLE 12.6-2. Estimation of Interfacial Tension

Equilibrium data for the system water (*A*)–acetic acid (*C*)–methylisobutyl ketone (MIBK) (*B*) are as follows in wt %, where the acetic acid concentration is dilute (P4):

| Water-rich (<i>A</i>) phase | | | MIBK-rich (<i>B</i>) phase | | |
|-------------------------------|-------------------|-------------------|------------------------------|-------------------|-------------------|
| Water (<i>A</i>) | Acid (<i>B</i>) | MIBK (<i>C</i>) | Water (<i>A</i>) | Acid (<i>C</i>) | MIBK (<i>B</i>) |
| 98.45 | 0 | 1.55 | 2.12 | 0 | 97.88 |
| 95.46 | 2.85 | 1.7 | 2.80 | 1.87 | 95.33 |

Estimate the interfacial tension for the data point containing some acetic acid.

Solution: The molecular weight for *A* is 18.02, for *B* is 100.16, and for *C* is 60.05. Converting 1.7 wt % (*B*) to mole fraction x_{BA} in the (*A*)-rich layer,

$$x_{BA} = \frac{1.7/100.16}{95.46/18.02 + 2.85/60.05 + 1.7/100.16} = 0.003163$$

Also, 2.85 wt % (*C*) in the (*A*)-rich layer becomes $x_{CA} = 0.00885$. Similarly, 2.80 wt % (*C*) becomes $x_{AB} = 0.1365$, and 1.87 wt % (*C*) becomes $x_{CB} = 0.02736$.

Substituting into Eq. (12.6-1),

$$\begin{aligned}\sigma &= -7.34 \ln[0.1365 + 0.003163 + (0.00885 + 0.02736)/2] - 4.90 \\ &= 8.65 \text{ dyn/cm}\end{aligned}$$

For the binary liquid system, water (A)–MIBK (B), the calculated mole fractions are $x_{BA} = 0.002825$ and $x_{AB} = 0.1074$. Then using Eq. (12.6-1), $\sigma = 11.49$ dyn/cm.

Perforated-Plate (Sieve-Tray) Extraction Towers

Perforated plates or sieve trays are also used for dispersion of liquid drops and coalescence on each tray, as shown in Fig. 12.6-4. This is similar to the sieve trays described in Fig. 10.6-1a for distillation and absorption. The downcomers carry the heavier continuous liquid phase from one tray to the next. The light dispersed phase coalesces below the tray, jets up to the tray above, and then coalesces on the tray above. Overflow weirs are not used on downcomers (S3).

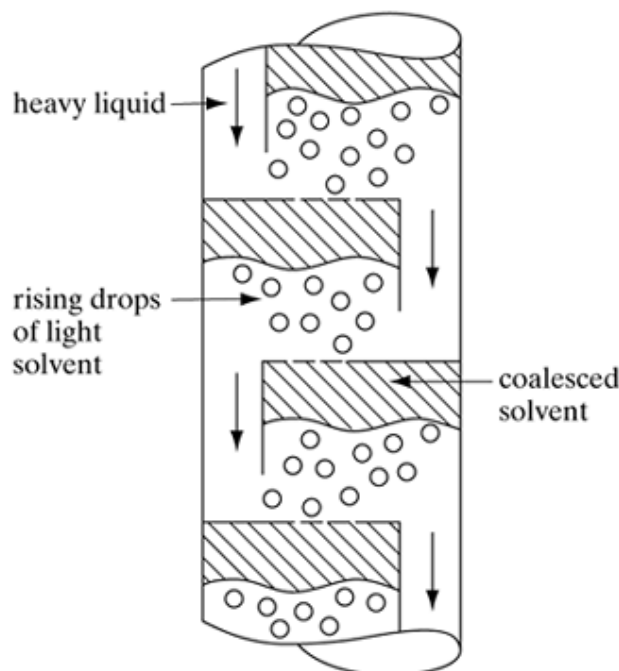


Figure 12.6-4. Perforated-plate or sieve-tray extraction tower.

The holes in the tray are 0.32–0.64 cm in diameter, and the % of open tray area is 15–25% of the column cross-sectional area. Tray spacings of 10–25 cm are used.

The following equation can be used to estimate the fractional tray efficiency E_o in a tray tower (P4):

Equation 12.6-2.

$$E_o = \frac{0.352T^{0.5}}{\sigma d_o^{0.35}} (V_D/V_C)^{0.42}$$

where σ is interfacial tension in dyn/cm, T is tray spacing in ft, d_o is hole diameter in ft, and V_D and V_C are superficial velocities in ft/s. For systems with high interfacial tensions, heights of transfer units are relatively high and stage efficiencies low.

Some typical operating conditions in tray towers are given in Table 12.6-1. To scale-up towers from small to larger sizes, the same sum of superficial velocities $V_C + V_D$ should be used (S3). A throughput design value of about 50% of flooding also should be used for all types of extraction towers.

EXAMPLE 12.6-3. Tray Efficiency for Perforated-Plate Tower

Acetic acid is being extracted from water by the solvent methylisobutyl ketone in a perforated-plate tower at 25°C. The flow rate of the continuous aqueous phase is 120 ft³/h and that of the dispersed solvent phase is 240 ft³/h. The interfacial tension is 9.1 dyn/cm. The tray spacing is 1.0 ft and the hole size on the tray is 0.25 in. Estimate the fraction tray efficiency E_o .

Solution: $V_D/V_C = 240/120$, $\sigma = 9.1$ dyn/cm, $T = 1.0$ ft, and $d_o = 0.25/12 = 0.02083$ ft. Substituting into Eq. (12.6-2),

$$E_o = \frac{0.352T^{0.5}(V_D/V_C)^{0.42}}{\sigma d_o^{0.35}} = \frac{0.35(1.0)^{0.5}(240/120)^{0.42}}{9.1(0.02083)^{0.35}}$$

$$E_o = 0.201$$

Pulsed Packed and Sieve-Tray Towers

There are many types of towers that are mechanically agitated to increase the mass-transfer efficiency and/or the throughput. An ordinary packed tower or one with special sieve plates can be pulsed by applying a rapid reciprocating motion of relatively short amplitude to the liquid contents. A reciprocating plunger pump, bellows pump, or high-pressure air pulse is externally connected to the space containing the continuous fluid so that the entire contents of the tower move up or down. Continuous inlet flows of continuous and dispersed phases enter and exit the tower.

Pulsed packed towers

Pulsing packed towers reduces the HETS considerably, by about a factor of 2 or so. Pulsing is also useful in handling liquids with high interfacial tensions, up to 30–40 dyn/cm (W1). Typical values for HETS of 0.15–0.3 m are given in Table 12.6-1. Since pulsing is uniform across the cross section, scale-up of tower size can be accomplished by using the same value of $V_D + V_C$ (W1).

Pulsed sieve-tray towers

Typical amplitudes used are from 0.6 to 2.5 cm and frequencies from 100 to 250 cycles/min (P4). Typical hole size is 0.32 cm diameter, with 20–25% free space on the tray and 5.1 cm (2 in.) tray spacing. The trays occupy the entire cross section of the tower and there are no downspouts. During upward pulsing, the light liquid is forced through the holes and droplets rise to the tray above. During downward pulsing, the heavy liquid behaves in a similar manner. Typical operating values are given in Table 12.6-1. Pulsing the tower markedly reduces the HETS.

Mechanically Agitated Extraction Towers

There are many types of mechanically agitated towers, two of the most important of which are the Scheibel tower shown in Fig. 12.6-5a and the Karr tower shown in Fig. 12.6-5b.

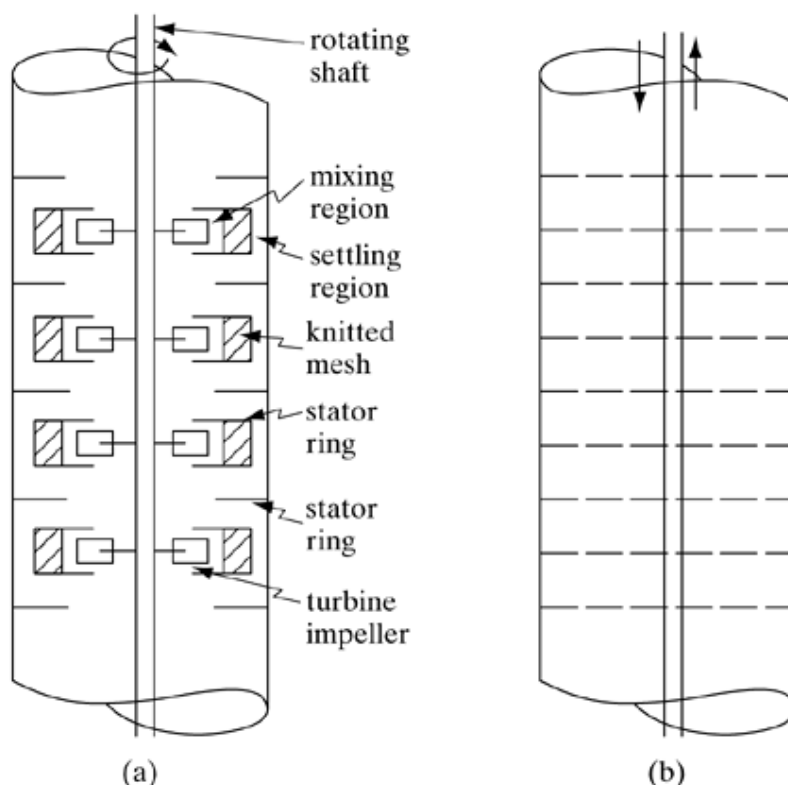


Figure 12.6-5. Mechanically agitated extraction towers: (a) Scheibel rotating-agitator tower, (b) Karr reciprocating-plate tower.

Scheibel tower

In the Scheibel tower, a series of rotating turbine agitators form dispersions which coalesce in passing through the knitted mesh. The mixture then passes through the outer settling zone. The tower thus operates as a series of mixer–settler extraction units.

The tower operates with high efficiencies, as shown in Table 12.6-1. In scaling up from a total combined flow rate Q_1 for both phases in m^3/s to Q_2 , the diameter D_2 is approximately related to D_1 by (L4, S2)

Equation 12.6-3.

$$\frac{D_2}{D_1} = \left(\frac{Q_2}{Q_1} \right)^{0.4}$$

Also, in scaling up from diameter D_1 to D_2 , the HETS varies as follows:

Equation 12.6-4.

$$(\text{HETS})_2 / (\text{HETS})_1 = (D_2 / D_1)^{0.5}$$

Equations for scale-up of the column internals are available (L4, S6).

Karr reciprocating-plate tower

As shown in Fig. 12.6-5b for the Karr column, the perforated trays are moved up and down to increase agitation and to pulse the liquids. This results in a more uniform drop-size distribution because the shear forces are more uniform over the tower cross section (K4, P4).

Typical parameters are an amplitude of plate movement of 2.5 cm (1 in.), 100–150 strokes/min, and plate spacing of 5–15 cm. Trays contain holes 1.4 cm in diameter and open space of 50–60% (W1). Scale-up procedures for the Karr column are relatively accurate. In scaling up a small tower with diameter D_1 to a larger size D_2 , the total throughput per unit area ($V_C + V_D$), plate spacing, and amplitude are kept constant. Then the HETS in m and the strokes per minute (SPM) are scaled up by (K4, P4)

Equation 12.6-5.

$$(\text{HETS}_2)/(\text{HETS}_1) = (D_2/D_1)^{0.38}$$

Equation 12.6-6.

$$(\text{SPM}_2)/(\text{SPM}_1) = (D_1/D_2)^{0.14}$$

Typical performance values are given in Table 12.6-1.

CONTINUOUS MULTISTAGE COUNTERCURRENT EXTRACTION

Introduction

In Section 12.5 single-stage equilibrium contact was used to transfer solute A from one liquid to another liquid phase. To transfer more solute, single-stage contact can be repeated by bringing the exit L_1 stream into contact with fresh solvent V_2 , as shown in Fig. 12.5-6. In this way a greater percentage removal of solute A is obtained. However, this is wasteful of the solvent stream as well as giving a dilute product of A in the outlet solvent extract streams. In order to use less solvent and to obtain a more concentrated exit extract stream, countercurrent multistage contacting is often employed.

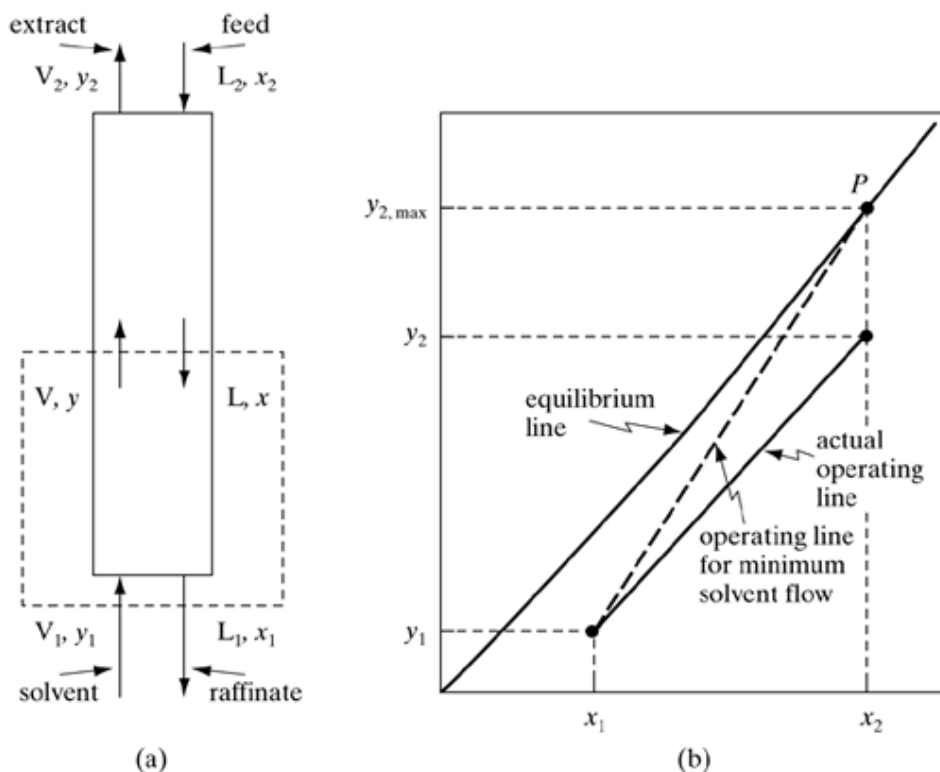


Figure 12.7-7. Extraction-tower flows: (a) process flow and material balance for countercurrent extraction tower, (b) operating line for minimum solvent flow for tower and actual operating line.

Many of the fundamental equations for countercurrent gas absorption and rectification are the same as or similar to those used in countercurrent extraction. Because of the frequently high solubility of the two liquid phases in each other, the equilibrium relationships in extraction are more complicated than in absorption and distillation.

Continuous Multistage Countercurrent Extraction

Countercurrent process and overall balance

The process flow for this extraction process is the same as given previously in Fig. 10.3-2 and is shown in Fig. 12.7-1. The feed stream containing the solute *A* to be extracted enters at one end of the process and the solvent stream enters at the other end. The extract and raffinate streams flow countercurrently from stage to stage, and the final products are the extract stream V_1 leaving stage 1 and the raffinate stream L_N leaving stage N .

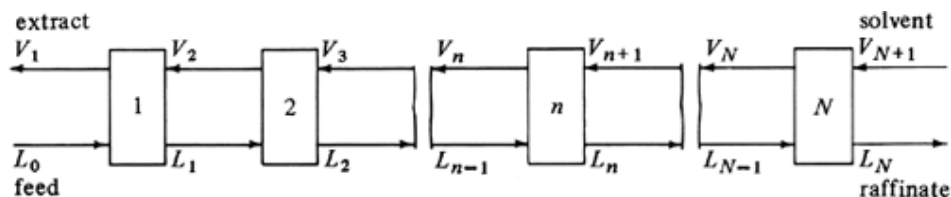


Figure 12.7-1. Countercurrent-multistage-extraction-process flow diagram.

Making an overall balance on all N stages,

Equation 12.7-1.

$$L_0 + V_{N+1} = L_N + V_1 = M$$

where M represents total kg/h (lb_m/h) and is a constant, L_0 the inlet feed flow rate in kg/h, V_{N+1} the inlet solvent flow rate in kg/h, V_1 the exit extract stream, and L_N the exit raffinate stream. Making an overall component balance on component C ,

Equation 12.7-2.

$$L_0 x_{C0} + V_{N+1} y_{CN+1} = L_N x_{CN} + V_1 y_{C1} = M x_{CM}$$

Combining Eqs. (12.7-1) and (12.7-2) and rearranging,

Equation 12.7-3.

$$x_{CM} = \frac{L_0 x_{C0} + V_{N+1} y_{CN+1}}{L_0 + V_{N+1}} = \frac{L_N x_{CN} + V_1 y_{C1}}{L_N + V_1}$$

A similar balance on component A gives

Equation 12.7-4.

$$x_{AM} = \frac{L_0 x_{A0} + V_{N+1} y_{AN+1}}{L_0 + V_{N+1}} = \frac{L_N x_{AN} + V_1 y_{A1}}{L_N + V_1}$$

Equations (12.7-3) and (12.7-4) can be used to calculate the coordinates of point M on the phase diagram, which ties together the two entering streams L_0 and V_{N+1} and the two exit streams V_1 and L_N . Usually, the flows and compositions of L_0 and V_{N+1} are known and the desired exit composition x_{AN} is set. If we plot points L_0 , V_{N+1} , and M as in Fig. 12.7-2, a straight line must connect these three points. Then L_N , M , and V_1 must lie on one line. Moreover, L_N and V_1 must also lie on the phase envelope, as shown. These balances also hold for lb_m and mass fraction, kg mol and mol fractions, and so on.

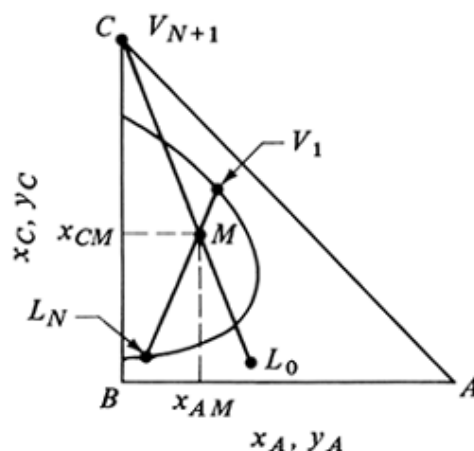


Figure 12.7-2. Use of the mixture point M for overall material balance in counter current solvent extraction.

EXAMPLE 12.7-1. Material Balance for Countercurrent Stage Process

Pure solvent isopropyl ether at the rate of $V_{N+1} = 600$ kg/h is being used to extract an aqueous solution of $L_0 = 200$ kg/h containing 30 wt % acetic acid (A) by countercurrent multistage extraction. The desired exit acetic acid concentration in the aqueous phase is 4%. Calculate the compositions and amounts of the ether extract V_1 and the aqueous raffinate L_N . Use equilibrium data from Appendix A.3.

Solution: The given values are $V_{N+1} = 600$, $y_{AN+1} = 0$, $y_{CN+1} = 1.0$, $L_0 = 200$, $x_{A0} = 0.30$, $x_{B0} = 0.70$, $x_{C0} = 0$, and $x_{AN} = 0.04$. In Fig. 12.7-3, V_{N+1} and L_0 are plotted. Also, since L_N is on the phase boundary, it can be plotted at $x_{AN} = 0.04$. For the mixture point M , substituting into Eqs. (12.7-3) and (12.7-4),

Equation 12.7-3.

$$x_{CM} = \frac{L_0 x_{C0} + V_{N+1} y_{CN+1}}{L_0 + V_{N+1}} = \frac{200(0) + 600(1.0)}{200 + 600} = 0.75$$

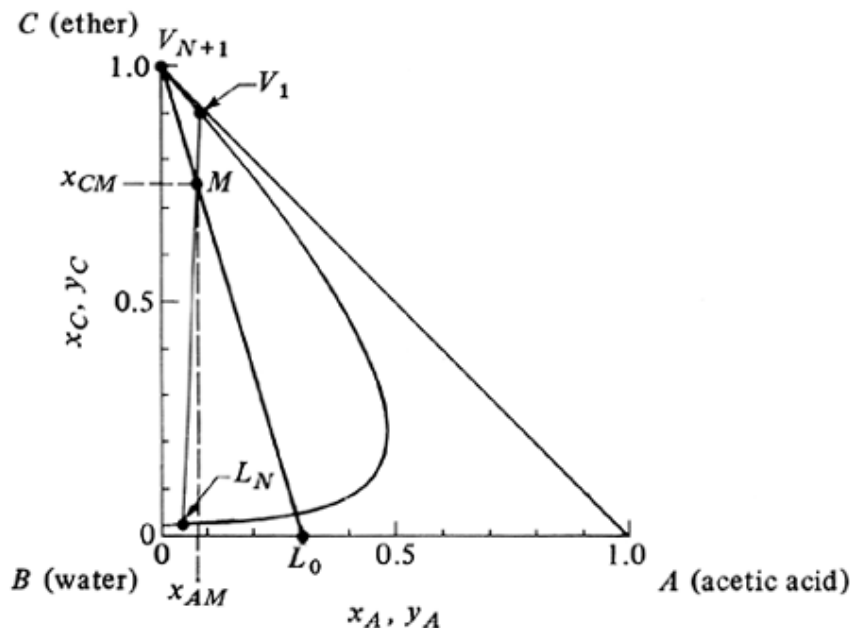


Figure 12.7-3. Method to perform overall material balance for Example 12.7-1.

Equation 12.7-4.

$$x_{AM} = \frac{L_0 x_{A0} + V_{N+1} y_{AN+1}}{L_0 + V_{N+1}} = \frac{200(0.30) + 600(0)}{200 + 600} = 0.075$$

Using these coordinates, the point M is plotted in Fig. 12.7-3. We locate V_1 by drawing a line from L_N through M and extending it until it intersects the phase boundary. This gives $y_{A1} = 0.08$ and $y_{C1} = 0.90$. For L_N a value of $x_{CN} = 0.017$ is obtained. By substituting into Eqs. (12.7-1) and (12.7-2) and solving, $L_N = 136$ kg/h and $V_1 = 664$ kg/h.

Stage-to-stage calculations for countercurrent extraction

The next step after an overall balance has been made is to go stage by stage to determine the concentrations at each stage and the total number of stages N needed to reach L_N in Fig. 12.7-1.

Making a total balance on stage 1,

Equation 12.7-5.

$$L_0 + V_2 = L_1 + V_1$$

Making a similar balance on stage n ,

Equation 12.7-6.

$$L_{n-1} + V_{n+1} = L_n + V_n$$

Rearranging Eq. (12.7-5) to obtain the difference Δ in flows,

Equation 12.7-7.

$$L_0 - V_1 = L_1 - V_2 = \Delta$$

This value of Δ in kg/h is constant, and for all stages,

Equation 12.7-8.

$$\Delta = L_0 - V_1 = L_n - V_{n+1} = L_N - V_{N+1} = \dots$$

This also holds for a balance on component A , B , or C .

Equation 12.7-9.

$$\Delta x_\Delta = L_0 x_0 - V_1 y_1 = L_n x_n - V_{n+1} y_{n+1} = L_N x_N - V_{N+1} y_{N+1} = \dots$$

Combining Eqs. (12.7-8) and (12.7-9) and solving for x_Δ ,

Equation 12.7-10.

$$x_\Delta = \frac{L_0 x_0 - V_1 y_1}{L_0 - V_1} = \frac{L_n x_n - V_{n+1} y_{n+1}}{L_n - V_{n+1}} = \frac{L_N x_N - V_{N+1} y_{N+1}}{L_N - V_{N+1}}$$

where x_Δ is the x coordinate of point Δ .

Equations (12.7-7) and (12.7-8) can be written as

Equation 12.7-11.

$$L_0 = \Delta + V_1 \quad L_n = \Delta + V_{n+1} \quad L_N = \Delta + V_{N+1}$$

From Eq. (12.7-11), we see that L_0 is on a line through Δ and V_1 , L_n is on a line through Δ and V_{n+1} , and so on. This means Δ is a point common to all streams passing each other, such as L_0 and V_1 , L_n and V_{n+1} , L_N and V_{N+1} , and so on. The coordinates for locating this Δ operating point are given for $x_{C\Delta}$ and $x_{A\Delta}$ in Eq. (12.7-10). Since the end points V_{N+1} , L_N or V_1 , and L_0 are known, x_Δ can be calculated and point Δ located. Alternatively, the Δ point is located graphically in Fig. 12.7-4 as the intersection of lines $L_0 V_1$ and $L_N V_{N+1}$.

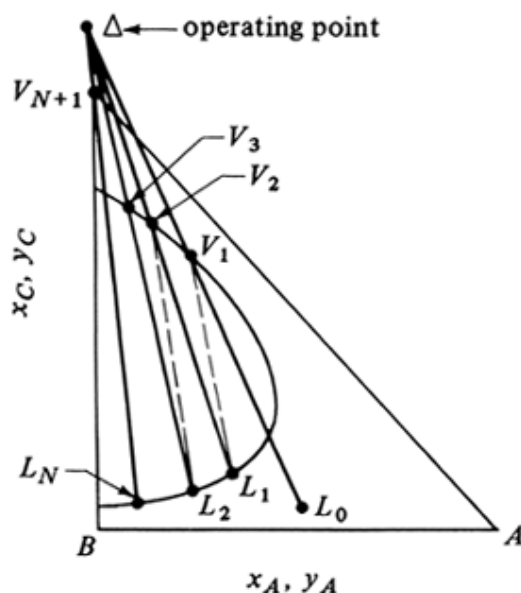


Figure 12.7-4. Operating point Δ and number of theoretical stages needed for countercurrent extraction.

In order to step off the number of stages using Eq. (12.7-11) we start at L_0 and draw the line $L_0\Delta$, which locates V_1 on the phase boundary. Next a tie line through V_1 locates L_1 , which is in equilibrium with V_1 . Then line $L_1\Delta$ is drawn giving V_2 . The tie line V_2L_2 is drawn. This stepwise procedure is repeated until the desired raffinate composition L_N is reached. The number of stages N required to perform the extraction is thus obtained.

EXAMPLE 12.7-2. Number of Stages in Countercurrent Extraction

Pure isopropyl ether of 450 kg/h is being used to extract an aqueous solution of 150 kg/h with 30 wt % acetic acid (A) by countercurrent multistage extraction. The exit acid concentration in the aqueous phase is 10 wt %. Calculate the number of stages required.

Solution: The known values are $V_{N+1} = 450$, $y_{AN+1} = 0$, $y_{CN+1} = 1.0$, $L_0 = 150$, $x_{A0} = 0.30$, $x_{B0} = 0.70$, $x_{C0} = 0$, and $x_{AN} = 0.10$. The points V_{N+1} , L_0 , and L_N are plotted in Fig. 12.7-5. For the mixture point M , substituting into Eqs. (12.7-3) and (12.7-4), $x_{CM} = 0.75$ and $x_{AM} = 0.075$. The point M is plotted and V_1 is located at the intersection of line L_NM with the phase boundary to give $y_{A1} = 0.072$ and $y_{C1} = 0.895$. (This construction is not shown. See Example 12.7-1 for construction of lines.)

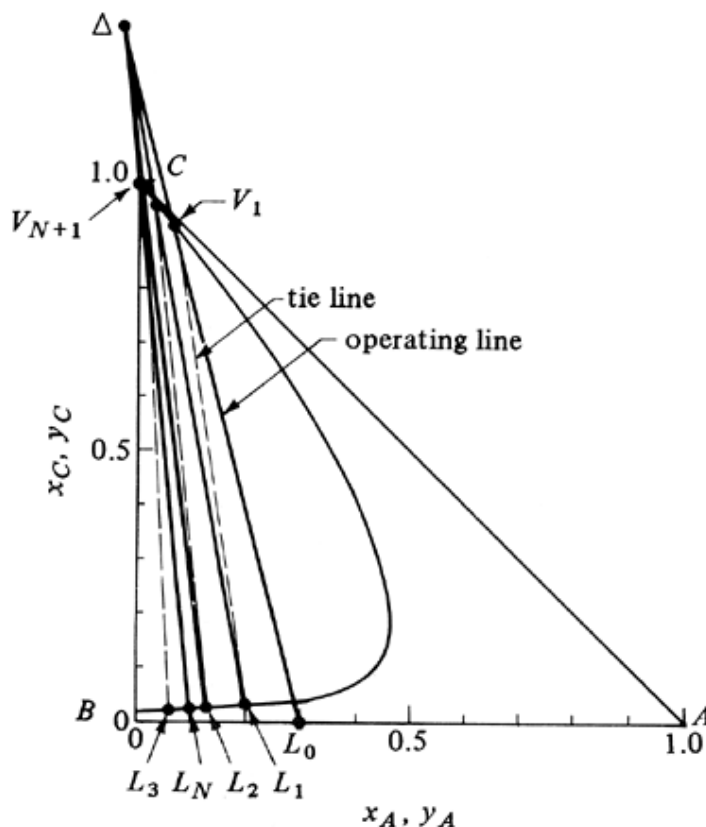


Figure 12.7-5. Graphical solution for countercurrent extraction in Example 12.7-2.

The lines $L_0 V_1$ and $L_N V_{N+1}$ are drawn and the intersection is the operating point $\Delta\Delta$ as shown. Alternatively, the coordinates of $\Delta\Delta$ can be calculated from Eq. (12.7-10) to locate point $\Delta\Delta$. Starting at L_0 we draw line $L_0 \Delta\Delta$, which locates V_1 . Then a tie line through V_1 locates L_1 in equilibrium with V_1 . (The tie-line data are obtained from an enlarged plot such as the bottom of Fig. 12.5-3.) Line $L_1 \Delta\Delta$ is next drawn locating V_2 . A tie line through V_2 gives L_2 . A line $L_2 \Delta\Delta$ gives V_3 . A final tie line gives L_3 , which has gone beyond the desired L_N . Hence, about 2.5 theoretical stages are needed.

Minimum solvent rate

If a solvent rate V_{N+1} is selected at too low a value, a limiting case will be reached, with a line through $\Delta\Delta$ and a tie line being the same. Then an infinite number of stages will be needed to reach the desired separation. The minimum amount of solvent has been reached. For actual operation a greater amount of solvent must be used.

The procedure for obtaining this minimum is as follows. A tie line is drawn through point L_0 (Fig. 12.7-4) to intersect the extension of line $L_N V_{N+1}$. Other tie lines to the left of this tie line are drawn, including one through L_N to intersect the line $L_N V_{N+1}$. The intersection of a tie line on line $L_N V_{N+1}$ which is nearest to V_{N+1} represents the $\Delta\Delta_{\min}$ point for minimum solvent. The actual position of $\Delta\Delta$ used must be closer to V_{N+1} than $\Delta\Delta_{\min}$ for a finite number of stages. This means that more solvent must be used. Usually, the tie line through L_0 represents the $\Delta\Delta_{\min}$.

Countercurrent-Stage Extraction with Immiscible Liquids

If the solvent stream V_{N+1} contains components A and C and the feed stream L_0 contains A and B, and if components B and C are relatively immiscible in each other, the stage calculations may be made more easily. The solute A is relatively dilute and is being transferred from L_0 to V_{N+1} .

Referring to Fig. 12.7-1 and making an overall balance for A over the whole system and then over the first n stages,

Equation 12.7-12.

$$L' \left(\frac{x_0}{1 - x_0} \right) + V' \left(\frac{y_{N+1}}{1 - y_{N+1}} \right) = L' \left(\frac{x_N}{1 - x_N} \right) + V' \left(\frac{y_1}{1 - y_1} \right)$$

Equation 12.7-13.

$$L' \left(\frac{x_0}{1 - x_0} \right) + V' \left(\frac{y_{n+1}}{1 - y_{n+1}} \right) = L' \left(\frac{x_n}{1 - x_n} \right) + V' \left(\frac{y_1}{1 - y_1} \right)$$

where $L \triangleq$ kg inert B/h , $V' \triangleq$ kg inert C/h , y = mass fraction A in V stream, and x = mass fraction A in L stream. This Eq. (12.7-13) is an operating-line equation whose slope $\cong L'/V$. If y and x are quite dilute, the line will be straight when plotted on an x - y diagram.

The number of stages are stepped off as shown previously for cases of distillation and absorption, as shown in Fig. 10.3-4.

If the equilibrium line is relatively dilute, then since the operating line is essentially straight, the analytical Eqs. (10.3-21)–(10.3-26) given in Section 10.3D can be used to calculate the number of stages.

EXAMPLE 12.7-3. Extraction of Nicotine with Immiscible Liquids.

An inlet water solution of 100 kg/h containing 0.010 wt fraction nicotine (A) in water is stripped with a kerosene stream of 200 kg/h containing 0.0005 wt fraction nicotine in a countercurrent-stage tower. The water and kerosene are essentially immiscible in each other. It is desired to reduce the concentration of the exit water to 0.0010 wt fraction nicotine. Determine the theoretical number of stages needed. The equilibrium data are as follows (C5), with x the weight fraction of nicotine in the water solution and y in the kerosene:

| x | y | x | y |
|----------|----------|---------|---------|
| 0.001010 | 0.000806 | 0.00746 | 0.00682 |
| 0.00246 | 0.001959 | 0.00988 | 0.00904 |
| 0.00500 | 0.00454 | 0.0202 | 0.0185 |

- Plot the equilibrium data and graphically determine the number of theoretical steps.
- Use the Kremser equation (10.3-21) and calculate the number of theoretical steps.

Solution: The given values are $L_0 = 100$ kg/h, $x_0 = 0.010$, $V_{N+1} = 200$ kg/h, $y_{N+1} = 0.0005$, $x_N = 0.0010$. The inert streams are

$$\begin{aligned} L' &= L(1 - x) = L_0(1 - x_0) = 100(1 - 0.010) \\ &= 99.00 \text{ kg water/h} \end{aligned}$$

$$\begin{aligned} V' &= V(1 - y) = V_{N+1}(1 - y_{N+1}) = 200(1 - 0.0005) \\ &= 199.9 \text{ kg kerosene/h} \end{aligned}$$

Making an overall balance on A using Eq. (12.7-12) and solving, $y_1 = 0.00498$. These points on the operating line are plotted in Fig. 12.7-6.

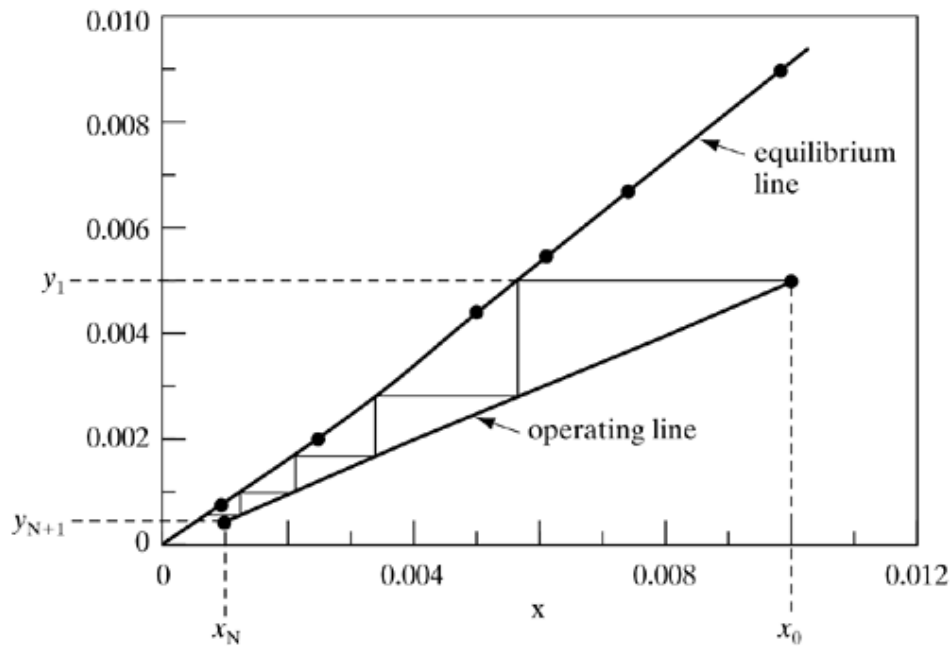


Figure 12.7-6. Solution for extraction with immiscible liquids in Example 12.7-3.

Since the operating-line equation is for dilute solutions, a straight line is drawn. The equilibrium data are plotted and the line is slightly curved.

For part (a), the number of stages are stepped off, giving $N = 4.5$ theoretical stages.

For part (b), to calculate the total flow rates L_N and V_1 , the following equations can be solved:

$$L' = 99.0 = L_N(1 - x_N) = L_N(1 - 0.0010).$$

$$L_N = 99.10 \text{ kg/h}$$

$$V' = 199.9 = V_1(1 - y_1) = V_1(1 - 0.00497).$$

$$V_1 = 200.9 \text{ kg/h}$$

Also, $L_0 = 100$ and $V_{N+1} = 200$ kg/h. To use Eq. (10.3-21) the slope of the equilibrium curve must be calculated at the top and bottom of the tower, since the line is not straight. At the top on the equilibrium curve, at the point $y_1 = 0.00498$, the tangent or slope at this point is determined to be $m_1 = 0.91$. At the bottom or dilute end, at $x_N = 0.0010$ on the equilibrium curve, the line is straight and m_2 can be calculated from the equilibrium data as $m_2 = 0.000806/0.001010 = 0.798$. Then $A_1 = L/(mV) = L_0/(m_1 V_1) = 100/(0.91 \times 200.9) = 0.547$. Also, $A_2 = L_N/(m_2 V_{N+1}) = 99.1/(0.798 \times 200) = 0.621$. The average value of $A = \sqrt{0.547 \times 0.621} = 0.583$.

Substituting into Eq. (10.3-22) using $m = m_2 = 0.798$,

$$N = \frac{\ln \left[\frac{x_0 - (y_{N+1}/m)}{x_N - (y_{N+1}/m)} (1 - A) + A \right]}{\ln(1/A)}$$

$$= \frac{\ln \left[\frac{0.010 - 0.0005/0.798}{0.001 - 0.0005/0.798} (1 - 0.583) + 0.583 \right]}{\ln(1/0.583)}$$

$N = 4.45$ theoretical stages. This compares closely with the graphical-method result of 4.5 theoretical stages.

Design of Towers for Extraction

Operating-line equation for relatively immiscible liquids

In this case, in Fig. 12.7-7a the liquid feed stream L and the solvent stream V are relatively immiscible in each other and solute A is relatively dilute in both streams. The outlet feed stream is commonly called the raffinate and the outlet solvent stream the extract. For the countercurrent extraction of A from the feed stream L to the solvent stream V , an overall material balance around the dashed-line box gives the following operating line equation:

Equation 12.7-14.

$$L' \left(\frac{x}{1-x} \right) + V' \left(\frac{y_1}{1-y_1} \right) = L' \left(\frac{x_1}{1-x_1} \right) + V' \left(\frac{y}{1-y} \right)$$

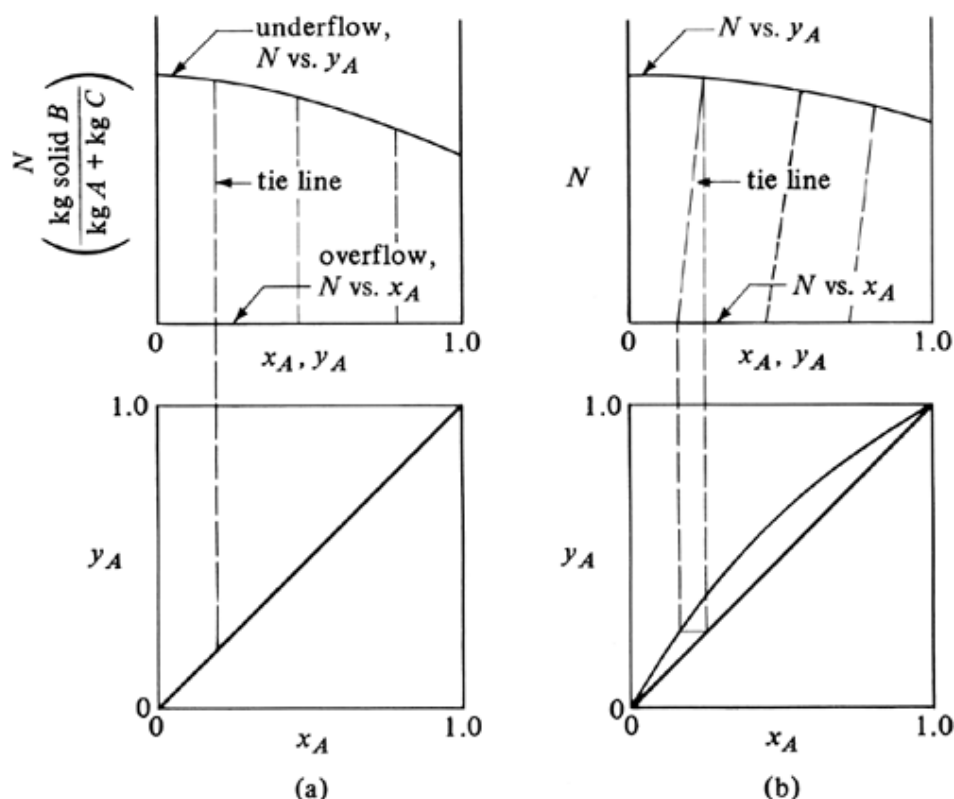


Figure 12.9-1. Several typical equilibrium diagrams: (a) case for vertical tie lines and $y_A = x_A$, (b) case where $y_A \neq x_A$ for tie lines.

where $L' = \text{kg feed } B/\text{h}$, $V' = \text{kg solvent}/\text{h}$, $y = \text{mass fraction } A \text{ in solvent } V \text{ stream}$, and $x = \text{mass fraction } A \text{ in feed } L \text{ stream}$.

This operating-line equation will be slightly curved when plotted on an x - y diagram as in Fig. 12.7-7b. Note that units of mole fraction and molar flow rates can also be used. The number of theoretical steps are stepped off as previously shown in Fig. 12.7-6. If the two liquid solvent and feed streams are immiscible in each other, L' and V' are constant.

Limiting solvent flows and optimum L'/V' ratios

In an extraction process, the inlet feed flow L_2 and its composition x_2 are usually set. The exit concentration x_1 in the raffinate (L_1 stream) is often set by the designer. The inlet concentration y_1 of the solvent (V_1 stream) is generally fixed by process requirements in regenerating the solvent for recycle back to the tower. Hence, the amount of the entering solvent flow V_1 or V' is open to choice.

In Fig. 12.7-7b, the concentrations x_1 , x_2 , and y_1 are set. When the operating line has a maximum slope and touches the equilibrium line at point P , then the solvent flow is at a minimum at V'_{\min} . The value of y_2 is at a maximum of $y_{2,\max}$. As in absorption and stripping, the optimum flow rate is taken as 1.2–1.5 times V'_{\min} , with 1.5 normally used (S6). Note that if the equilibrium line is curved and highly concave upward, then, for the minimum value, the operating line is tangent to the equilibrium line instead of intersecting it. Then the optimum is taken as 1.2–1.5 times V'_{\min} .

Analytical equations for number of trays

The analytical equation to calculate the number of theoretical trays N for extraction is the same as Eq. (10.6-8) for stripping in gas–liquid separations and is given as

Equation 12.7-15.

$$N = \frac{\ln \left[\frac{(x_2 - y_1/m)(1 - A) + A}{(x_1 - y_1/m)} \right]}{\ln(1/A)}$$

where $A = L/mV$. The value of A may vary in the tower if the operating and equilibrium lines are curved somewhat. Referring to Fig. 12.7-7b, at the concentrated top of the tower, the slope m_2 or tangent at point y_2 on the equilibrium line is used. At the bottom or dilute end, the slope m_1 at point x_1 on the equilibrium line is used. Then $A_1 = L_1/m_1 V_1$, $A_2 = L_2/m_2 V_2$, and $A = \sqrt{A_1 A_2}$. Also, the dilute m_1 is used in Eq. (12.7-15). A useful equation is Eq. (12.7-16), which allows one to calculate the performance of an existing tower when the number of theoretical steps N are known:

Equation 12.7-16.

$$\frac{x_2 - x_1}{x_2 - y_1/m} = \frac{(1/A)^{N+1} - (1/A)}{(1/A)^{N+1} - 1}$$

Design of Packed Towers for Extraction Using Mass-Transfer Coefficients

The use of mass-transfer coefficients in extraction is similar to their use in stripping in absorption. The equations for dilute solutions and essentially immiscible solvents using overall coefficients are essentially identical to those for stripping with dilute solutions as given previously in Section 10.6G as Eq. (10.6-46) and (10.6-47). For extraction,

Equation 12.7-17.

$$z = H_{OL} N_{OL} = H_{OL} \int_{x_2}^{x_1} \frac{dx}{x^* - x}$$

Equation 12.7-18.

$$H_{OL} = \frac{L}{K'_x a S}$$

If both the operating and equilibrium lines are straight and dilute, the integral in Eq. (12.7-17) can be integrated to give

Equation 12.7-19.

$$N_{OL} = \frac{(x_1 - x_2)}{(x^* - x)_M}$$

where

Equation 12.7-20.

$$(x^* - x)_M = \frac{(x_1^* - x_1) - (x_2^* - x_2)}{\ln[(x_1^* - x_1)/(x_2^* - x_2)]}$$

In terms of the V phase,

Equation 12.7-21.

$$N_{OV} = \frac{(y_1 - y_2)}{(y - y^*)_M}$$

where $(y - y^*)_M$ is defined in Eq. (10.6-28). The value of the overall number of transfer units N_{OL} can also be determined using Eq. (10.6-53) as

Equation 12.7-22.

$$N_{OL} = \frac{1}{(1 - A)} \ln \left[(1 - A) \left(\frac{x_2 - y_1/m}{x_1 - y_1/m} \right) + A \right]$$

EXAMPLE 12.7-4. Extraction of Acetone from Water with Trichloroethane in a Tower

An inlet water solution of 800 kg/h containing 12.0 wt % acetone is extracted with the solvent trichloroethane containing 0.5 wt % acetone in a countercurrent tray tower at 25°C. The solvents water and trichloroethane are essentially immiscible in each other up to a concentration of acetone in water of 27 wt %. The exit concentration in the water (raffinate) stream is set at 1.0 wt % acetone. The equilibrium data are as follows (T3), where x is the weight fraction of acetone in the water solution and y in the trichloroethane solution:

| x | y | x | y |
|--------|--------|--------|--------|
| 0.0120 | 0.0196 | 0.0833 | 0.1304 |
| 0.0294 | 0.0476 | 0.1081 | 0.1666 |
| 0.0462 | 0.0741 | 0.1316 | 0.2000 |
| 0.0571 | 0.0909 | | |

- Determine the minimum solvent rate needed.
- Using 1.3 times the minimum rate, graphically determine the number of theoretical steps needed.
- Calculate the number of steps using the analytical equation.
- Using a packed tower, the height of a transfer unit H_{OL} is estimated to be 1.2 m. Calculate the number of transfer units N_{OL} and the tower height.

Solution: For part (a), the given values are $L_2 = 800$ kg/h, $x_2 = 0.12$, $x_1 = 0.01$, $y_1 = 0.005$. The inlet stream is

$$L' = L_2(1 - x_2) = 800(1 - 0.12) = 704.0 \text{ kg water/h}$$

The equilibrium data are plotted in Fig. 12.7-8, and the line is curved somewhat. The operating line for minimum solvent flow is plotted from point x_1, y_1 to point P , where $x_2 = 0.12$ on the equilibrium line and $y_{2,\max} = 0.184$.

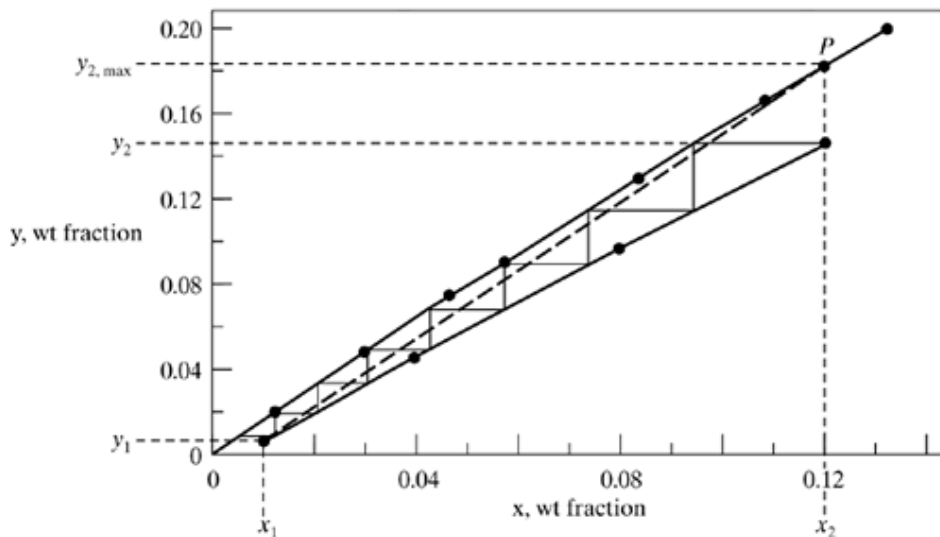


Figure 12.7-8. Operating and equilibrium line for Example 12.7-4.

Rewriting Eq. (12.7-14) for an overall balance, and substituting the known values,

$$L' \left(\frac{x_2}{1 - x_2} \right) + V' \left(\frac{y_1}{1 - y_1} \right) = L' \left(\frac{x_1}{1 - x_1} \right) + V' \left(\frac{y_{2,\max}}{1 - y_{2,\max}} \right)$$

$$704 \left(\frac{0.12}{1 - 0.12} \right) + V' \left(\frac{0.005}{1 - 0.005} \right) = 704 \left(\frac{0.01}{1 - 0.01} \right) + V' \left(\frac{0.184}{1 - 0.184} \right)$$

Solving, $V' = V'_{\min} = 403.2$ kg solvent/h. Setting $x = 0.07$ in Eq. (12.7-14) and solving, $y = 0.1062$. Repeating this for several other x values, these points on the operating line are plotted in Fig. 12.7-8. This operating line for minimum solvent flow (dashed line) is slightly curved and does not intersect or become tangent to the equilibrium line at any point other than P .

For part (b), $V' = 1.3 V'_{\min} = 1.3(403.2) = 524.2$ kg solvent/h. Substituting into the operating-line Eq. (12.7-14) and solving for y_2 ,

$$L' \left(\frac{x_2}{1 - x_2} \right) + V' \left(\frac{y_1}{1 - y_1} \right) = L' \left(\frac{x_1}{1 - x_1} \right) + V' \left(\frac{y_2}{1 - y_2} \right)$$

$$704 \left(\frac{0.12}{1 - 0.12} \right) + 524.2 \left(\frac{0.005}{1 - 0.005} \right) = 704 \left(\frac{0.01}{1 - 0.01} \right) + 524.2 \left(\frac{y_2}{1 - y_2} \right)$$

Then, $y_2 = 0.1486$. As before, calculating several points on the operating line, which is curved, for $x = 0.04$, $y = 0.0453$; for $x = 0.08$, $y = 0.0977$. Plotting these points shows a curved operating line. Stepping off the trays, a total of 7.4 steps are obtained.

For part (c), the total flows are first calculated as

$$L_1 = \frac{L'}{1 - x_1} = \frac{704}{1 - 0.01} = 711.1, \quad V_1 = \frac{V'}{1 - y_1} = \frac{524.2}{1 - 0.005} = 526.8$$

$$L_2 = 800, \quad V_2 = \frac{V'}{1 - y_2} = \frac{524.2}{1 - 0.1486} = 615.7$$

The value of m_2 is the slope or tangent at point y_2 on the equilibrium line, which gives $m_2 = 1.49$. The value of m_1 at point x_1 at the dilute end on the equilibrium line is, from the first set of equilibrium data points, equal to $y/x = 0.0196/0.0120 = 1.633 = m_1$. Then

$$A_1 = \frac{L_1}{m_1 V_1} = \frac{711.1}{1.633(526.8)} = 0.827$$

$$A_2 = \frac{L_2}{m_2 V_2} = \frac{800}{1.49(615.7)} = 0.872$$

$$A = \sqrt{A_1 A_2} = \sqrt{0.827(0.872)} = 0.849$$

Using Eq. (12.7-15),

$$N = \frac{\ln \left[\frac{x_2 - (y_1/m)}{x_1 - (y_1/m)} (1 - A) + A \right]}{\ln(1/A)}$$

$$= \frac{\ln \left[\frac{0.12 - 0.0005/1.633}{0.01 - 0.0005/1.633} (1 - 0.849) + 0.849 \right]}{\ln(1/0.849)}$$

Then, $N = 7.46$ theoretical steps. This agrees closely with the graphical value of 7.4.

For part (d), Eq. (12.7-19) will not be used, because the operating and equilibrium lines are slightly curved. Using Eq. (12.7-22),

$$N_{OL} = \frac{1}{(1 - A)} \ln \left[(1 - A) \left(\frac{x_2 - y_1/m}{x_1 - y_1/m} \right) + A \right]$$

$$= \frac{1}{(1 - 0.849)} \ln \left[(1 - 0.849) \left(\frac{0.12 - 0.005/1.633}{0.01 - 0.005/1.633} \right) + 0.849 \right]$$

Solving, $N_{OL} = 8.09$ transfer units. Then, $z = H_{OL} N_{OL} = 1.2(8.09) = 9.71$ m.

INTRODUCTION AND EQUIPMENT FOR LIQUID–SOLID LEACHING

Leaching Processes

Introduction

Many biological and inorganic and organic substances occur in a mixture of different components in a solid. In order to separate the desired solute constituent or remove an undesirable solute component from the solid phase, the solid is contacted with a liquid phase. The two phases are in intimate contact and the solute or solutes can diffuse from the solid to the liquid phase, resulting in a separation of the components originally in the solid. This separation process is called *liquid–solid leaching* or simply *leaching*. The term *extraction* is also used to describe this separation process, although it also refers to liquid–liquid extraction. In leaching, when an undesirable component is removed from a solid with water, the process is called *washing*.

Leaching processes for biological substances

In the biological and food processing industries, many products are separated from their original natural structure by liquid–solid leaching. An important process, for example, is the leaching of sugar from sugar beets with hot water. In the production of vegetable oils, organic solvents such as hexane, acetone, and ether are used to extract the oil from peanuts, soybeans, flax seeds, castor beans, sunflower seeds, cotton seeds, tung meal, and halibut livers. In the pharmaceutical industry, many different pharmaceutical products are obtained by leaching plant roots, leaves, and stems. For the production of soluble “instant” coffee, ground roasted coffee is leached with fresh water. Soluble tea is produced by water leaching of tea leaves. Tannin is removed from tree barks by leaching with water.

Leaching processes for inorganic and organic materials

Leaching processes are used extensively in the metals processing industries. The useful metals usually occur in mixtures with very large amounts of undesirable constituents, and leaching is used to remove the metals as soluble salts. Copper salts are dissolved or leached from ground ores containing other minerals by sulfuric acid or ammoniacal solutions. Cobalt and nickel salts are leached from their ores by sulfuric acid–ammonia–oxygen mixtures. Gold is leached from its ore using an aqueous sodium cyanide solution. Sodium hydroxide is leached from a slurry of calcium carbonate and sodium hydroxide prepared by reacting Na_2CO_3 with $\text{Ca}(\text{OH})_2$.

Preparation of Solids for Leaching**Inorganic and organic materials**

The method of preparation of the solid depends to a large extent upon the proportion of the soluble constituent present, its distribution throughout the original solid, the nature of the solid—that is, whether it is composed of plant cells or whether the soluble material is completely surrounded by a matrix of insoluble matter—and the original particle size.

If the soluble material is surrounded by a matrix of insoluble matter, the solvent must diffuse inside to contact and dissolve the soluble material and then diffuse out. This occurs in many hydrometallurgical processes where metal salts are leached from mineral ores. In these cases crushing and grinding of the ores is used to increase the rate of leaching, since the soluble portions are made more accessible to the solvent. If the soluble substance is in solid solution in the solid or is widely distributed throughout the whole solid, the solvent leaching action may form small channels. The passage of additional solvent is then made easier, and grinding to very small sizes may not be needed. Grinding of the particles is not necessary if the soluble material is dissolved in solution adhering to the solid. Then simple washing can be used, as in washing of chemical precipitates.

Animal and vegetable materials

Biological materials are cellular in structure and the soluble constituents are generally found inside the cells. The rate of leaching may be comparatively slow because the cell walls provide another resistance to diffusion. However, to grind the biological material sufficiently small to expose the contents of individual cells is impractical. Sugar beets are cut into thin, wedge-shaped slices for leaching so that the distance required for the water solvent to diffuse in order to reach individual cells is reduced. The cells of the sugar beet are kept essentially intact so that sugar will diffuse through the semipermeable cell walls, while the undesirable albuminous and colloidal components cannot pass through the walls.

For the leaching of pharmaceutical products from leaves, stems, and roots, drying of the material before extraction helps rupture the cell walls. Thus, the solvent can directly dissolve the solute. The cell walls of soybeans and many vegetable seeds are largely ruptured when the original materials are reduced in size to about 0.1 mm to 0.5 mm by rolling or flaking. Cells are smaller in size, but the walls are ruptured and the vegetable oil is easily accessible to the solvent.

Rates of Leaching

Introduction and general steps

In the leaching of soluble materials from inside a particle by means of a solvent, the following general steps can occur in the overall process. The solvent must be transferred from the bulk solvent solution to the surface of the solid. Next, the solvent must penetrate or diffuse into the solid. The solute dissolves into the solvent. The solute then diffuses through the solid solvent mixture to the surface of the particle. Finally, the solute is transferred to the bulk solution. The many different phenomena encountered make it virtually impracticable if not impossible to apply any one theory to the leaching action.

In general, the rate of transfer of the solvent from the bulk solution to the solid surface is quite rapid, while the rate of transfer of the solvent into the solid may be somewhat rapid or slow. These are not, in many cases, the rate-limiting steps in the overall leaching process. This solvent transfer usually occurs initially, when the particles are first contacted with the solvent. The dissolving of the solute into the solvent inside the solid may be a simple physical dissolution process or an actual chemical reaction that frees the solute for dissolution. Our knowledge of the dissolution process is limited and the mechanism may be different for each solid (K1).

The rate of diffusion of the solute through the solid and solvent to the surface of the solid is often the controlling resistance in the overall leaching process and may depend on a number of different factors. If the solid is made up of an inert porous solid structure, with the solute and solvent in the pores in the solid, the diffusion through the porous solid can be described by an effective diffusivity. The void fraction and tortuosity are needed. This is described in Section 6.5C for diffusion in porous solids.

In biological or natural substances, additional complexity occurs because of the cells present. In the leaching of thin sugar beet slices, about one-fifth of the cells are ruptured in the slicing of the beets. The leaching of the sugar is then similar to a washing process (Y1). In the remaining cells, sugar must diffuse out through the cell walls. The net result of the two transfer processes does not follow the simple diffusion law with a constant effective diffusivity.

With soybeans, whole beans cannot be leached effectively. The rolling and flaking of the soybeans ruptures cell walls so that the solvent can more easily penetrate by capillary action. The rate of diffusion of the soybean oil solute from the soybean flakes does not permit simple interpretation. A method for designing large-scale extractors involves using small-scale laboratory experiments (O2) with flakes.

The resistance to mass transfer of the solute from the solid surface to the bulk solvent is in general quite small compared to the resistance to diffusion within the solid (O1) itself. This has been found for leaching soybeans, where the degree of agitation of the external solvent has no appreciable effect on the extraction rate (O3, Y1).

Rate of leaching when dissolving a solid

When a material is being dissolved from the solid to the solvent solution, however, the rate of mass transfer from the solid surface to the liquid is the controlling factor. There is essentially no resistance in the solid phase if it is a pure material. The equation for this can be derived as follows for a batch system. The following can also be used for the case when diffusion in the solid is very rapid compared to diffusion from the particle.

The rate of mass transfer of solute A being dissolved to the solution of volume $V\text{ m}^3$ is

Equation 12.8-1.

$$\frac{\bar{N}_A}{A} = k_L(c_{AS} - c_A)$$

where \bar{N}_A is kg mol of A dissolving to the solution/s. A is surface area of particles in m^2 , k_L is a mass-transfer coefficient in m/s , c_{AS} is the saturation solubility of the solid solute A in the solution in kg mol/m^3 , and c_A is the concentration of A in the solution at time t sec in kg mol/m^3 . By a material balance, the rate of accumulation of A in the solution is equal to Eq. (12.8-1) times the area A :

Equation 12.8-2.

$$V \frac{dc_A}{dt} = \bar{N}_A = Ak_L(c_{AS} - c_A)$$

Integrating from $t = 0$ and $c_A = c_{A0}$ to $t = t$ and $c_A = c_A$,

Equation 12.8-3.

$$\int_{c_{A0}}^{c_A} \frac{dc_A}{c_{AS} - c_A} = \frac{Ak_L}{V} \int_{t=0}^t dt$$

Equation 12.8-4.

$$\frac{c_{AS} - c_A}{c_{AS} - c_{A0}} = e^{-(k_L A/V)t}$$

The solution approaches a saturated condition exponentially. Often the interfacial area A will increase during the extraction if the external surface becomes very irregular. If the soluble material forms a high proportion of the total solid, disintegration of the particles may occur. If the solid is completely dissolving, the interfacial area changes markedly. Also, the mass-transfer coefficient may then change.

If the particles are very small, the mass-transfer coefficient to the particle in an agitated system can be predicted by using equations given in Section 7.4. For larger particles, which are usually present in leaching, equations for predicting the mass-transfer coefficient k_L in agitated mixing vessels are given in Section 7.4 and reference (B1).

Rate of leaching when diffusion in solid controls

In the case where unsteady-state diffusion in the solid is the controlling resistance in the leaching of the solute by an external solvent, the following approximations can be used. If the average diffusivity D_{Aeff} of solute A is approximately constant, then for extraction in a batch process, unsteady-state mass-transfer equations can be used, as discussed in Section 7.1. If the particle is approximately spherical, Fig. 5.3-13 can be used.

EXAMPLE 12.8-1. Prediction of Time for Batch Leaching

Particles having an average diameter of approximately 2.0 mm are leached in a batch-type apparatus with a large volume of solvent. The concentration of the solute A in the solvent is kept approximately constant. A time of 3.11 h is needed to leach 80% of the available solute from the solid. Assuming that diffusion in the solid is controlling and the effective diffusivity is constant, calculate the time of leaching if the particle size is reduced to 1.5 mm.

Solution: For 80% extraction, the fraction unextracted E_s is 0.20. Using Fig. 5.3-13 for a sphere, for $E_s = 0.20$, a value of $D_{Aeff} t/a^2 = 0.112$ is obtained, where D_{Aeff} is the effective diffusivity in mm^2/s , t is time in s, and a is radius in mm. For the same fraction E_s , the value of $D_{Aeff} t/a^2$ is constant for a different size. Hence,

Equation 12.8-5.

$$t_2 = \frac{t_1 a_2^2}{a_1^2}$$

where t_2 is time for leaching with a particle size a_2 . Substituting into Eq. (12.8-5),

$$t_2 = (3.11) \frac{(1.5/2)^2}{(2.0/2)^2} = 1.75 \text{ h}$$

Methods of operation in leaching

There are a number of general methods of operation in the leaching of solids. The operations can be carried out under batch or unsteady-state conditions as well as under continuous or steady-state conditions. Both continuous and stagewise types of equipment are used in steady or unsteady-state operation.

In unsteady-state leaching, a method commonly used in the mineral industries is *in-place leaching*, where the solvent is allowed to percolate through the actual ore body. In other cases the leach liquor is pumped over a pile of crushed ore and collected at the ground level as it drains from the heap. Copper is leached by sulfuric acid solutions from sulfide ores in this manner.

Crushed solids are often leached by percolation through stationary solid beds in a vessel with a perforated bottom to permit drainage of the solvent. The solids should not be too fine, or a high resistance to flow will be encountered. Sometimes a number of tanks are used in series, called an *extraction battery*, and fresh solvent is fed to the solid that is most nearly extracted. The tanks can be open tanks or closed tanks called *diffusers*. The solvent flows through the tanks in series, being withdrawn from the freshly charged tank. This simulates a continuous countercurrent stage operation. As a tank is completely leached, a fresh charge is added to the tank at the other end. Multiple piping is used so that tanks do not have to be moved for countercurrent operation. This is often called the *Shanks system*. It is used widely in leaching sodium nitrate from ore, recovering tannins from barks and woods, in the mineral industries, in the sugar industry, and in other processes.

In some processes the crushed solid particles are moved continuously by bucket-type conveyors or a screw conveyor. The solvent flows countercurrent to the moving bed.

Finely ground solids may be leached in agitated vessels or in thickeners. The process can be unsteady-state batch or the vessels can be arranged in a series to obtain a countercurrent stage process.

Types of Equipment for Leaching

Fixed-bed leaching

Fixed-bed leaching is used in the beet sugar industry and is also used for the extraction of tanning extracts from tanbark, for the extraction of pharmaceuticals from barks and seeds, and in other processes. In Fig. 12.8-1 a typical sugar beet diffuser or extractor is shown. The cover is removable so that sugar beet slices called *cossettes* can be dumped into the bed. Heated water at 344 K (71°C) to 350 K (77°C) flows into the bed to leach out the sugar. The leached sugar solution flows out the

bottom onto the next tank in series. Countercurrent operation is used in the Shanks system. The top and bottom covers are removable so that the leached beets can be removed and a fresh charge added. About 95% of the sugar in the beets is leached to yield an outlet solution from the system of about 12 wt %.

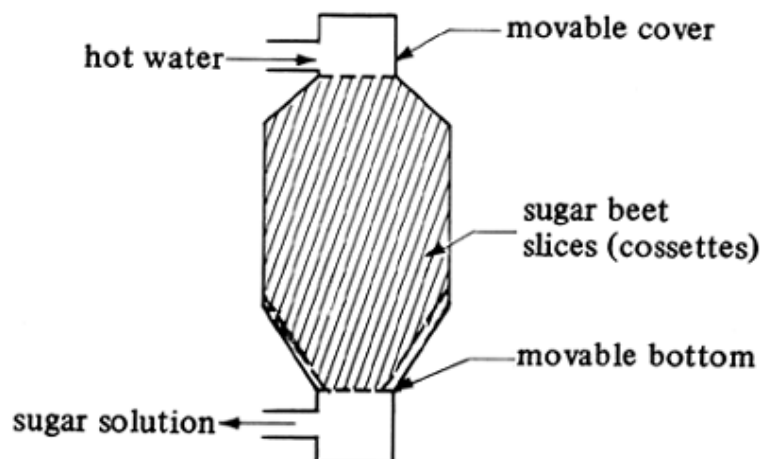


Figure 12.8-1. Typical fixed-bed apparatus for sugar beet leaching.

Moving-bed leaching

There are a number of devices for stagewise countercurrent leaching where the bed or stage moves instead of being stationary. These are used widely in extracting oil from vegetable seeds such as cottonseeds, peanuts, and soybeans. The seeds are usually dehulled first, sometimes precooked, often partially dried, and rolled or flaked. Sometimes preliminary removal of oil is accomplished by expression. The solvents are usually petroleum products, such as hexane. The final solvent–vegetable solution, called *miscella*, may contain some finely divided solids.

In Fig. 12.8-2a an enclosed moving-bed bucket elevator device is shown. This is called the *Bollman extractor*. Dry flakes or solids are added at the upper right side to a perforated basket or bucket. As the buckets on the right side descend, they are leached by a dilute solution of oil in solvent called *half miscella*. This liquid percolates downward through the moving buckets and is collected at the bottom as the strong solution or *full miscella*. The buckets moving upward on the left are leached countercurrently by fresh solvent sprayed on the top bucket. The wet flakes are dumped as shown and removed continuously.

The *Hildebrandt extractor* in Fig. 12.8-2b consists of three screw conveyors arranged in a U shape. The solids are charged at the top right, conveyed downward, across the bottom, and then up the other leg. The solvent flows countercurrently.

Agitated solid leaching

When the solid can be ground fine to about 200 mesh (0.074 mm), it can be kept in suspension by small amounts of agitation. Continuous countercurrent leaching can be accomplished by placing a number of agitators in series, with settling tanks or thickeners between each agitator.

Sometimes the thickeners themselves are used as combination contactor-agitators and settlers, as shown in Fig. 12.8-3. In this countercurrent-stage system, fresh solvent enters the first stage thickener as shown. The clear, settled liquid leaves and flows from stage to stage. The feed solids enter the last stage, where they are contacted with solvent from the previous stage and then enter the settler. The slowly rotating rake moves the solids to the bottom discharge. The solids together with some liquid are pumped as a slurry to the next tank. If the contact is insufficient, a mixer can be installed between the settlers.

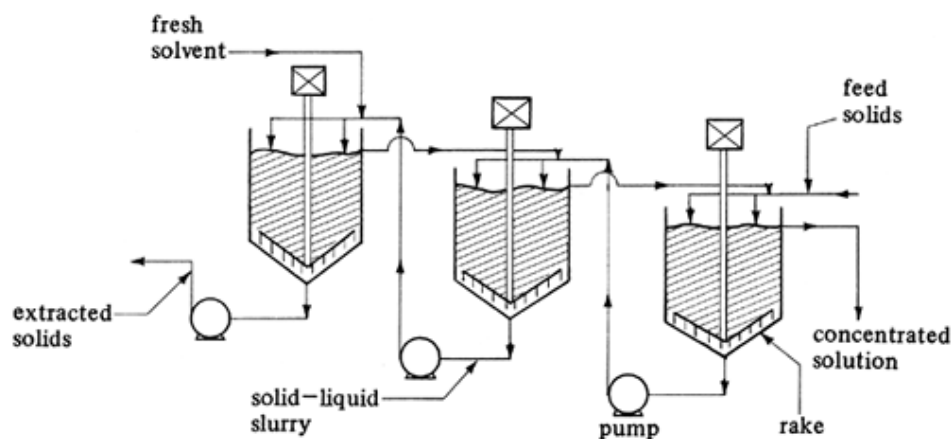


Figure 12.8-3. Countercurrent leaching using thickeners.

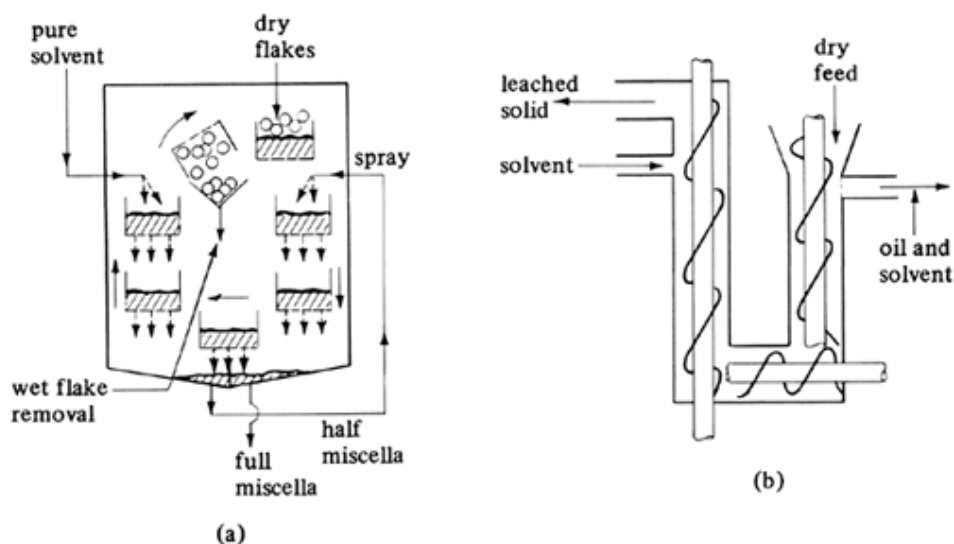


Figure 12.8-2. Equipment for moving-bed leaching: (a) Bollman bucket-type extractor, (b) Hildebrandt screw-conveyor extractor.

EQUILIBRIUM RELATIONS AND SINGLE-STAGE LEACHING

Equilibrium Relations in Leaching

Introduction

To analyze single-stage and countercurrent-stage leaching, an operating-line equation or material-balance relation and the equilibrium relations between the two streams are needed, as in liquid-liquid extraction. It is assumed that the solute-free solid is insoluble in the solvent. In leaching, assuming there is sufficient solvent present so that all the solute in the entering solid can be dissolved into the liquid, equilibrium is reached when the solute is dissolved. Hence, all the solute is completely dissolved in the first stage. There usually is sufficient time for this to occur in the first stage.

It is also assumed that there is no adsorption of the solute by the solid in the leaching. This means that the solution in the liquid phase leaving a stage is the same as the solution that remains with the solid matrix in the settled slurry leaving the stage. In the settler in a stage it is not possible or feasible to separate all the liquid from the solid. Hence, the settled solid leaving a stage always contains some liquid in which dissolved solute is present. This solid–liquid stream is called the *underflow* or *slurry stream*. Consequently, the concentration of oil or solute in the liquid or *overflow stream* is equal to the concentration of solute in the liquid solution accompanying the slurry or underflow stream. Hence, on an x - y plot the equilibrium line is on the 45° line.

The amount of solution retained with the solids in the settling portion of each stage may depend upon the viscosity and density of the liquid in which the solid is suspended. This, in turn, depends upon the concentration of the solute in the solution. Hence, experimental data showing the variation of the amount and composition of solution retained in the solids as a function of the solute composition must be obtained. These data should be obtained under conditions of concentrations, time, and temperature similar to those in the process for which the stage calculations are to be made.

Equilibrium diagrams for leaching

The equilibrium data can be plotted on the rectangular diagram as wt fraction for the three components: solute (A), inert or leached solid (B), and solvent (C). The two phases are the overflow (liquid) phase and the underflow (slurry) phase. This method is discussed elsewhere (B2). Another convenient method of plotting the equilibrium data will be used, instead, which is similar to the method discussed in the enthalpy–concentration plots in Section 11.6.

The concentration of inert or insoluble solid B in the solution mixture or the slurry mixture can be expressed in kg (lb_m) units:

Equation 12.9-1.

$$N = \frac{\text{kg } B}{\text{kg } A + \text{kg } C} = \frac{\text{kg solid}}{\text{kg solution}} = \frac{\text{lb solid}}{\text{lb solution}}$$

There will be a value of N for the overflow where $N = 0$, and for the underflow N will have different values, depending on the solute concentration in the liquid. The compositions of solute A in the liquid will be expressed as wt fractions:

Equation 12.9-2.

$$x_A = \frac{\text{kg } A}{\text{kg } A + \text{kg } C} = \frac{\text{kg solute}}{\text{kg solution}} \quad (\text{overflow liquid})$$

Equation 12.9-3.

$$y_A = \frac{\text{kg } A}{\text{kg } A + \text{kg } C} = \frac{\text{kg solute}}{\text{kg solution}} \quad (\text{liquid in slurry})$$

where x_A is the wt fraction of solute A in the overflow liquid and y_A is the wt fraction of A on a solid- B -free basis in the liquid associated with the slurry or underflow. For the entering solid feed to be leached, N is kg inert solid/kg solute A and $y_A = 1.0$. For pure entering solvent $N = 0$ and $x_A = 0$.

In Fig. 12.9-1a a typical equilibrium diagram is shown, where solute A is infinitely soluble in solvent C , which would occur, for example, in the system soybean oil (A)–soybean inert solid meal (B)–hexane solvent (C). The upper curve of N versus y_A for the slurry underflow represents the separated solid under experimental conditions similar to the actual stage process. The bottom line of N versus x_A , where $N = 0$ on the axis, represents the overflow liquid composition where all the solid has been

removed. In some cases small amounts of solid may remain in the overflow. The tie lines are vertical, and on a y - x diagram, the equilibrium line is $y_A = x_A$ on the 45° line. In Fig. 12.9-1b the tie lines are not vertical, which can result from insufficient contact time, so that all the solute is not dissolved; adsorption of solute A on the solid; or the solute being soluble in the solid B .

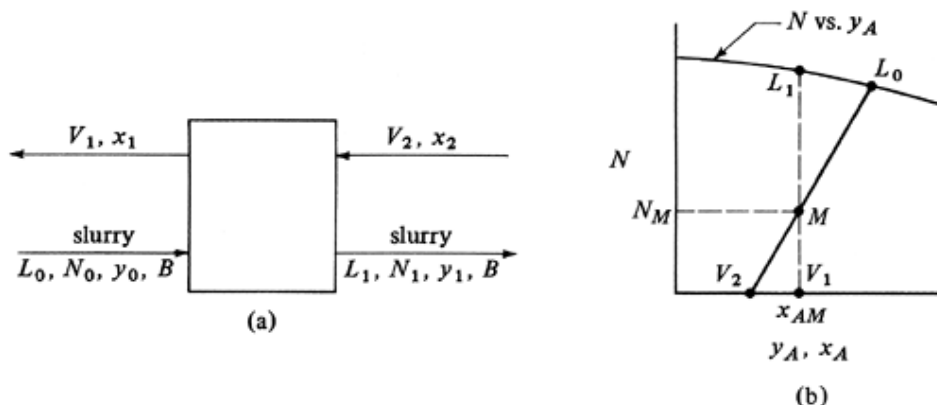


Figure 12.9-2. Process flow and material balance for single-stage leaching: (a) process flow, (b) material balance.

If the underflow line of N versus y is straight and horizontal, the amount of liquid associated with the solid in the slurry is constant for all concentrations. This would mean that the underflow liquid rate is constant throughout the various stages as well as the overflow stream. This is a special case which is sometimes approximated in practice.

Single-Stage Leaching

In Fig. 12.9-2a a single-stage leaching process is shown where V is kg/h (lb_m/h) of overflow solution with composition x_A and L is kg/h of liquid in the slurry solution with composition y_A based on a given flow rate B kg/h of dry, solute-free solid. The material-balance equations are almost identical to Eqs. (12.5-12)–(12.5-14) for single-stage liquid–liquid extraction and are as follows for a total solution balance (solute A + solvent C), a component balance on A , and a solids balance on B , respectively:

Equation 12.9-4.

$$L_0 + V_2 = L_1 + V_1 = M$$

Equation 12.9-5.

$$L_0 y_{A0} + V_2 x_{A2} = L_1 y_{A1} + V_1 x_{A1} = M x_{AM}$$

Equation 12.9-6.

$$B = N_0 L_0 + 0 = N_1 L_1 + 0 = N_M M$$

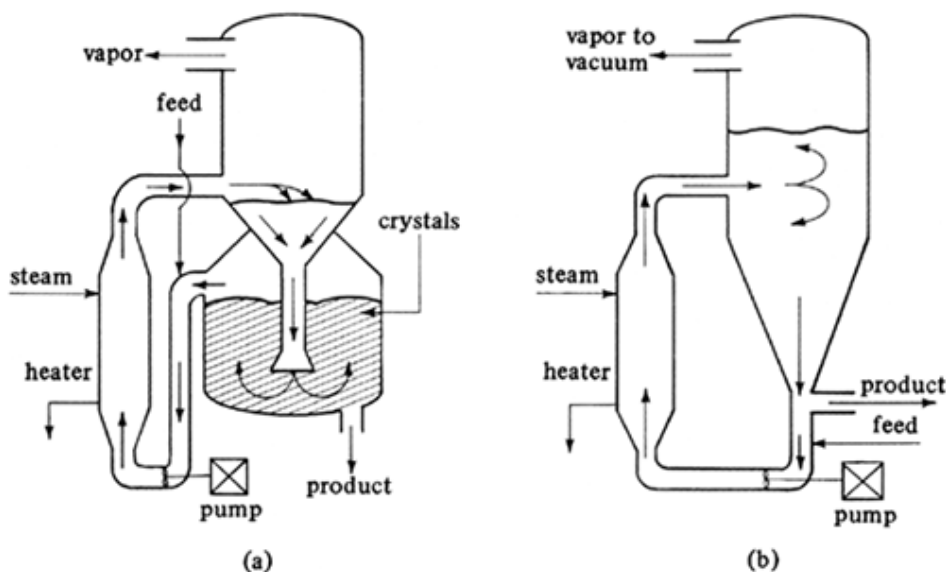


Figure 12.11-3. Types of crystallizers: (a) circulating-liquid evaporator-crystallizer, (b) circulating-magma vacuum crystallizer.

where M is the total flow rate in kg $A + C/h$ and x_{AM} and N_M are the coordinates of this point M . A balance on C is not needed, since $x_A + x_C = 1.0$ and $y_A + y_C = 1.0$. As shown before, L_1MV_1 must lie on a straight line and L_0MV_2 must also lie on a straight line. This is shown in Fig. 12.9-2b. Also, L_1 and V_1 must lie on the vertical tie line. The point M is the intersection of the two lines. If L_0 entering is the fresh solid feed to be leached with no solvent C present, it will be located above the N -versus- y line in Fig. 12.9-2b.

EXAMPLE 12.9-1. Single-Stage Leaching of Flaked Soybeans

In a single-stage leaching of soybean oil from flaked soybeans with hexane, 100 kg of soybeans containing 20 wt % oil is leached with 100 kg of fresh hexane solvent. The value of N for the slurry underflow is essentially constant at 1.5 kg insoluble solid/kg solution retained. Calculate the amounts and compositions of the overflow V_1 and the underflow slurry L_1 leaving the stage.

Solution: The process flow diagram is the same as given in Fig. 12.9-2a. The known process variables are as follows: for the entering solvent flow, $V_2 = 100$ kg, $x_{A2} = 0$, $x_{C2} = 1.0$; for the entering slurry stream, $B = 100(1.0 - 0.2) = 80$ kg insoluble solid, $L_0 = 100(1.0 - 0.8) = 20$ kg A , $N_0 = 80/20 = 4.0$ kg solid/kg solution, $y_{A0} = 1.0$.

To calculate the location of M , substituting into Eqs. (12.9-4), (12.9-5), and (12.9-6) and solving,

$$L_0 + V_2 = 20 + 100 = 120 \text{ kg} = M$$

$$L_0 y_{A0} + V_2 x_{A2} = 20(1.0) + 100(0) = 120 x_{AM}$$

Hence, $x_{AM} = 0.167$.

$$B = N_0 L_0 = 4.0(20) = 80 = N_M(120)$$

$$N_M = 0.667$$

The point M is plotted in Fig. 12.9-3 along with V_2 and L_0 . The vertical tie line is drawn locating L_1 and V_1 in equilibrium with each other. Then $N_1 = 1.5$, $y_{A1} = 0.167$, $x_{A1} = 0.167$. Substituting into Eqs. (12.9-4) and (12.9-6) and solving or using the lever-arm rule, $L_1 = 53.3$ kg and $V_1 = 66.7$ kg.

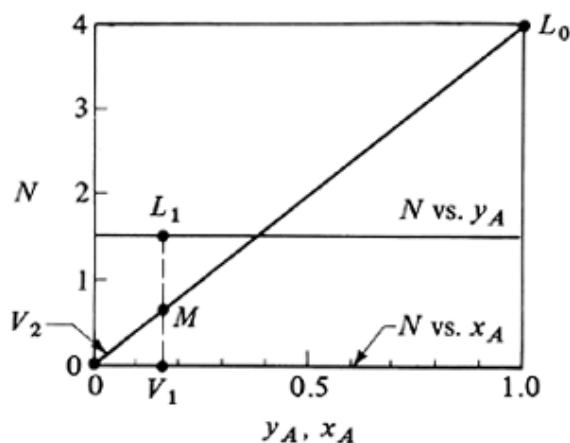


Figure 12.9-3. Graphical solution of single-stage leaching for Example 12.9-1.

COUNTERCURRENT MULTISTAGE LEACHING

Introduction and Operating Line for Countercurrent Leaching

A process flow diagram for countercurrent multistage leaching is shown in Fig. 12.10-1 and is similar to Fig. 12.7-1 for liquid–liquid extraction. The ideal stages are numbered in the direction of the solids or underflow stream. The solvent (C)–solute (A) phase or V phase is the liquid phase that overflows continuously from stage to stage countercurrent to the solid phase, dissolving solute as it moves along. The slurry phase L composed of inert solids (B) and a liquid phase of A and C is the continuous underflow from each stage. Note that the composition of the V phase is denoted by x and the composition of the L phase by y , which is the reverse of that for liquid–liquid extraction.

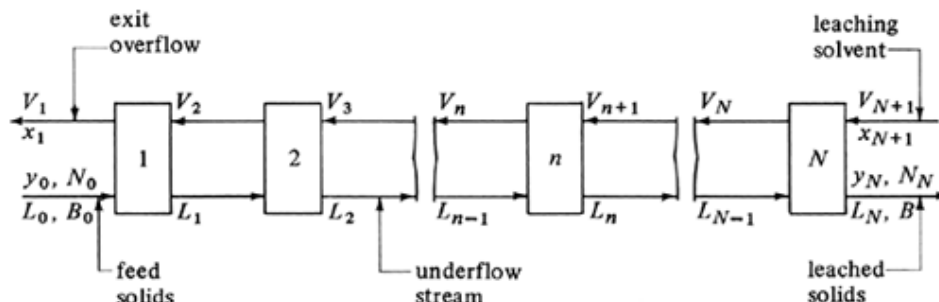


Figure 12.10-1. Process flow for countercurrent multistage leaching.

It is assumed that solid B is insoluble and is not lost in the liquid V phase. The flow rate of the solids is constant throughout the cascade of stages. As in single-stage leaching, V is kg/h (lb_m/h) of overflow solution and L is kg/h of liquid solution in the slurry retained by the solid.

In order to derive the operating-line equation, an overall balance and a component balance on solute A is made over the first n stages:

Equation 12.10-1.

$$V_{n+1} + L_0 = V_1 + L_n$$

Equation 12.10-2.

$$V_{n+1}x_{n+1} + L_0y_0 = V_1x_1 + L_ny_n$$

Solving for x_{n+1} and eliminating V_{n+1} ,

Equation 12.10-3.

$$x_{n+1} = \frac{1}{1 + (V_1 - L_0)/L_n} y_n + \frac{V_1 x_1 - L_0 x_0}{L_n + V_1 - L_0}$$

The operating-line equation (12.10-3), when plotted on an x - y plot, passes through the terminal points x_1, y_0 and x_{N+1}, y_N .

In the leaching process, if the viscosity and density of the solution change appreciably with the solute (A) concentration, the solids from the lower-numbered stages where solute concentrations are high may retain more liquid solution than the solids from the higher-numbered stages, where the solute concentration is dilute. Then L_n , the liquid retained in the solids underflow, will vary, and the slope of Eq. (12.10-3) will vary from stage to stage. This condition of variable underflow will be considered first. The overflow will also vary. If the amount of solution L_n retained by the solid is constant and independent of concentration, then constant underflow occurs. This simplifies somewhat the stage-to-stage calculations. This case will be considered later.

Variable Underflow in Countercurrent Multistage Leaching

The methods in this section are very similar to those used in Section 12.7B for countercurrent solvent extraction, where the L and V flow rates varied from stage to stage. Making an overall total solution (solute A + solvent C) balance on the process shown in Fig. 12.10-1,

Equation 12.10-4.

$$L_0 + V_{N+1} = L_N + V_1 = M$$

where M is the total mixture flow rate in kg A + C/h. Next, making a component balance on A,

Equation 12.10-5.

$$L_0 y_{A0} + V_{N+1} x_{AN+1} = L_N y_{AN} + V_1 x_{A1} = M x_{AM}$$

Making a total solids balance on B,

Equation 12.10-6.

$$B = N_0 L_0 = N_N L_N = N_M M$$

where N_M and x_{AM} are the coordinates of point M shown in Fig. 12.10-2, which is the operating diagram for the process. As demonstrated previously, $L_0 M V_{N+1}$ must lie on a straight line and $V_1 M L_N$ must also lie on a straight line. Usually the flows and compositions of L_0 and V_{N+1} are known and the desired exit concentration y_{AN} is set. Then the coordinates N_M and x_{AM} can be calculated from Eqs. (12.10-4)–(12.10-6) and point M plotted. Then L_N, M , and V_1 must lie on one line, as shown in Fig. 12.10-2.

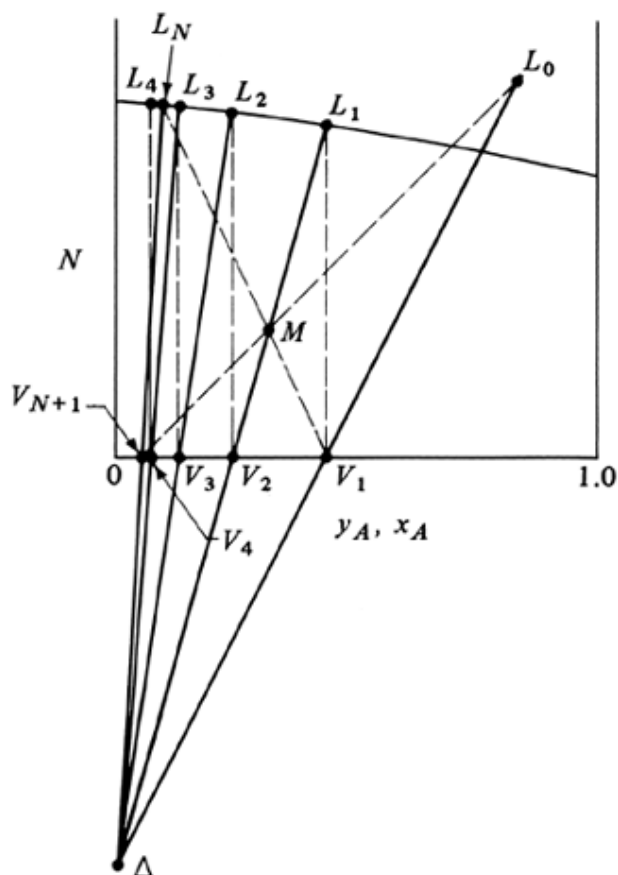


Figure 12.10-2. Number of stages for multistage countercurrent leaching.

In order to go stage by stage on Fig. 12.10-2, we must derive the operating-point equation. Making a total balance on stage 1 and then on stage n ,

Equation 12.10-7.

$$L_0 + V_2 = L_1 + V_1$$

Equation 12.10-8.

$$L_{n-1} + V_{n+1} = L_n + V_n$$

Rearranging Eq. (12.10-7) for the difference flows Δ in kg/h,

Equation 12.10-9.

$$L_0 - V_1 = L_1 - V_2 = \Delta$$

This value Δ is constant and also holds for Eq. (12.10-8) rearranged and for all stages:

Equation 12.10-10.

$$\Delta = L_0 - V_1 = L_n - V_{n+1} = L_N - V_{N+1} = \dots$$

This can also be written for a balance on solute A to give

Equation 12.10-11.

$$x_{A\Delta} = \frac{L_0 y_{A0} - V_1 x_{A1}}{L_0 - V_1} = \frac{L_N y_{AN} - V_{N+1} x_{AN+1}}{L_N - V_{N+1}}$$

where $x_{A\Delta}$ is the x coordinate of the operating point Δ . A balance made on solids gives

Equation 12.10-12.

$$N_{\Delta} = \frac{B}{L_0 - V_1} = \frac{N_0 L_0}{L_0 - V_1}$$

where N_{Δ} is the N coordinate of the operating point Δ .

As shown in Section 12.7B, Δ is the operating point. This point Δ is located graphically in Fig. 12.10-2 as the intersection of lines $L_0 V_1$ and $L_N V_{N+1}$. From Eq. (12.10-10) we see that V_1 is on a line between L_0 and Δ , V_2 is on a line between L_1 and Δ , V_{n+1} is on a line between L_n and Δ , and so on.

To graphically determine the number of stages, we start at L_0 and draw line $L_0 \Delta$ to locate V_1 . A tie line through V_1 locates L_1 . Line $L_1 \Delta$ is drawn given V_2 . A tie line gives L_2 . This is continued until the desired L_N is reached. In Fig. 12.10-2, about 3.5 stages are required.

EXAMPLE 12.10-1. Countercurrent Leaching of Oil from Meal

A continuous countercurrent multistage system is to be used to leach oil from meal by benzene solvent (B3). The process is to treat 2000 kg/h of inert solid meal (B) containing 800 kg oil (A) and also 50 kg benzene (C). The inlet flow per hour of fresh solvent mixture contains 1310 kg benzene and 20 kg oil. The leached solids are to contain 120 kg oil. Settling experiments similar to those in the actual extractor show that the solution retained depends upon the concentration of oil in the solution. The data (B3) are tabulated below as N /kg inert solid B /kg solution and y_A kg oil A /kg solution:

| N | y_A | N | y_A |
|------|-------|------|-------|
| 2.00 | 0 | 1.82 | 0.4 |
| 1.98 | 0.1 | 1.75 | 0.5 |
| 1.94 | 0.2 | 1.68 | 0.6 |
| 1.89 | 0.3 | 1.61 | 0.7 |

Calculate the amounts and concentrations of the stream leaving the process and the number of stages required.

Solution: The underflow data from the table are plotted in Fig. 12.10-3 as N versus y_A . For the inlet solution with the untreated solid, $L_0 = 800 + 50 = 850$ kg/h, $y_{A0} = 800/(800 + 50) = 0.941$, $B = 2000$ kg/h, $N_0 = 2000/(800 + 50) = 2.36$. For the inlet leaching solvent, $V_{N+1} = 1310 + 20 = 1330$ kg/h and $x_{AN+1} = 20/1330 = 0.015$. The points V_{N+1} and L_0 are plotted.

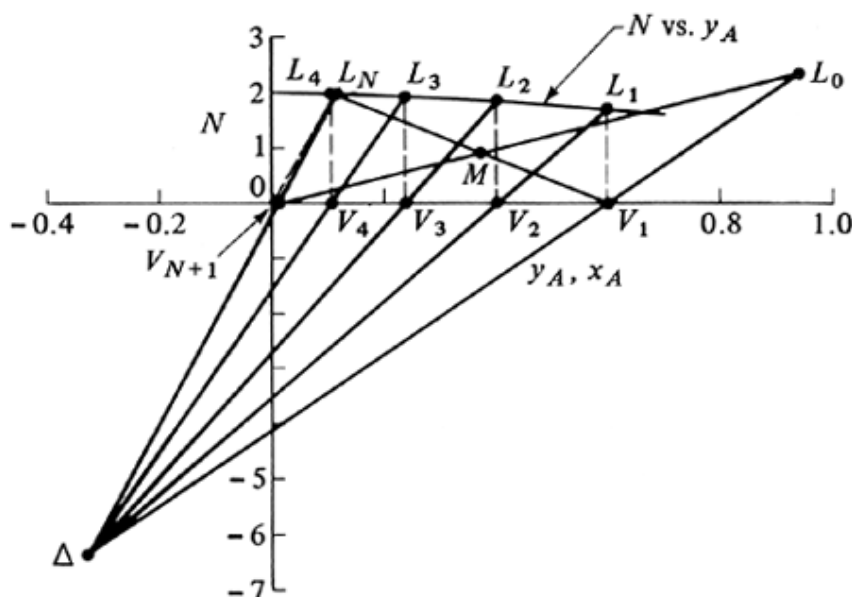


Figure 12.10-3. Graphical construction for number of stages for Example 12.10-1.

The point L_N lies on the N -versus- y_A line in Fig. 12.10-3. Also for this point, the ratio $N_N/y_{AN} = (\text{kg solid/kg solution})/(\text{kg oil/kg solution}) = \text{kg solid/kg oil} = 2000/120 = 16.67$. Hence, a dashed line through the origin at $y_A = 0$ and $N = 0$ is plotted with a slope of 16.67 and intersects the N -versus- y_A line at L_N . The coordinates of L_N at this intersection are $N_N = 1.95$ kg solid/kg solution and $y_{AN} = 0.118$ kg oil/kg solution.

Making an overall balance by substituting into Eq. (12.10-4) to determine point M ,

$$L_0 + V_{N+1} = 850 + 1330 = 2180 \text{ kg/h} = M$$

Substituting into Eq. (12.10-5) and solving,

$$L_0 y_{A0} + V_{N+1} x_{AN+1} = 850(0.941) + 1330(0.015) = 2180 x_{AM}$$

$$x_{AM} = 0.376$$

Substituting into Eq. (12.10-6) and solving,

$$B = 2000 = N_M M = N_M(2180) \quad N_M = 0.918$$

The point M is plotted with the coordinates $x_{AM} = 0.376$ and $N_M = 0.918$ in Fig. 12.10-3. The line $V_{N+1}M$ is drawn, as is line $L_N M$, which intersects the abscissa at point V_1 where $x_{A1} = 0.600$.

The amounts of streams V_1 and L_N are calculated by substituting into Eqs. (12.10-4) and (12.10-5), and solving simultaneously:

$$L_N + V_1 = M = 2180$$

$$L_N y_{AN} + V_1 x_{A1} = L_N(0.118) + V_1(0.600) = 2180(0.376)$$

Hence, $L_N = 1016$ kg solution/h in the outlet underflow stream and $V_1 = 1164$ kg solution/h in the exit overflow stream. Alternatively, the amounts could have been calculated using the lever-arm rule.

The operating point Δ is obtained as the intersection of lines $L_0 V_1$ and $L_N V_{N+1}$ in Fig. 12.10-3. Its coordinates can also be calculated from Eqs. (12.10-11) and (12.10-12). The stages are stepped off as shown. The fourth stage for L_4 is slightly past the desired L_N . Hence, about 3.9 stages are required.

Constant Underflow in Countercurrent Multistage Leaching

In this case the liquid L_n retained in the underflow solids is constant from stage to stage. This means that a plot of N versus y_A is a horizontal straight line and N is constant. Then the operating-line equation (12.10-3) is a straight line when plotted as y_A versus x_A . The equilibrium line can also be plotted on the same diagram. In many cases the equilibrium line may also be straight, with $y_A = x_A$. Special treatment must be given the first stage, however, as L_0 is generally not equal to L_n , since it contains little or no solvent. A separate material and equilibrium balance is made on stage 1 to obtain L_1 and V_2 (see Fig. 12.10-1). Then the straight operating line can be used and the McCabe–Thiele method used to step off the number of stages.

Since this procedure for constant underflow requires almost as many calculations as the general case for variable underflow, the general procedure can be used for constant underflow by simply using a horizontal line of N versus y_A in Fig. 12.10-2 and stepping off the stages with the Δ point.

INTRODUCTION AND EQUIPMENT FOR CRYSTALLIZATION

Crystallization and Types of Crystals

Introduction

Separation processes for gas–liquid and liquid–liquid systems have been treated in this and previous chapters. Also, the separation process of leaching was discussed for a solid–liquid system. Crystallization is another solid–liquid separation process, in which mass transfer of a solute from the liquid solution to a pure solid crystalline phase occurs. An important example is in the production of sucrose from sugar beet, where the sucrose is crystallized out from an aqueous solution.

Crystallization is a process where solid particles are formed from a homogeneous phase. This process can occur in the freezing of water to form ice, in the formation of snow particles from a vapor, in the formation of solid particles from a liquid melt, or in the formation of solid crystals from a liquid solution. The last process mentioned, crystallization from a solution, is the most important one commercially and will be treated in the present discussion. In crystallization the solution is concentrated and usually cooled until the solute concentration becomes greater than its solubility at that temperature. Then the solute comes out of the solution, forming crystals of approximately pure solute.

In commercial crystallization not only are the yield and purity of the crystals important but also the sizes and shapes of the crystals. It is often desirable that crystals be uniform in size. Size uniformity is desirable to minimize caking in the package, for ease of pouring, for ease in washing and filtering, and for uniform behavior when used. Sometimes large crystals are requested by the purchaser, even though smaller crystals are just as useful. Also, crystals of a certain shape are sometimes required, such as needles rather than cubes.

Types of crystal geometry

A crystal can be defined as a solid composed of atoms, ions, or molecules which are arranged in an orderly and repetitive manner. It is a highly organized type of matter. The atoms, ions, or molecules are located in three-dimensional arrays or space lattices. The interatomic distances between these imaginary planes or space lattices in a crystal are measured by X-ray diffraction, as are the angles between these planes. The pattern or arrangement of these space lattices is repeated in all directions.

Crystals appear as polyhedrons having flat faces and sharp corners. The relative sizes of the faces and edges of different crystals of the same material may differ greatly. However, the angles between the corresponding faces of all crystals of the same material are equal and are characteristic of that particular material. Therefore, crystals are classified on the basis of these interfacial angles.

There are seven classes of crystals, depending upon the arrangement of the axes to which the angles are referred:

1. Cubic system. Three equal axes at right angles to each other.
2. Tetragonal system. Three axes at right angles to each other, one axis longer than the other two.
3. Orthorhombic system. Three axes at right angles to each other, all of different lengths.
4. Hexagonal system. Three equal axes in one plane at 60° to each other, and a fourth axis at right angles to this plane and not necessarily the same length.
5. Monoclinic system. Three unequal axes, two at right angles in a plane and a third at some angle to this plane.
6. Triclinic system. Three unequal axes at unequal angles to each other and not 30° , 60° , or 90° .
7. Trigonal system. Three equal and equally inclined axes.

The relative development of different types of faces of a crystal may differ depending on the solute crystallizing. Sodium chloride crystallizes from aqueous solutions with cubic faces only. But if sodium chloride crystallizes from an aqueous solution with a given slight impurity present, the crystals will have octahedral faces. Both types of crystals, however, are in the cubic system. The crystallization in overall shapes of plates or needles has no relation to the type of crystal system and usually depends upon the process conditions under which the crystals are grown.

Equilibrium Solubility in Crystallization

In crystallization equilibrium is attained when the solution or mother liquor is saturated. This is represented by a *solubility curve*. Solubility is dependent mainly upon temperature. Pressure has a negligible effect on solubility. Solubility data are given in the form of curves where solubilities in some convenient units are plotted versus temperature. Tables of solubilities are given in many chemical handbooks (P1). Solubility curves for some typical salts in water were given in Fig. 8.1-1. In general, the solubilities of most salts increase slightly or markedly with increasing temperature.

A very common type of curve is shown in Fig. 8.1-1 for KNO_3 , where the solubility increases markedly with temperature and there are no hydrates. Over the whole range of temperatures, the solid phase is KNO_3 . The solubility of NaCl is marked by its small change with temperature. In solubility plots the solubility data are ordinarily given as parts by weight of anhydrous material per 100 parts by weight of total solvent (i.e., water in many cases).

In Fig. 12.11-1 the solubility curve is shown for sodium thiosulfate, $\text{Na}_2\text{S}_2\text{O}_3$. The solubility increases rapidly with temperature, but there are definite breaks in the curve which indicate different hydrates. The stable phase up to 48.2°C is the pentahydrate $\text{Na}_2\text{S}_2\text{O}_3 \cdot 5\text{H}_2\text{O}$. This means that at concentrations above the solubility line (up to 48.2°C), the solid crystals formed are $\text{Na}_2\text{S}_2\text{O}_3 \cdot 5\text{H}_2\text{O}$. At concentrations below the solubility line, only a solution exists. From 48.2 to about 65°C , the stable phase is $\text{Na}_2\text{S}_2\text{O}_3 \cdot 2\text{H}_2\text{O}$. A half-hydrate is present between 65 to 70°C , and the anhydrous salt is the stable phase above 70°C .

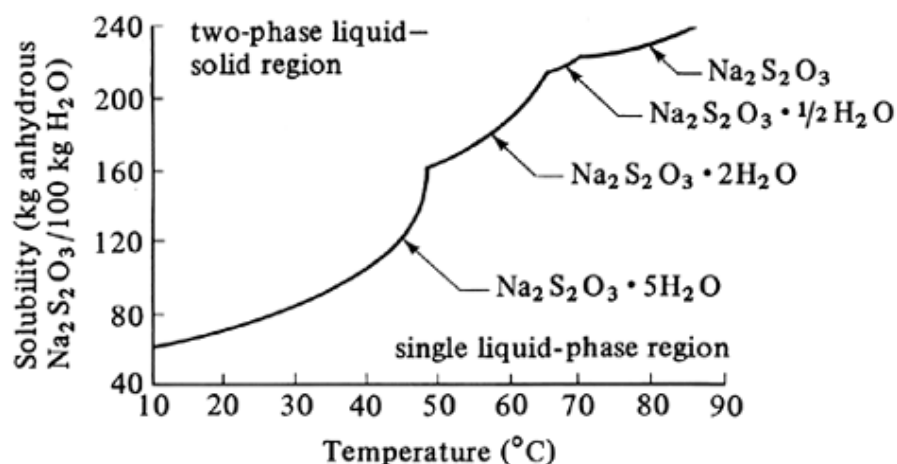


Figure 12.11-1. Solubility of sodium thiosulfate, $\text{Na}_2\text{S}_2\text{O}_3$, in water.

Yields and Heat and Material Balances in Crystallization

Yields and material balances in crystallization

In most of the industrial crystallization processes, the solution (mother liquor) and the solid crystals are in contact for enough time to reach equilibrium. Hence, the mother liquor is saturated at the final temperature of the process, and the final concentration of the solute in the solution can be obtained from the solubility curve. The yield of crystals from a crystallization process can then be calculated knowing the initial concentration of solute, the final temperature, and the solubility at this temperature.

In some instances in commercial crystallization, the rate of crystal growth may be quite slow, due to a very viscous solution or a small surface of crystals exposed to the solution. Hence, some supersaturation may still exist, giving a lower yield of crystals than predicted.

In making the material balances, the calculations are straightforward when the solute crystals are anhydrous. Simple water and solute material balances are made. When the crystals are hydrated, some of the water in the solution is removed with the crystals as a hydrate.

EXAMPLE 12.11-1. Yield of a Crystallization Process

A salt solution weighing 10000 kg with 30 wt % Na_2CO_3 is cooled to 293 K (20°C). The salt crystallizes as the decahydrate. What will be the yield of $\text{Na}_2\text{CO}_3 \cdot 10\text{H}_2\text{O}$ crystals if the solubility is 21.5 kg anhydrous $\text{Na}_2\text{CO}_3/100$ kg of total water? Do this for the following cases:

- Assume that no water is evaporated.
- Assume that 3% of the total weight of the solution is lost by evaporation of water in cooling.

Solution: The molecular weights are 106.0 for Na_2CO_3 , 180.2 for $10\text{H}_2\text{O}$, and 286.2 for $\text{Na}_2\text{CO}_3 \cdot 10\text{H}_2\text{O}$. The process flow diagram is shown in Fig. 12.11-2, with W being kg H_2O evaporated, S kg solution (mother liquor), and C kg crystals of $\text{Na}_2\text{CO}_3 \cdot 10\text{H}_2\text{O}$. Making a material balance around the dashed-line box for water for part (a), where $W = 0$,

Equation 12.11-1.

$$0.70(10\,000) = \frac{100}{100 + 21.5}(S) + \frac{180.2}{286.2}(C) + 0$$

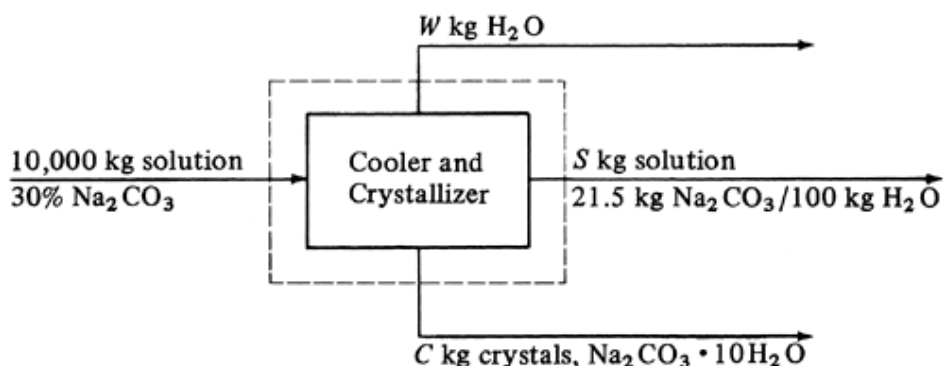


Figure 12.11-2. Process flow for crystallization in Example 12.11-1.

where $(180.2)/(286.2)$ is wt fraction of water in the crystals. Making a balance for Na_2CO_3 ,

Equation 12.11-2.

$$0.30(10\,000) = \frac{21.5}{100 + 21.5}(S) + \frac{106.0}{286.2}(C) + 0$$

Solving the two equations simultaneously, $C = 6370$ kg of $\text{Na}_2\text{CO}_3 \cdot 10\text{H}_2\text{O}$ crystals and $S = 3630$ kg solution.

For part (b), $W = 0.03(10\,000) = 300$ kg H_2O . Equation (12.11-1) becomes

Equation 12.11-3.

$$0.70(10\,000) = \frac{100}{100 + 21.5}(S) + \frac{180.2}{286.2}(C) + 300$$

Equation (12.11-2) does not change, since no salt is in the W stream. Solving Eqs. (12.11-2) and (12.11-3) simultaneously, $C = 6630$ kg of $\text{Na}_2\text{CO}_3 \cdot 10\text{H}_2\text{O}$ crystals and $S = 3070$ kg solution.

Heat effects and heat balances in crystallization

When a compound whose solubility increases as temperature increases dissolves, there is an absorption of heat, called the *heat of solution*. An evolution of heat occurs when a compound dissolves whose solubility decreases as temperature increases. For compounds dissolving whose solubility does not change with temperature, there is no heat evolution on dissolution. Most data on heats of solution are given as the change in enthalpy in kJ/kg mol (kcal/g mol) of solute occurring with the dissolution of 1 kg mol of the solid in a large amount of solvent at essentially infinite dilution.

In crystallization the opposite of dissolution occurs. At equilibrium the heat of crystallization is equal to the negative of the heat of solution at the same concentration in solution. If the heat of dilution from saturation in the solution to infinite dilution is small, this can be neglected, and the negative of the heat of solution at infinite dilution can be used for the heat of crystallization. With many materials this heat of dilution is small compared with the heat of solution, and this approximation is reasonably accurate. Heat-of-solution data are available in several references (P1, N1).

Probably the most satisfactory method for calculating heat effects during a crystallization process is to use the enthalpy–concentration chart for the solution and the various solid phases which are present for the system. However, only a few such charts are available, including the following systems: calcium chloride–water (H1), magnesium sulfate–water (P2), and ferrous sulfate–water (K2). When such a chart is available, the following procedure is used. The enthalpy H_1 of the entering solution at the initial temperature is read off the chart, where H_1 is kJ (btu) for the total feed. The enthalpy H_2 of the final mixture of crystals and mother liquor at the final temperature is also read off the chart. If some evaporation occurs, the enthalpy H_v of the water vapor is obtained from the steam tables. Then the total heat absorbed q in kJ is

Equation 12.11-4.

$$q = (H_2 + H_V) - H_1$$

If q is positive, heat must be added to the system. If it is negative, heat is evolved or given off.

EXAMPLE 12.11-2. Heat Balance in Crystallization

A feed solution of 2268 kg at 327.6 K (54.4°C) containing 48.2 kg MgSO_4 /100 kg total water is cooled to 293.2 K (20°C), where $\text{MgSO}_4 \cdot 7\text{H}_2\text{O}$ crystals are removed. The solubility of the salt is 35.5 kg MgSO_4 /100 kg total water (P1). The average heat capacity of the feed solution can be assumed as 2.93 kJ/kg · K (H_1). The heat of solution at 291.2 K (18°C) is -13.31×10^3 kJ/kg mol $\text{MgSO}_4 \cdot 7\text{H}_2\text{O}$ (P1). Calculate the yield of crystals and make a heat balance to determine the total heat absorbed, q , assuming that no water is vaporized.

Solution: Making a water balance and a balance for MgSO_4 using equations similar to (12.11-1) and (12.11-2) in Example 12.11-1, $C = 616.9$ kg $\text{MgSO}_4 \cdot 7\text{H}_2\text{O}$ crystals and $S = 1651.1$ kg solution.

To make a heat balance, a datum of 293.2 K (20°C) will be used. The molecular weight of $\text{MgSO}_4 \cdot 7\text{H}_2\text{O}$ is 246.49. The enthalpy of the feed is H_1 :

$$H_1 = 2268(327.6 - 293.2)(2.93) = 228\,600 \text{ kJ}$$

The heat of solution is $-(13.31 \times 10^3)/246.49 = -54.0$ kJ/kg crystals. Then the heat of crystallization is $-(-54.0) = +54.0$ kJ/kg crystals, or $54.0(616.9) = 33\,312$ kJ. This assumes that the value at 291.2 K is the same as at 293.2 K. The total heat absorbed, q , is

$$q = -228\,600 - 33\,312 = -261\,912 \text{ kJ} (-248\,240 \text{ btu})$$

Since q is negative, heat is given off and must be removed.

Equipment for Crystallization

Introduction and classification of crystallizers

Crystallizers may be classified according to whether they are batch or continuous in operation. Batch operation is done for certain special applications. Continuous operation of crystallizers is generally preferred.

Crystallization cannot occur without *supersaturation*. A main function of any crystallizer is to cause a supersaturated solution to form. Crystallizing equipment can be classified according to the methods used to bring about supersaturation as follows: (1) supersaturation produced by cooling the solution with negligible evaporation—tank and batch-type crystallizers; (2) supersaturation produced by evaporation of the solvent with little or no cooling—evaporator–crystallizers and crystallizing evaporators; (3) supersaturation by combined cooling and evaporation in an adiabatic evaporator—vacuum crystallizers.

In crystallizers producing supersaturation by cooling, the substances must have a solubility curve that decreases markedly with temperature. This occurs for many substances, and this method is commonly used. When the solubility curve changes little with temperature, as for common salt, evaporation of the solvent to produce supersaturation is often used. Sometimes evaporation with some cooling may be used. In the method of cooling adiabatically in a vacuum, a hot solution is introduced into a vacuum, where the solvent flashes or evaporates and the solution is cooled adiabatically. This method for producing supersaturation is the most important one for large-scale production.

In another method of classification of crystallizers, the equipment is classified according to the method of suspending the growing product crystals. Examples are crystallizers where the suspension is agitated in a tank, is circulated by a heat exchanger, or is circulated in a scraped surface exchanger.

An important difference between many commercial crystallizers is the manner in which the supersaturated liquid contacts the growing crystals. In one method, called the *circulating magma method*, the entire magma of crystals and supersaturated liquid is circulated through both the supersaturation and crystallization steps without separating the solid from the liquid into two streams. Crystallization and supersaturation are occurring together in the presence of the crystals. In the second method, called the *circulating liquid method*, a separate stream of supersaturated liquid is passed through a fluidized bed of crystals, where the crystals grow and new ones form by nucleation. Then the saturated liquid is passed through an evaporating or cooling region to produce supersaturation again for recycling.

Tank crystallizers

In tank crystallization, which is an old method still used in some specialized cases, hot saturated solutions are allowed to cool in open tanks. After a period of time the mother liquor is drained and the crystals removed. Nucleation and the size of crystals are difficult to control. Crystals contain considerable amounts of occluded mother liquor. Labor costs are very high. In some cases the tank is cooled by coils or a jacket and an agitator used to improve the heat-transfer rate. However, crystals often build up on these surfaces. This type of crystallizer has limited application; it is sometimes used to produce certain fine chemicals and pharmaceutical products.

Scraped surface crystallizers

One type of scraped surface crystallizer is the Swenson–Walker crystallizer, which consists of an open trough 0.6 m wide with a semicircular bottom having a cooling jacket outside. A slow-speed spiral agitator rotates and suspends the growing crystals on turning. The blades pass close to the wall and break off any deposits of crystals on the cooled wall. The product generally has a somewhat wide crystal-size distribution.

In the double-pipe scraped surface crystallizer, cooling water passes in the annular space. An internal agitator is fitted with spring-loaded scrapers that wipe the wall and provide good heat-transfer coefficients. This type is called a *votator* and is used in crystallizing ice cream and plasticizing margarine. A sketch is given in Fig. 4.13-2.

Circulating-liquid evaporator–crystallizer

In a combination evaporator–crystallizer, shown in Fig. 12.11-3a, supersaturation is generated by evaporation. The circulating liquid is drawn by the screw pump down inside the tube side of the condensing steam heater. The heated liquid then flows into the vapor space, where flash evaporation occurs, giving some supersaturation. The vapor leaving is condensed. The supersaturated liquid flows down the downflow tube and then up through the bed of fluidized and agitated crystals, which are growing in size. The leaving saturated liquid then goes back as a recycle stream to the heater, where it is joined by the entering feed. The larger crystals settle out and a slurry of crystals and mother liquor is withdrawn as product. This type is also called the *Oslo crystallizer*.

Circulating-magma vacuum crystallizer

In the circulating-magma vacuum-type crystallizer shown in Fig. 12.11-3b, the magma or suspension of crystals is circulated out of the main body through a circulating pipe by a screw pump. The magma flows through a heater, where its temperature is raised 2–6 K. The heated liquor then mixes with body slurry and boiling occurs at the liquid surface. This causes supersaturation in the swirling liquid near the surface, which results in deposits on the swirling suspended crystals until they leave again via the circulating pipe. The vapors leave through the top. A steam-jet ejector provides the vacuum.

CRYSTALLIZATION THEORY

Introduction

When crystallization occurs in a homogeneous mixture, a new solid phase is created. An understanding of the mechanisms by which crystals form and then grow is helpful in designing and operating crystallizers. Much experimental and theoretical work has been done to help understand crystallization.

The overall process of crystallization from a supersaturated solution is considered to consist of the basic steps of nucleus formation or nucleation and of crystal growth. If the solution is free of all solid particles, whether foreign or of the crystallizing substance, then nucleus formation must first occur, before crystal growth starts. New nuclei may continue to form while the nuclei present are growing. The driving force for the nucleation step as well as the growth step is supersaturation. These two steps do not occur in a saturated or undersaturated solution.

Nucleation Theories

Solubility and crystal size

In a solution at a given temperature, the thermodynamic difference between small and large particles or crystals is that the small particle has a significant amount of surface energy per unit mass, whereas the large particle does not. As a result, the solubility of a small crystal, of less than micrometer size, is greater than that of a larger-size crystal.

The ordinary solubility applies only to moderately large crystals. Hence, in a supersaturated solution a small crystal can be in equilibrium. If a larger crystal is also present, the larger crystal will grow and the smaller crystal will dissolve. This effect of particle size is an important factor in nucleation.

Homogeneous nucleation

As a result of rapid random fluctuations of molecules in a homogeneous solution, the molecules may come together and associate into a cluster. This loose aggregate may quickly disappear. However, if the supersaturation is large enough, then enough particles may associate to form a nucleus which can grow and become oriented into a fixed lattice to form a crystal. The number of particles needed to form a stable nucleus ranges up to a few hundred. In solutions with high supersaturation and no agitation, homogeneous nucleation may be important.

Contact nucleation

This is due to two types of contact nucleation. In the first type, the formation of new nuclei by contact nucleation is due to interference of the contacting agent (walls of a container or agitator blades) with clusters of solute molecules becoming organized into the existing crystals and by actual breakage of microscopic growths on the surface of the growing crystals. In the second type, the formation of new nuclei occurs in collisions between crystals. The intensity of agitation is an important factor in contact nucleation.

This phenomenon of contact nucleation has been isolated and studied experimentally (B9, C4) and a correlation has been developed. In practice, experimental data from an actual crystallizer are required for design.

Nucleation in commercial crystallizers

In commercial crystallizers, supersaturation is low and agitation is used to keep the crystals suspended. At low supersaturation the crystal growth rate is at the optimum for more-uniform crystals. The predominant mechanism is contact nucleation. Homogeneous nucleation is largely absent because of the agitation and low supersaturation.

Rate of Crystal Growth and ΔL Law

Rate of crystal growth and growth coefficients

The rate of growth of a crystal face is the distance moved per unit time in a direction that is perpendicular to the face. Crystal growth is a layer-by-layer process, and since growth can occur only at the outer face of the crystal, the solute material must be transported to that face from the bulk of the solution. The solute molecules reach the face by diffusion through the liquid phase. The usual mass-transfer coefficient k_y applies in this case. At the surface the resistance to integration of the molecules into the space lattice at the face must be considered. This reaction at the surface occurs at a finite rate, and the overall process consists of two resistances in series. The solution must be supersaturated for the diffusion and interfacial steps to proceed.

The equation for mass transfer of solute A from the bulk solution of supersaturation concentration y_A , mole fraction of A , to the surface where the concentration is, y'_A , is

Equation 12.12-1.

$$\frac{\bar{N}_A}{A_i} = k_y(y_A - y'_A)$$

where k_y is the mass-transfer coefficient in $\text{kg mol}/\text{sm}^2\text{mol frac}$, \bar{N}_A is rate in $\text{kg mol } A/\text{s}$, and A_i is area in m^2 of surface i . Assuming that the rate of reaction at the crystal surface is also dependent on the concentration difference,

Equation 12.12-2.

$$\frac{\bar{N}_A}{A_i} = k_s(y'_A - y_{Ae})$$

where k_s is a surface-reaction coefficient in $\text{kg mol}/\text{s} \cdot \text{m}^2 \cdot \text{mol frac}$ and y_{Ae} is the saturation concentration. Combining Eqs. (12.12-1) and (12.12-2),

Equation 12.12-3.

$$\frac{\bar{N}_A}{A_i} = \frac{y_A - y_{Ae}}{1/k_y + 1/k_s} = K(y_A - y_{Ae})$$

where K is the overall transfer coefficient.

The mass-transfer coefficient k_y can be predicted by methods given in Section 7.4 for convective mass-transfer coefficients. When the mass-transfer coefficient k_y is very large, the surface reaction is controlling and $1/k_y$ is negligible. Conversely, when the mass-transfer coefficient is very small, diffusional resistance is controlling. Surface-reaction coefficients and overall transfer coefficients have been measured and reported for a number of systems (B4, H2, P3, V1). Much of the infor-

mation in the literature is not directly applicable, because the conditions of measurement differ greatly from those in a commercial crystallizer. Also, the velocities and the level of supersaturation in a system are difficult to determine, and vary with position of the circulating magma in the crystallizer.

The ΔL law of crystal growth.

McCabe (M1) has shown that all crystals that are geometrically similar and of the same material in the same solution grow at the same rate. Growth is measured as the increase in length ΔL , in mm, in linear dimension of one crystal. This increase in length is for geometrically corresponding distances on all crystals. This increase is independent of the initial size of the initial crystals, provided that all the crystals are subject to the same environmental conditions. This law follows from Eq. (12.12-3), where the overall transfer coefficient is the same for each face of all crystals.

Mathematically, this can be written

Equation 12.12-4.

$$\frac{\Delta L}{\Delta t} = G$$

where Δt is time in h and growth rate G is a constant in mm/h. Hence, if D_1 is the linear dimension of a given crystal at time t_1 and D_2 at time t_2 ,

Equation 12.12-5.

$$\Delta L = D_2 - D_1 = G(t_2 - t_1)$$

The total growth ($D_2 - D_1$) or ΔL is the same for all crystals.

The ΔL law fails in cases where the crystals are given any different treatment based on size. It has been found to hold for many materials, particularly when the crystals are under 50 mesh in size (0.3 mm). Even though this law is not applicable in all cases, it is reasonably accurate in many situations.

Particle-Size Distribution of Crystals

An important factor in the design of crystallization equipment is the expected particle-size distribution of the crystals obtained. Usually, the dried crystals are screened to determine the particle sizes. The percent retained on different-sized screens is recorded. The screens or sieves used are the Tyler standard screens, whose sieve or clear openings in mm are given in Appendix A.5-3.

The data are plotted as particle diameter (sieve opening in screen) in mm versus the cumulative percent retained at that size on arithmetic probability paper. Data for urea particles from a typical crystallizer (B5) are shown in Fig. 12.12-1. Many types of such data will show an approximate straight line for a large portion of the plot.

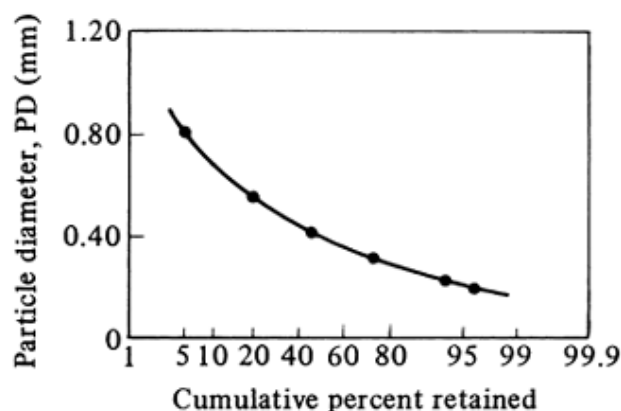


Figure 12.12-1. Typical particle-size distribution from a crystallizer. [From R. C. Bennett and M. Van Buren, *Chem. Eng. Progr. Symp.*, **65**(95), 46 (1969).]

A common parameter used to characterize the size distribution is the coefficient of variation, CV, as a percent:

Equation 12.12-6.

$$CV = 100 \frac{PD_{16\%} - PD_{84\%}}{2PD_{50\%}}$$

where $PD_{16\%}$ is the particle diameter at 16 percent retained. By giving the coefficient of variation and mean particle diameter, a description of the particle-size distribution is obtained if the line is approximately straight between 90 and 10%. For a product removed from a mixed-suspension crystallizer, the CV value is about 50% (R1). In a mixed-suspension system, the crystallizer is at steady state and contains a well-mixed-suspension magma with no product classification and no solids entering with the feed.

Model for Mixed Suspension–Mixed Product Removal Crystallizer

Introduction and model assumptions

This model will be derived for a mixed suspension–mixed product removal (MSMPR) crystallizer, which is by far the most important type of crystallizer in use in industry today. Conditions assumed are as follows: steady state, suspension completely mixed, no product classification, uniform concentration, no crystals in feed, and the ΔL law of crystal growth applies. All continuous crystallizers have mixing by an agitator or by pump around. In ideal mixing, the effluent composition is the same as in the vessel. This is similar to a CSTR continuous-stirred tank reactor.

Crystal population-density function n

To analyze data from a crystallizer, an overall theory must consider combining the effects of nucleation rate, growth rate, and material balance. Randolph and Larson (R1, R2, R3) derived such a model. They plotted the total cumulative number of crystals N per unit volume of suspension (usually 1 L) of size L and smaller versus this size L , as in Fig. 12.12-2. The slope dN/dL of this line is defined as the crystal population density n .

Equation 12.12-7.

$$n = dN/dL$$

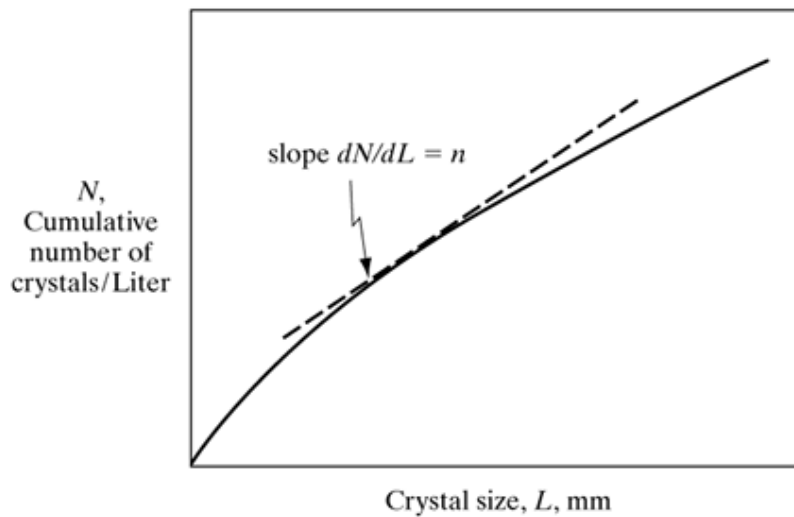


Figure 12.12-2. Determination of population density n of crystals.

where n is the number of crystals/(L · mm). This characterizes the nuclear growth rate of this crystallizer. For this model a relation between population density n and size L is desired.

This population density is obtained experimentally by screen analysis of the total crystal content of a given volume, such as 1.0 L of magma suspension. Each sieve fraction by weight is obtained by collection between two closely spaced and adjacent screens. Then, $L_{av} = (L_1 + L_2)/2$, where L_1 and L_2 are the openings in mm in the two adjacent screens. Also, $\Delta L = (L_1 - L_2)$, where L_1 is the size opening of the upper screen. Then the volume of a particle v_p is

Equation 12.12-8.

$$v_p = aL_{av}^3$$

where v_p is mm³/particle and a is a constant shape factor. Knowing the total weight of the crystals in this fraction, the density ρ in g/mm³, and the weight of each crystal, which is ρv_p , the total number of crystals ΔN is obtained for the size range ΔL .

Then, rewriting Eq. (12.12-7) for this ΔL size,

Equation 12.12-9.

$$n = \frac{dN}{dL} \cong \frac{\Delta N}{\Delta L}$$

This method permits the calculation of n for each fraction collected in the screen analysis with an average size of L_{av} mm.

Population material balance

To make a population material balance, in Δt time, $\Delta n \Delta L$ crystals are withdrawn. Since the effluent composition in the outflow of Q L/h is the same as that in the crystallizer, then the ratio $(\Delta n \Delta L)/(n \Delta L)$, or fraction of particles withdrawn during Δt time, is the same as the volume ratio $Q \Delta t$ withdrawn divided by the total volume V of the crystallizer. Hence,

Equation 12.12-10.

$$\frac{-\Delta n \Delta L}{n \Delta L} = \frac{Q \Delta t}{V}$$

During this time period Δt , the growth ΔL of a crystal is

Equation 12.12-11.

$$\Delta L = G \Delta t$$

where G is growth rate in mm/h. Combining Eqs. (12.12-10) and (12.12-11),

Equation 12.12-12.

$$\frac{-\Delta n}{n} = \frac{Q \Delta L}{VG}$$

Letting $\Delta L \rightarrow 0$, $\Delta n \rightarrow 0$, and integrating,

Equation 12.12-13.

$$\int_{n^0}^n \frac{dn}{n} = -\frac{1}{G\tau} \int_0^L dL$$

Equation 12.12-14.

$$\ln n = -\frac{L}{G\tau} + \ln n^0$$

where n^0 is population of nuclei when $L = 0$, n is population when the size is L , and VQ is the total retention or holdup time in h in the crystallizer. A plot of Eq. (12.12-14) of $\ln n$ versus L is a straight line with intercept n^0 and slope $-1/G\tau$. If the line is not straight, this could be an indication of the violation of the ΔL law. These calculations are well suited for being done with a computer spreadsheet.

Average particle size and nucleation rate

Further derivation of the population approach results in the equation for the average size L_a in mm of the mass distribution:

Equation 12.12-15.

$$L_a = 3.67 G\tau$$

Here, 50% of the mass of the product is smaller or larger in size than this value. Also, the predominant particle size is given as

Equation 12.12-16.

$$L_d = 3.00 G\tau$$

This predominant particle size means more of the mass is in this differential size interval than in any other size interval.

Another relation can be obtained from this model, which relates the nucleation rate B^0 to the value of the zero-size particle population density n^0 and the growth rate G . For the condition $L \rightarrow 0$, the limit of dN/dt (nucleation rate) can be written as

Equation 12.12-17.

$$\lim_{L \rightarrow 0} \frac{dN}{dt} = \lim_{L \rightarrow 0} \frac{dN}{dL} \frac{dL}{dt}$$

However, when $L \rightarrow 0$, the slope $dL/dt = G$, the slope $dN/dL = n^0$, and $B^0 = dN/dt$. Hence,

Equation 12.12-18.

$$B^0 = Gn^0$$

where B^0 is nucleation rate in number of nuclei/h · L.

Prediction of cumulative weight fraction obtained

The population equation can be used to perform a reverse calculation when only values of G and τ are known. The following equation has been derived from the population density function (L4):

Equation 12.12-19.

$$(1 - W_f) = e^{-x}(1 + x + x^2/2 + x^3/6)$$

where $x = L/G\tau$, and $(1 - W_f)$ is the cumulative wt fraction at opening L mm, which is in the same form of results as from a screen analysis.

Use of population-model approach for process design

The data for experimental crystal growth rate G and nucleation rate B^0 obtained by means of the population material balance are for one given set of conditions in the crystallizer. Then additional experiments can be conducted to determine the effect of residence time τ (production rate) and, possibly, pump-around rate (mixing) on B^0 and G . This is done until the desired distribution W_f from Eq. (12.12-19) is achieved. Or, in some cases, the goal may be for a desired dominant size L_d to be obtained. In many cases, as the residence time τ is increased, the experimental growth rate G decreases. Additional useful references are (B6, C2, C4, L5, M2, P1, R4, S2).

EXAMPLE 12.12-1. Growth and Nucleation Rates in MSMPR Crystallizer

Calculate the population density and nucleation growth rates for crystal samples of urea from a screen analysis. The slurry density (g of crystals) is 450 g/liter, the crystal shape factor a is 1.00, the crystal density ρ is 1.335 g/cm³, and the residence time τ is 3.38 h. The screen analysis from reference (B5) is as follows:

| Mesh | Wt % | Mesh | Wt % |
|----------|------|-----------|------|
| -14, +20 | 4.4 | -48, +65 | 15.5 |
| -20, +28 | 14.4 | -65, +100 | 7.4 |
| -28, +35 | 24.2 | -100 | 2.5 |
| -35, +48 | 31.6 | | |

Solution: The data above are tabulated in Table 12.12-1 using data from Appendix A.5-3. The value of L is the screen opening. For the 14–20 mesh portion, $L_{av} = (1.168 + 0.833)/2 = 1.001$ mm and $\Delta L = 1.168 - 0.833$

$= 0.335$ mm. For $L_{av} = 1.001$ mm, using Eq. (12.12-8), $v_p = aL_{av}^3 = 1.00(1.001)^3 = 1.003$ mm³/particle. The density $\rho = 1.335$ g/cm³ $= 1.335 \times 10^{-3}$ g/mm³ and the mass/particle $= \rho v_p = 1.335 \times 10^{-3}(1.003) = 1.339 \times 10^{-3}$ g. The total mass of crystals $= (450 \text{ g/L})(0.044 \text{ wt frac})$.

Table 12.12-1. Data and Calculations for Example 12.12-1

| Mesh | L (mm) | Mesh | L (mm) | L_{av} (mm) | ΔL (mm) | $\ln n$ | wt % |
|------|----------|------|----------|---------------|-----------------|---------|------|
| 14 | 1.168 | 20 | 0.833 | 1.001 | 0.335 | 10.695 | 4.4 |
| 20 | 0.833 | 28 | 0.589 | 0.711 | 0.244 | 13.224 | 14.4 |
| 28 | 0.589 | 35 | 0.417 | 0.503 | 0.172 | 15.131 | 24.2 |
| 35 | 0.417 | 48 | 0.295 | 0.356 | 0.122 | 16.778 | 31.6 |
| 48 | 0.295 | 65 | 0.208 | 0.252 | 0.087 | 17.441 | 15.5 |
| 65 | 0.208 | 100 | 0.147 | 0.178 | 0.061 | 18.099 | 7.4 |

Using Eq. (12.12-9) to calculate n for the 14–20 mesh size range,

$$\begin{aligned} n &= \frac{\Delta N}{\Delta L} = \frac{(450 \text{ g/L})(\text{wt frac})}{\rho(aL^3) \Delta L} \\ &= \frac{(450 \text{ g/L})(0.044)}{(1.335 \times 10^{-3} \text{ g/mm}^3)(1.00)(1.001 \text{ mm})^3(0.335 \text{ mm})} \\ &= 4.414 \times 10^4 \text{ number of crystals/L} \cdot \text{mm} \end{aligned}$$

Then $\ln n = \ln 4.414 \times 10^4 = 10.695$. For the 20–28 mesh size range, $L_{av} = 0.711/\text{mm}$, and $\Delta L = 0.244$. Then,

$$n = \frac{(450)(0.144)}{(1.335 \times 10^{-3})(1.00)(0.711)^3(0.244)} = 5.535 \times 10^5$$

Then $\ln n = 13.224$. Other values are calculated in a similar manner using a computer spreadsheet and are given in Table 12.12-1.

The $\ln n$ is plotted versus L in Fig. 12.12-3. The equation of this line is Eq. (12.12-14), where the slope is -9.12 and the intercept = 19.79:

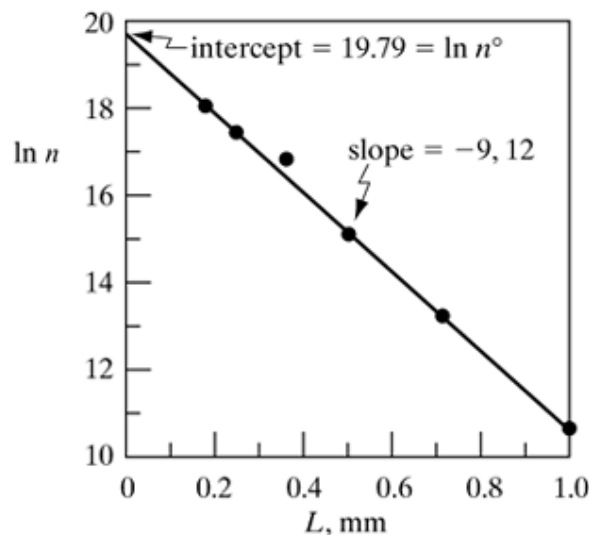


Figure 12.12-3. Plot of population density n versus length for Example 12.12-1.

$$\ln n = -9.12L + 19.79 = \frac{-L}{G\tau} + \ln n^0$$

The slope $-9.12 = -1/G\tau = -1/(G)(3.38)$. Hence, $G = 0.03244 \text{ mm/h}$. The intercept $\ln n^0 = 19.79$. Hence, $n^0 = 3.933 \times 10^8$. From Eq. (12.12-18), the nucleation rate B^0 is

$$B^0 = Gn^0 = 0.03244(3.933 \times 10^8) = 1.276 \times 10^7 \text{ nuclei/h} \cdot \text{L}$$

$$B^0 = Gn^0 = 0.03244(3.933 \times 10^8) = 1.26 \times 10^7 \text{ nuclei/h} \cdot \text{L}$$

The average size is, from Eq. (12.12-15), $L_a = 3.67G\tau = 3.67(0.03244)(3.38) = 0.402 \text{ mm}$. The predominant size, from Eq. (12.12-16), is $L_d = 3.00G\tau = 3.00(0.03244)(3.38) = 0.329 \text{ mm}$.

PROBLEMS

12.1-1.

Equilibrium Isotherm for Glucose Adsorption. Equilibrium isotherm data for adsorption of glucose from an aqueous solution to activated alumina are as follows (H3):

| | | | | | | |
|--------------------------|-------|--------|-------|-------|-------|-------|
| C (g/cm ³) | 0.004 | 0.0087 | 0.019 | 0.027 | 0.094 | 0.195 |
| | 0 | | | | | |
| q (g solute/g alumina) | 0.026 | 0.053 | 0.075 | 0.082 | 0.123 | 0.129 |

Determine the isotherm that fits the data and give the constants of the equation using the given units.

A1:

Ans. Langmuir isotherm, $q = 0.145c/(0.0174 + c)$

12.2-1.

Batch Adsorption for Phenol Solution. A wastewater solution having a volume of 2.5 m³ contains 0.25 kg phenol/m³ of solution. This solution is mixed thoroughly in a batch process with 3.0 kg of granular activated carbon until equilibrium is reached. Use the isotherm from Example 12.2-1 and calculate the final equilibrium values and the percent phenol extracted.

12.3-1.

Scale-Up of Laboratory Adsorption-Column Data. Using the break-point time and other results from Example 12.3-1, do as follows:

- The break-point time for a new column is to be 8.5 h. Calculate the new total length of the column required, column diameter, and the fraction of total capacity used up to the break point. The flow rate is to remain constant at 754 cm³/s.
- Use the same conditions as in part (a), but the flow rate is to be increased to 2000 cm³/s.

A3:

Ans. (a) $H_T = 27.2$ cm, 0.849 fraction; (b) $D = 6.52$ cm

12.3-2.

Drying of Nitrogen and Scale-Up of Column. Using molecular sieves, water vapor was removed from nitrogen gas in a packed bed (C3) at 28.3°C. The column height was 0.268 m, with the bulk density of the solid bed being equal to 712.8 kg/m³. The initial water concentration in the solid was 0.01 kg water/kg solid and the mass velocity of the nitrogen gas was 4052 kg/m² · h. The initial water concentration in the gas was $c_o = 926 \times 10^{-6}$ kg water/kg nitrogen. The breakthrough data are as follows:

| | | | | | | |
|--|------|-------|------|------|------|------|
| t (h) | 0 | 9 | 9.2 | 9.6 | 10 | 10.4 |
| c (kg H ₂ O/kg N ₂ × 10 ⁶) | <0.6 | 0.6 | 2.6 | 21 | 91 | 235 |
| t (h) | 10.8 | 11.25 | 11.5 | 12.0 | 12.5 | 12.8 |
| c (kg H ₂ O/kg N ₂ × 10 ⁶) | 418 | 630 | 717 | 855 | 906 | 926 |

A value of $dc_o = 0.02$ is desired at the break point. Do as follows:

- Determine the break-point time, the fraction of total capacity used up to the break point, the length of the unused bed, and the saturation loading capacity of the solid.
- For a proposed column length $H_T = 0.40$ m, calculate the break-point time and fraction of total capacity used.

A4:

Ans. (a) $t_b = 9.58$ h, fraction used = 0.878

12.4-1.

Scale-Up of Ion-Exchange Column. An ion-exchange process using a resin to remove copper ions from aqueous solution is conducted in a 1.0-in.-diameter column 1.2 ft high. The flow rate is 1.5 gph and the break point occurred at 7.0 min. Integrating the breakthrough curve gives a ratio of usable capacity to total capacity of 0.60. Design a new tower that will be 3.0 ft high and operate at 4.5 gph. Calculate the new tower size and break-point time.

A5:

Ans. $t_b = 24.5$ min, $D = 1.732$ in.

12.4-2.

Height of Tower in Ion Exchange. In a given run using a flow rate of $0.2 \text{ m}^3/\text{h}$ in an ion-exchange tower with a column height of 0.40 m, the break point occurred at 8.0 min. The ratio of usable capacity to total equilibrium capacity is 0.65. What is the height of a similar column operating for 13.0 min to the break point at the same flow rate?

12.4-3.

Ion Exchange of Copper in Column. An ion-exchange column containing 99.3 g of amberlite ion-exchange resin was used to remove Cu^{2+} from a solution where $c_o = 0.18 \text{ M CuSO}_4$. The tower height = 30.5 cm and the diameter = 2.59 cm. The flow rate was 1.37 cm^3 solution/s to the tower. The breakthrough data are shown below:

| | | | | | | |
|------------------|--------|--------|--------|--------|--------|--------|
| t (s) | 420 | 480 | 510 | 540 | 600 | 660 |
| c (g mol Cu/L) | 0 | 0.0033 | 0.0075 | 0.0157 | 0.0527 | 0.1063 |
| t (s) | 720 | 780 | 810 | 870 | 900 | |
| c (g mol Cu/L) | 0.1433 | 0.1634 | 0.1722 | 0.1763 | 0.180 | |

The concentration desired at the break point is $c/c_o = 0.010$. Determine the break-point time, fraction of total capacity used up to the break point, length of unused bed, and the saturation loading capacity of the solid.

12.4-4.

Effect of Total Concentration on Loading of Ion-Exchange Resin. Use the conditions of Example 12.4-1 for ion exchange of Cu^{2+} with H^+ . However, determine the effect of total concentration in the solution on the loading of Cu^{2+} on the resin. Do this for a total concentration C of 0.010 N in the solution at equilibrium instead of 0.10 N. Also, the concentration of Cu^{2+} in the solution is 0.002 M (0.004 N) instead of 0.02 M.

A8:

Ans. $q_{\text{CuR}_2} = 0.9132$ equiv/L

12.4-5.

Equilibrium in Ion Exchange of NH_4^+ for H^+ . For the case where the cation NH_4^+ (A) replaces H^+ (B) in a polystyrene resin with 8% DVB, calculate the equilibrium constant $K_{A,B}$. The total resin capacity $Q = 2.0$ equiv/L wet bed volume. The total concentration $C = 0.20 \text{ N}$ in the solution. Calculate at equilibrium the equivalents of NH_4^+ in the resin when the concentration of NH_4^+ in solution is 0.04 N.

A9:

Ans. $q_{\text{NH}_4\text{R}} = 0.6684$ equiv/L

- 12.5-1.** *Composition of Two Liquid Phases in Equilibrium.* An original mixture weighing 200 kg and containing 50 kg of isopropyl ether, 20 kg of acetic acid, and 130 kg of water is equilibrated in a mixer–settler and the phases separated. Determine the amounts and compositions of the raffinate and extract layers. Use equilibrium data from Appendix A.3.
- 12.5-2.** *Single-Stage Extraction.* A single-stage extraction is performed in which 400 kg of a solution containing 35 wt % acetic acid in water is contacted with 400 kg of pure isopropyl ether. Calculate the amounts and compositions of the extract and raffinate layers. Solve for the amounts both algebraically and by the lever-arm rule. What percent of the acetic acid is removed? Use equilibrium data from Appendix A.3.
- A11:** **Ans.** $L_1 = 358$ kg, $x_{B1} = 0.715$, $x_{C1} = 0.03$, $V_1 = 442$ kg, $y_{A1} = 0.11$, $y_{C1} = 0.86$, 34.7% removed.
- 12.5-3.** *Single-Stage Extraction with Unknown Composition.* A feed mixture weighing 200 kg of unknown composition containing water, acetic acid, and isopropyl ether is contacted in a single stage with 280 kg of a mixture containing 40 wt % acetic acid, 10 wt % water, and 50 wt % isopropyl ether. The resulting raffinate layer weighs 320 kg and contains 29.5 wt % acetic acid, 66.5 wt % water, and 4.0 wt % isopropyl ether. Determine the original composition of the feed mixture and the composition of the resulting extract layer. Use equilibrium data from Appendix A.3.
- A12:** **Ans.** $x_{A0} = 0.032$, $x_{B0} = 0.948$, $y_{A1} = 0.15$
- 12.5-4.** *Extraction of Acetone in a Single Stage.* A mixture weighing 1000 kg contains 23.5 wt % acetone and 76.5 wt % water and is to be extracted by 500 kg methyl isobutyl ketone in a single-stage extraction. Determine the amounts and compositions of the extract and raffinate phases. Use equilibrium data from Appendix A.3.
- 12.6-1.** *Flooding Velocity and Tower Diameter.* Using the same flow rates for each stream and feed conditions as in Ex. 12.6-1, with 1-in. Pall rings, design a tower for 50% of flooding with the aqueous phase dispersed instead of the toluene phase. Compare results.
- A14:** **Ans.** Diameter = 1.274 ft
- 12.6-2.** *Interfacial Tension in Extraction System.* Equilibrium data for the system water (A)–acetic acid (C)–isopropyl ether (B) are given in the Appendix, Table A.3-24. Using the data in dilute solution, where the wt fraction of acetic acid in the water-rich phase is 0.69%, calculate the interfacial tension.
- A15:** **Ans.** $\sigma = 20.28$ dyn/cm
- 12.6-3.** *Perforated-Plate Tray Efficiency.* An organic solvent is extracting an acid from a water solution in a perforated plate tower. The dispersed organic solvent flow rate is 600 ft³/h and the continuous aqueous flow rate is 400 ft³/h. The interfacial tension is 15 dyn/cm and the tray spacing is 1.1 ft. The hole size is 0.40 cm. Estimate the tray efficiency. What happens if the solvent flow rate is reduced to 400 ft³/h?
- A16:** **Ans.** $E_o = 0.133$ (solvent 600 ft³/h)

12.7-1.

Multiple-Stage Extraction with Fresh Solvent in Each Stage. Pure water is to be used to extract acetic acid from 400 kg of a feed solution containing 25 wt % acetic acid in isopropyl ether. Use equilibrium data from Appendix A.3.

- If 400 kg of water is used, calculate the percent recovery in the water solution in a one-stage process.
- If a multiple three-stage system is used and 133.3 kg fresh water is used in each stage, calculate the overall percent recovery of the acid in the total outlet water. (*Hint:* First, calculate the outlet extract and raffinate streams for the first stage using 400 kg of feed solution and 133 kg of water. For the second stage, 133 kg of water contacts the outlet organic phase from the first stage. For the third stage, 133.3 kg of water contacts the outlet organic phase from the second stage, and so on.)

12.7-2.

Overall Balance in Countercurrent Stage Extraction. An aqueous feed of 200 kg/h containing 25 wt % acetic acid is being extracted by pure isopropyl ether at the rate of 600 kg/h in a countercurrent multistage system. The exit acid concentration in the aqueous phase is to contain 3.0 wt % acetic acid. Calculate the compositions and amounts of the exit extract and raffinate streams. Use equilibrium data from Appendix A.3.

12.7-3.

Minimum Solvent and Countercurrent Extraction of Acetone. An aqueous feed solution of 1000 kg/h containing 23.5 wt % acetone and 76.5 wt % water is being extracted in a countercurrent multistage extraction system using pure methylisobutyl ketone solvent at 298–299 K. The outlet water raffinate will contain 2.5 wt % acetone. Use equilibrium data from Appendix A.3.

- Calculate the minimum solvent that can be used. [*Hint:* In this case the tie line through the feed L_0 represents the condition for minimum solvent flow rate. This gives $V_{1\min}$. Then draw lines $L_N V_{1\min}$ and $L_0 V_{N+1}$ to give the mixture point M_{\min} and the coordinate $x_{AM\min}$. Using Eq. (12.7-4), solve for $V/V_{N+1\min}$, the minimum value of the solvent flow rate V_{N+1} .]
- Using a solvent flow rate of 1.5 times the minimum, calculate the number of theoretical stages.

12.7-4.

Countercurrent Extraction of Acetic Acid and Minimum Solvent. An aqueous feed solution of 1000 kg/h of acetic acid–water solution contains 30.0 wt % acetic acid and is to be extracted in a countercurrent multistage process with pure isopropyl ether to reduce the acid concentration to 2.0 wt % acid in the final raffinate. Use equilibrium data from Appendix A.3.

- Calculate the minimum solvent flow rate that can be used. (*Hint:* See Problem 12.7-3 for the method to use.)
- If 2500 kg/h of ether solvent is used, determine the number of theoretical stages required. (*Note:* It may be necessary to replot on an expanded scale the concentrations at the dilute end.)

A20:

Ans. (a) Minimum solvent flow rate $V_{N+1} = 1630$ kg/h; (b) 7.5 stages

12.7-5. *Number of Stages in Countercurrent Extraction.* Repeat Example 12.7-2 but use an exit acid concentration in the aqueous phase of 4.0 wt %.

12.7-6. *Extraction with Immiscible Solvents.* A water solution of 1000 kg/h containing 1.5 wt % nicotine in water is stripped with a kerosene stream of 2000 kg/h containing 0.05 wt % nicotine in a countercurrent stage tower. The exit water is to contain only 10% of the original nicotine, that is, 90% is removed. Use equilibrium data from Example 12.7-3. Calculate the number of theoretical stages needed.

A22: **Ans.** 3.7 stages

12.7-7. *Numbers of Transfer Units for Extraction of Nicotine.* Using the data from Example 12.7-3 for nicotine extraction, replot the equilibrium and operating lines. For this system using a packed tower, the height of a transfer unit has been estimated as $H_{OL} = 1.1$ m. Calculate the number of transfer units by two different methods and compare the values. Also calculate the tower height.

A23: **Ans.** $N_{OL} = 5.76$ transfer units (Eq. 12.7-22), $z = 6.34$ m

12.7-8. *Minimum Solvent Rate with Immiscible Solvents.* Determine the minimum solvent kerosene rate to perform the desired extraction in Example 12.7-3. Using 1.50 times this minimum rate, determine the number of theoretical stages needed graphically and also by using the analytical equation.

A24: **Ans.** $V' = 153.8$ kg/h, $N = 6.86$ analytically

12.7-9. *Stripping Nicotine from Kerosene.* A kerosene flow of 100 kg/h contains 1.4 wt % nicotine and is to be stripped with pure water in a countercurrent multistage tower. It is desired to remove 90% of the nicotine. Using a water rate of 1.50 times the minimum, determine the number of theoretical stages required. (Use the equilibrium data from Example 12.7-3.)

12.7-10. *Extraction of Acetone from Water and Number of Transfer Units.* Repeat Example 12.7-4 for the extraction of acetone from water using 1.5 times the minimum solvent flow rate. Do as follows:

- Graphically determine the number of theoretical steps needed.
- Calculate the number of steps using the analytical equation.
- For a packed tower with this system, the height of the transfer unit H_{OL} has been estimated as 0.9 m. Calculate the number of transfer units N_{OL} and the tower height.

A26: **Ans.** (b) $N = 5.34$ steps analytically; (c) $N_{OL} = 6.21$ transfer units

12.7-11. *Predicting Extraction for Existing Tower with a Given Number of Steps.* An existing tower contains 5.0 theoretical steps. It is desired to predict its performance under the following conditions using the system water–acetone–trichloroethane given in Example 12.7-4. An inlet water stream of 1000 kg/h containing 8.0 wt % acetone is extracted with 750 kg/h trichloroethane containing 1.0 wt % acetone in this countercurrent tower at 25°C. Determine the outlet concentration x_1 in the water solution and in the trichloroethane solution using an analytical equation. Also plot the equilibrium and operating lines and step off 5.0 steps. Assume dilute solutions.

A27: **Ans.** $x_1 = 0.01205$, $y_2 = 0.0932$

- 12.8-1.** *Effective Diffusivity in Leaching Particles.* In Example 12.8-1 a time of leaching of the solid particle of 3.11 h is needed to remove 80% of the solute. Perform the following calculations:
- Using the experimental data, calculate the effective diffusivity, D_{Aeff} .
 - Predict the time to leach 90% of the solute from the 2.0 mm particle.
- A28:** **Ans.** (a) $D_{\text{Aeff}} = 1.0 \times 10^{-5} \text{ mm}^2/\text{s}$; (b) $t = 5.00 \text{ h}$
- 12.9-1.** *Leaching of Oil from Soybeans in a Single Stage.* Repeat Example 12.9-1 for single-stage leaching of oil from soybeans. The 100 kg of soybeans contains 22 wt % oil and the solvent feed is 80 kg of solvent containing 3 wt % soybean oil.
- A29:** **Ans.** $L_1 = 52.0 \text{ kg}$, $y_{A1} = 0.239$, $V_1 = 50.0 \text{ kg}$, $x_{A1} = 0.239$, $N_1 = 1.5$
- 12.9-2.** *Leaching a Soybean Slurry in a Single Stage.* A slurry of flaked soybeans weighing a total of 100 kg contains 75 kg of inert solids and 25 kg of solution with 10 wt % oil and 90 wt % solvent hexane. This slurry is contacted with 100 kg of pure hexane in a single stage so that the value of N for the outlet underflow is 1.5 kg insoluble solid/kg solution retained. Calculate the amounts and compositions of the overflow V_1 and the underflow L_1 leaving the stage.
- 12.10-1.** *Constant Underflow in Leaching Oil from Meal.* Use the same conditions as given in Example 12.10-1, but assume constant underflow of $N = 1.85 \text{ kg solid/kg solution}$. Calculate the exit flows and compositions and the number of stages required. Compare with Example 12.10-1.
- A31:** **Ans.** $y_{AN} = 0.111$, $x_{A1} = 0.623$, 4.3 stages
- 12.10-2.** *Effect of Less Solvent Flow in Leaching Oil from Meal.* Use the same conditions as given in Example 12.10-1, but the inlet fresh-solvent-mixture flow rate per hour is decreased by 10%, to 1179 kg of benzene and 18 kg of oil. Calculate the number of stages needed.
- 12.10-3.** *Countercurrent Multistage Washing of Ore.* A treated ore containing inert solid gangue and copper sulfate is to be leached in a countercurrent multistage extractor using pure water to leach the CuSO_4 . The solid charge rate per hour consists of 10 000 kg of inert gangue (B), 1200 kg of CuSO_4 (solute A), and 400 kg of water (C). The exit wash solution is to contain 92 wt % water and 8 wt % CuSO_4 . A total of 95% of the CuSO_4 in the inlet ore is to be recovered. The underflow is constant at $N = 0.5 \text{ kg inert gangue solid/kg aqueous solution}$. Calculate the number of stages required.
- A33:** **Ans.** 9 stages, $L_N = 20\,000 \text{ kg/h}$, $y_{AN} = 0.0030$, $V_1 = 14\,250 \text{ kg/h}$
- 12.10-4.** *Countercurrent Multistage Leaching of Halibut Livers.* Fresh halibut livers containing 25.7 wt % oil are to be extracted with pure ethyl ether to remove 95% of the oil in a countercurrent multistage leaching process. The feed rate is 1000 kg of fresh livers per hour. The final exit overflow solution is to contain 70 wt % oil. The retention of solution by the inert solids (oil-free liver) of the liver varies as follows (C_1), where N is kg inert solid/kg solution retained and y_A is kg oil/kg solution:

| N | y_A | N | y_A | N | y_A |
|------|-------|------|-------|------|-------|
| 4.88 | 0 | 2.47 | 0.4 | 1.39 | 0.81 |
| 3.50 | 0.2 | 1.67 | 0.6 | | |

Calculate the amounts and compositions of the exit streams and the total number of theoretical stages.

12.10-5.

Countercurrent Leaching of Flaked Soybeans. Soybean flakes containing 22 wt % oil are to be leached in a countercurrent multi-stage process to contain 0.8 kg oil/100 kg inert solid using fresh and pure hexane solvent. For every 1000 kg soybeans, 1000 kg hexane is used. Experiments (S1) give the following retention of solution with the solids in the underflow, where N is kg inert solid/kg solution retained and y_A is wt fraction of oil in solution:

| N | y_A |
|------|-------|
| 1.73 | 0 |
| 1.52 | 0.20 |
| 1.43 | 0.30 |

Calculate the exit flows and compositions and the number of theoretical stages needed.

12.11-1.

Crystallization of $\text{Ba}(\text{NO}_3)_2$. A hot solution of $\text{Ba}(\text{NO}_3)_2$ from an evaporator contains 30.6 kg $\text{Ba}(\text{NO}_3)_2$ /100 kg H_2O and goes to a crystallizer, where the solution is cooled and $\text{Ba}(\text{NO}_3)_2$ crystallizes. On cooling, 10% of the original water present evaporates. For a feed solution of 100 kg total, calculate the following:

- The yield of crystals if the solution is cooled to 290 K (17°C), where the solubility is 8.6 kg $\text{Ba}(\text{NO}_3)_2$ /100 kg total water.
- The yield if cooled instead to 283 K, where the solubility is 7.0 kg $\text{Ba}(\text{NO}_3)_2$ /100 kg total water.

A36:

Ans. (a) 17.47 kg $\text{Ba}(\text{NO}_3)_2$ crystals

12.11-2.

Dissolving and Subsequent Crystallization. A batch of 1000 kg of KCl is dissolved in sufficient water to make a saturated solution at 363 K, where the solubility is 35 wt % KCl in water. The solution is cooled to 293 K, at which temperature its solubility is 25.4 wt %.

- What is the weight of water required for solution and the weight of crystals of KCl obtained?
- What is the weight of crystals obtained if 5% of the original water evaporates on cooling?

A37:

Ans. (a) 1857 kg water, 368 kg crystals; (b) 399 kg crystals

12.11-3.

Crystallization of $\text{MgSO}_4 \cdot 7\text{H}_2\text{O}$. A hot solution containing 1000 kg of MgSO_4 and water having a concentration of 30 wt % MgSO_4 is cooled to 288.8 K, where crystals of $\text{MgSO}_4 \cdot 7\text{H}_2\text{O}$ are precipitated. The solubility at 288.8 K is 24.5 wt % anhydrous MgSO_4 in the solution. Calculate the yield of crystals obtained if 5% of the original water in the system evaporates on cooling.

12.11-4.

Heat Balance in Crystallization. A feed solution of 10 000 lb_m at 130°F containing 47.0 lb FeSO₄/100 lb total water is cooled to 80°F, where FeSO₄ · 7H₂O crystals are removed. The solubility of the salt is 30.5 lb FeSO₄/100 lb total water (P1). The average heat capacity of the feed solution is 0.70 btu/lb_m · °F. The heat of solution at 18°C is -4.4 kcal/g mol (-18.4 kJ/g mol) FeSO₄ · 7H₂O (P1). Calculate the yield of crystals and make a heat balance. Assume that no water is vaporized.

A39:

Ans. 2750 lb_m FeSO₄ · 7H₂O crystals, $q = -428\,300$ btu (-451 900 kJ)

12.11-5.

Effect of Temperature on Yield and Heat Balance in Crystallization. Use the conditions given in Example 12.11-2, but the solution is cooled instead to 283.2 K, where the solubility is 30.9 kg MgSO₄/100 kg total water (P1). Calculate the effect on yield and the heat absorbed by using 283.2 K instead of 293.2 K for the crystallization.

12.12-1.

Growth and Nucleation Rate in MSMPR Crystallizer. Experimental data were obtained for an MSMPR crystallizer (S2). The slurry density is 169 g/L, the crystal density ρ is 1.65 g/m³, the residence time τ is 6.57 h, and the shape factor a is 0.98. The screen analysis of the crystals is as follows:

| Mesh | Wt % | Mesh | Wt % |
|----------|------|-----------|------|
| -14, +20 | 4.5 | -35, +48 | 31.5 |
| -20, +28 | 14.5 | -48, +65 | 15.5 |
| -28, +35 | 24.0 | -65, +100 | 7.5 |
| | | -100 | 2.5 |

Using these data, do as follows:

- Calculate the population density, growth rate, and nucleation rate. Also calculate the average size L_a .
- Using these calculated values, predict the cumulative weight fraction versus size L from the experimental value of G and τ . Compare the predicted and experimental values.

A41:

Ans. (a) $G = 0.01673$ mm/h; (b) For $L = 0.589$ mm, $(1 - W_{\hat{L}}) = 0.218$

12.12-2.

Prediction of Cumulative Weight Fraction of Crystals from Growth Rate. In Example 12.12-1, the growth rate G was determined to be 0.03244 mm/h for a residence time τ of 3.38 h. Using these values, predict the cumulative weight fraction versus size L . Compare the predicted values with the experimental values.

A42:

Ans. $L = 0.589$ mm, $(1 - W_{\hat{L}}) = 0.217$; $L = 0.417$ mm, $(1 - W_{\hat{L}}) = 0.473$

REFERENCES

Bibliography

- [ch12biblio01entry01] (B1) N. Blakebrough, *Biochemical and Biological Engineering Science*, Vol. 1. New York: Academic Press, Inc., 1968.
- [ch12biblio01entry02] (B2) W. L., Badger, and J. T. Banchero, *Introduction to Chemical Engineering*. New York: McGraw-Hill Book Company, 1955.
- [ch12biblio01entry03] (B3) W. L., Badger, and W. L. McCabe, *Elements of Chemical Engineering*. New York: McGraw-Hill Book Company, 1936.
- [ch12biblio01entry04] (B4) H. E. Buckley, *Crystal Growth*. New York: John Wiley & Sons, Inc., 1951.
- [ch12biblio01entry05] (B5) R. C., Bennett, and M. Van Buren, *Chem. Eng. Progr. Symp.*, **65**(95), 46 (1969).
- [ch12biblio01entry06] (B6) R. C., Bennett, H., Fieldelman, and A. D. Randolph, *Chem. Eng. Progr.*, **69**(7), 86 (1972).
- [ch12biblio01entry07] (B7) P. A., Belter, E. L., Cussler, and W. S. Hu, *Bioseparations*. New York: John Wiley & Sons, Inc., 1988.
- [ch12biblio01entry08] (B8) O. D., Bonner, and L. L. Smith, *J. Phys. Chem.*, **61**, 236 (1957).
- [ch12biblio01entry09] (B9) R. C., Bennett, H., Fiedelman, and A. D. Randolph, *Chem. Eng. Progr.*, **69**(7), 86 (1973).
- [ch12biblio01entry10] (C1) S. E. Charm, *The Fundamentals of Food Engineering*, 2nd ed. Westport, Conn.: Avi Publishing Co., Inc., 1971.
- [ch12biblio01entry11] (C2) Crystallization from Solutions and Melts, *Chem. Eng. Progr. Symp.*, **65**(95), (1969).
- [ch12biblio01entry12] (C3) J. J. Collins, *Chem. Eng. Progr. Symp. Series*, **63**(74), 31 (1967).
- [ch12biblio01entry13] (C4) N. A., Clontz, and W. L. McCabe, *A.I.Ch.E. Symp. Ser. No. 110*, **67**, 6 (1971).
- [ch12biblio01entry14] (C5) J. B., Claffey, C. O., Badgett, C. D., Skalamera, and G. W. Phillips, *Ind. Eng. Chem.*, **42**, 166 (1950).
- [ch12biblio01entry15] (C6) R. W., Cusack, and A. E. Karr, *Chem. Eng.*, **98**(4), 112 (1991).
- [ch12biblio01entry16] (C7) R. W., Cusack, P., Fremeaux, and D Glatz, *Chem. Eng.*, **98**(2), 66 (1991).
- [ch12biblio01entry17] (C8) R. W., Cusack, and P. Fremeaux, *Chem. Eng.*, **98**(3), 132 (1991).
- [ch12biblio01entry18] (C9) J. W., Crawford, and C. R. Wilke, *Chem. Eng. Prog.*, **47**, 423 (1951).
- [ch12biblio01entry19] (H1) O. A., Hougen, K. M., Watson, and R. A. Ragatz, *Chemical Process Principles*, Part I, 2nd ed. New York: John Wiley & Sons, Inc., 1954.
- [ch12biblio01entry20] (H2) A. W., Hixson, and K. L. Knox, *Ind. Eng. Chem.*, **43**, 2144 (1951).
- [ch12biblio01entry21] (H3) M. C., Hu, E. R., Haering, and C. J. Geankoplis, *Chem. Eng. Sci.*, **40**, 2241 (1985).

- [ch12biblio01entry22] (H4) J. L., Humphry, and G. E. Keller, *Separation Process Technology*. New York: McGraw-Hill Book Company, 1997.
- [ch12biblio01entry23] (K1) G. J. Karnofsky, *Am. Oil Chemist's Soc.*, **26**, 564 (1949).
- [ch12biblio01entry24] (K2) K. A., Kobe, and E. J., Couch,, Jr. *Ind. Eng. Chem.*, **46**, 377 (1954).
- [ch12biblio01entry25] (K3) A. E. Karr, and T. C. Lo, *Proc. Int. Solv. Ext. Conf. (ISEC)*, **1**, 299 (1971).
- [ch12biblio01entry26] (K4) A. E. Karr, *Sepr. Sci. Tech.*, **15**(No. 4), 877 (1980).
- [ch12biblio01entry27] (L1) G. M. Lukchis, *Chem. Eng.*, **80** (June 11), 111 (1973).
- [ch12biblio01entry28] (L2) M. A. Larson, *Chem. Eng.*, **85** (Feb. 13), 90 (1978).
- [ch12biblio01entry29] (L3) T. C., Lo, and A. E. Karr, *I.E.C. Proc. Des. Dev.*, **11**(4), 495 (1972).
- [ch12biblio01entry30] (L4) T. C., Lo, M. H.I., Baird, and C. Hanson, *Handbook of Solvent Extraction*. New York: John Wiley & Sons, Inc., 1983.
- [ch12biblio01entry31] (L5) M. A., Larson, and A. D. Randolph, *Chem. Eng. Progr. Symp.*, **65**(95), 1 (1969).
- [ch12biblio01entry32] (M1) A. S. Michaels, *Ind. Eng. Chem.*, **44**(8), 1922 (1952).
- [ch12biblio01entry33] (M2) D. C., Murray, and M. A. Larson, *A.I.Ch.E. J.*, **11**, 728 (1965).
- [ch12biblio01entry34] (M3) W. L., McCabe, J. C., Smith, and P. Harriott, *Unit Operations of Chemical Engineering*, 4th ed. New York: McGraw-Hill Book Company, 1985.
- [ch12biblio01entry35] (M4) W. L., McCabe, J. C., Smith, and P. Harriott, *Unit Operations of Chemical Engineering*, 5th ed. New York: McGraw-Hill Book Company, 1992.
- [ch12biblio01entry36] (N1) National Research Council. *International Critical Tables*, Vol. 5. New York: McGraw-Hill Book Company, 1929.
- [ch12biblio01entry37] (O1) J. Q., Osburn, and D. L. Katz, *Trans. A.I.Ch.E.*, **40**, 511 (1944).
- [ch12biblio01entry38] (O2) D. F., Othmer, and W. A. Jaatinen, *Ind. Eng. Chem.*, **51**, 543 (1959).
- [ch12biblio01entry39] (O3) D. F., Othmer, and J. C. Agarwal, *Ind. Eng. Chem.*, **51**, 372 (1955).
- [ch12biblio01entry40] (P1) R. H., Perry, and D. Green, *Perry's Chemical Engineers' Handbook*, 6th ed. New York: McGraw-Hill Book Company, 1984.
- [ch12biblio01entry41] (P2) J. H. Perry, *Chemical Engineers' Handbook*, 4th ed. New York: McGraw-Hill Book Company, 1963.
- [ch12biblio01entry42] (P3) R. H., Perry, and C. H. Chilton, *Chemical Engineers' Handbook*, 5th ed. New York: McGraw-Hill Book Company, 1973.
- [ch12biblio01entry43] (P4) R. H., Perry, and D. Green, *Perry's Chemical Engineers' Handbook*, 7th ed. New York: McGraw-Hill Book Company, 1997.
- [ch12biblio01entry44] (R1) A. D., Randolph, and M. A. Larson, *Theory of Particulate Systems*. New York: Academic Press, Inc., 1971.
- [ch12biblio01entry45] (R2) A. D., Randolph, and M. Larson, *A. A.I.Ch.E. J.*, **8**, 639 (1962).
- [ch12biblio01entry46] (R3) A. D. Randolph, *A.I.Ch.E. J.*, **11**, 424 (1965).
- [ch12biblio01entry47] (R4) Rousseau, R.W. (ed.). *Handbook of Separation Process Technology*. New York: John Wiley & Sons, Inc., 1987.
- [ch12biblio01entry48] (R5) T. D. Reynolds, *Unit Operations and Processes in Environmental Engineering*. Boston: PWS Publishers, 1982.
- [ch12biblio01entry49] (R6) D. M. Ruthven, *Principles of Adsorption and Adsorption Processes*. New York: John Wiley & Sons, Inc., 1984.

- [ch12biblio01entry50] (S1) C. T. Smith, *J. Am. Oil Chemists' Soc.*, **28**, 274 (1951).
- [ch12biblio01entry51] (S2) P. A. Schweitzer, *Handbook of Separation Techniques for Chemical Engineers*. New York: McGraw-Hill Book Company, 1997.
- [ch12biblio01entry52] (S3) J. D., Seader, and E. J. Henley, *Separation Process Principles*. New York: John Wiley & Sons, Inc., 1998.
- [ch12biblio01entry53] (S4) J. Stichlmair, *Chemie Ingenieur Technik*, **52**, 253 (1980).
- [ch12biblio01entry54] (S5) R. F. Strigle, *Packed Tower Design and Applications*. Houston: Gulf Publishing Company, 1994.
- [ch12biblio01entry55] (T1) R. E. Treybal, *Mass Transfer Operations*, 3rd ed. New York: McGraw-Hill Book Company, 1980.
- [ch12biblio01entry56] (T2) R. E. Treybal, *Liquid Extraction*, 2nd ed. New York: McGraw-Hill Book Company, 1963.
- [ch12biblio01entry57] (T3) R. E. Treybal, D. W., Lawrence, and F. Daley, *Ind. Eng. Chem.*, **38**, 817 (1946).
- [ch12biblio01entry58] (V1) A. Van Hook, *Crystallization, Theory and Practice*. New York: John Wiley & Sons, Inc., 1951.
- [ch12biblio01entry59] (W1) S. M. Walas, *Chemical Process Equipment*. Boston: Butterworth-Heinemann, 1990.
- [ch12biblio01entry60] (Y1) H. H., Yang, and J. Brier, *C. A.I.Ch.E. J.*, **4**, 453 (1958).